



REVIEW ARTICLE

Tuning of graphitic carbon nitride (g-C₃N₄) for photocatalysis: A critical review



Y.S. Wudil^{a,b,*}, U.F. Ahmad^c, M.A. Gondal^{a,d}, Mohammed A. Al-Osta^{b,e},
Abdullah Almohammedi^f, R.S. Sa'id^g, F. Hrahsheh^h, K. Harunaⁱ,
M.J.S. Mohamed^a

^a Laser Research Group, Physics Department, King Fahd University of Petroleum & Minerals (KFUPM), Mailbox 5047, Dhahran 31261, Saudi Arabia

^b Interdisciplinary Research Center for Construction and Building Materials, King Fahd University of Petroleum and Minerals, Dhahran 31261, Saudi Arabia

^c Center for Renewable Energy Research, Bayero University, Kano, Nigeria

^d K.A.CARE Energy Research & Innovation Center, King Fahd University of Petroleum and Minerals, Dhahran 31261, Saudi Arabia

^e Department of Civil and Environmental Engineering, King Fahd University of Petroleum and Minerals, 31261 Dhahran, Eastern Province, Saudi Arabia

^f Department of Physics, Faculty of Science, Islamic University of Madinah, Prince Naif bin Abdulaziz, Al Jamiah, Madinah 42351, Saudi Arabia

^g Department of Physics, Faculty of Physical Sciences, Bayero University, Kano, Nigeria

^h Higher Colleges of Technology, ETS, MZWC, 58855, Abu Dhabi, UAE

ⁱ Chemistry Department, King Fahad University of Petroleum and Mineral, Dhahran 31261, Saudi Arabia

Received 14 November 2022; accepted 1 January 2023

Available online 5 January 2023

KEYWORDS

Clean energy;
Clean water;
CO₂ conversion;
Graphitic carbon nitride;
Hydrogen production;
Photocatalysis

Abstract Graphitic carbon nitride (g-C₃N₄) is a remarkable semiconductor catalyst that has attracted widespread attention as a visible light photo-responsive, metal-free, low-cost photocatalytic material. Pristine g-C₃N₄ suffers fast recombination of photogenerated electron-hole pairs, low surface area, and insufficient visible light absorption, resulting in low photocatalytic efficiency. This review presents the recent progress, perspectives, and persistent challenges in the development of g-C₃N₄-based photocatalytic materials. Several approaches employed to improve the visible light absorption of the materials including metal and non-metal doping, co-doping, and heterojunction engineering have been extensively discussed. These approaches, in general, were found to decrease

* Corresponding author.

E-mail address: yswudil@yahoo.com (Y.S. Wudil).

Peer review under responsibility of King Saud University.



the material's bandgap, increase the surface area, reduce charge carrier recombination, and promote visible light absorption, thereby enhancing the overall photocatalytic performance. The material has been widely used for different applications such as photocatalytic hydrogen production, water splitting, CO₂ conversion, and water purification. The work has also identified various limitations and weaknesses associated with the material that hinders its maximum utilization under visible illumination and presented state-of-the-art solutions that have been reported recently. The summary presented in this review would add an invaluable contribution to photocatalysis research and facilitate the development of efficient visible light-responsive semiconducting materials.

© 2023 The Author(s). Published by Elsevier B.V. on behalf of King Saud University. This is an open access article under the CC BY-NC-ND license (<http://creativecommons.org/licenses/by-nc-nd/4.0/>).

1. Introduction

The ever-increasing demand for clean and sustainable energy for domestic and industrial applications has been a source of concern for both policymakers and researchers as witnessed in deliberations at the international energy summits (Xie et al., 2022; Sharma et al., 2022; Li et al., 2022). This is especially important considering the rising global warming and climate change impacts on our environment (Kanimba et al., 2019; Wudil et al., 2021; Hrahsheh et al., 2017). Sunlight has been considered an incredible and inexhaustible energy source that does not pose any threat to the environment (Zhang et al., 2022). It is considered one of the solutions to the lingering energy scarcity and environmental pollution.

Semiconductor photocatalysts have been employed for various applications including selective synthesis of organic compounds, water splitting, bacteria disinfection, removal of organic pollutants, and CO₂ reduction (Zhang et al., 2022; Al-Ahmed, 2022; Boumeriame et al., 2022; Zhao et al., 2022). They are considered clean, safe, economic, and renewable technology. However, the main impediment to the practical applications of these compounds is their wide bandgap which results in low solar energy utilization. For instance, TiO₂ has been regarded as an excellent photocatalyst since the discovery of Fujishima et al. (Fujishima and Honda, 1972), who found that by using TiO₂ as a photoanode, water can be split into hydrogen. However, the relatively large bandgap of the compound (~3.2 eV) has become a barrier to its deployment, especially under visible light irradiation. Multiple works have been conducted to overcome the drawbacks of the wide bandgap of TiO₂ to enable it to harness the visible portion of solar energy (Su et al., 2017; Ahmed et al., 2010).

Hitherto, it is remarkably challenging to develop a novel photocatalytic material that is efficient, abundant, stable, and facile in synthesis (Zhang et al., 2022; Cheng et al., 2022; Wang et al., 2022; Long et al., 2022). Recently, some 2D materials with outstanding properties such as hexagonal boron nitrides, transition-metal dichalcogenides, graphitic carbon nitrides (g-C₃N₄), and graphene have been extensively used for different applications including energy storage and generation, chemical sensors, electronic and optical devices, and environmental remediation (Liu et al., 2022; Lu et al., 2022; Zhang et al., 2022; Li et al., 2022; Wan et al., 2022). Specifically, g-C₃N₄ (Fig. 1) has generated vast interest for its exceptional photocatalytic applications as a metal-free polymer.

Basically, g-C₃N₄ falls in the range of medium bandgap semiconducting compounds that respond to visible light (up to 460 nm) (Kong et al., 2022; Shi et al., 2022). This optimum energy gap together with high chemical stability, facile synthesis, low cost, and environmental friendliness makes it one of the excellent candidates for CO₂ reduction and organic synthesis, water splitting, and degradation of organic pollutants under visible light radiation (Altan et al., 2022; Choong et al., 2022; Dong et al., 2022; Rana et al., 2022; Kumar et al., 2022). However, the intrinsic g-C₃N₄ generally exhibits low photocatalytic performance due to the fast recombination of electron-hole pairs, low surface area, and inadequate light absorption (Mo et al., 2022). The structural lattice architecture and the calculated electronic

band structure of the g-C₃N₄ photocatalyst are presented in Fig. 2. g-C₃N₄ at varying dimensions has been used for different applications as depicted in Fig. 3. It is evident that g-C₃N₄ possesses a tunable bandgap with the ability to control the highest occupied molecular orbital (HOMO) and lowest unoccupied molecular orbital (LUMO). This makes it easier to enhance its photoelectronic efficiency. The tunable bandgap allows modifying the material's property through heterostructure design or by elemental doping (Wudil et al., 2022; Wudil et al., 2020; Al-Najjar et al., 2022). The latter has been reported as an effective means of tuning the material's energy gap and facilitating visible light absorption, thereby accelerating charge carrier separation (Cheng et al., 2022). Elsewhere (Fronczak et al., 2022), the electronic structure and texture of g-C₃N₄ have been modified by substitutional and interstitial doping with B, I, C, S, or P, and enhanced photocatalytic efficiency was achieved. Similarly, transition metals and Alkali metals have been doped on g-C₃N₄ to improve its photo-response.

Herein, we report the recent progress and persistent challenges in the development of g-C₃N₄ photocatalytic systems to enhance the utilization of solar radiation in the visible range for different applications such as water splitting, hydrogen evolution, water purification, and CO₂ reduction. We also present the current challenges that need to be addressed in future works.

2. Fundamentals of heterogeneous photocatalysis mediated by semiconductors

The basics of photocatalysis has been explained in numerous articles (Liang et al., 2022; Wang et al., 2020; Fattahimoghaddam et al., 2022; Meng et al., 2022), therefore, our focus in this work is to give a brief insight into the subject to enable the reader to digest the important aspects of the photocatalytic process (Wang et al., 2020; Wang et al., 2020; Wang et al., 2022). Fig. 4 summarizes the fundamental principles of photocatalysis starting from light harvesting, excitation of charge carriers and separation, charge transfer, recombination of charges, and surface reactions (Koutsouroubi et al., 2022; Rajan and Neppolian, 2022; Shahsavandi et al., 2022). Briefly, the mechanism of photocatalysis involves three main steps: photon absorption, electron-hole generation, and surface activity (Lin et al., 2022; Gao et al., 2022; You et al., 2022; Song et al., 2022). Thus, multiple strategies have been adopted to improve the photocatalytic efficiency of g-C₃N₄ such as dye sensitization, nanocomposite structure formation, using conductive materials, and exfoliation to 2D nanosheets, fabricating mesoporous g-C₃N₄, molecular and elemental doping (Yu et al., 2022; Tao et al., 2022; Azami et al., 2022; Zehtab Salmasi et al., 2022; Zhao et al., 2022; Van Thuan et al., 2022; Wang et al., 2022; Niu et al., 2022; Tipllook et al., 2022; Mandari et al., 2022).

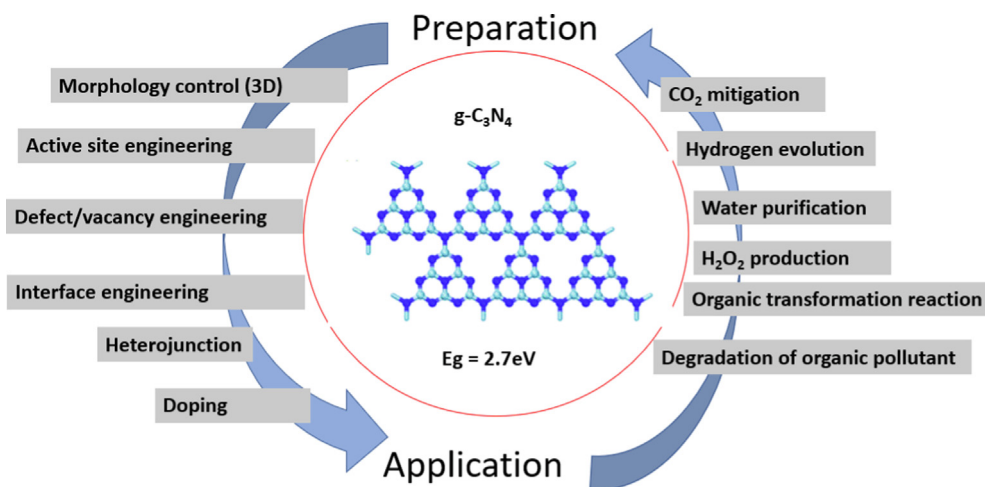


Fig. 1 Polymerized $g\text{-C}_3\text{N}_4$ structure (nitrogen: gray, carbon: blue). (). Adapted from Sun et al., 2018

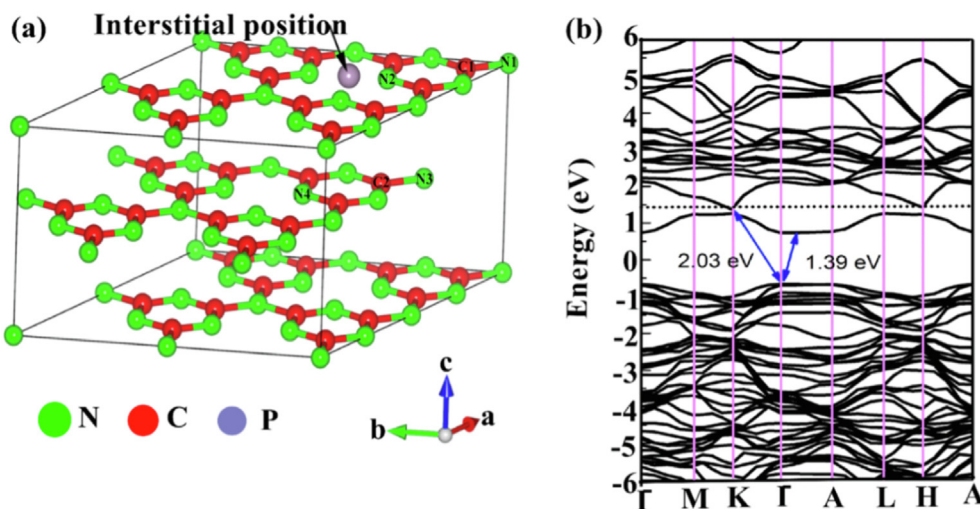


Fig. 2 (a) Lattice structure of $g\text{-C}_3\text{N}_4$ with 2:2:1 supercell, (b) calculated band structure of $g\text{-C}_3\text{N}_4$. (). Adapted from Liu, 2016

Several industries (leather, energy, paper, textiles, etc.) employ the application of dyes or synthetic pigments which makes colored wastewater a significant problem to deal with related to these industries, especially as they release large quantity of heat to the environment which often complicate the issue (Wudil et al., 2020; Almessiere et al., 2021; Salhi et al., 2018; Alrebdi et al., 2022). These pollutants are made up of extensive organic compounds and hazardous substances that are poisonous to organisms that live below water. In addition, the increased use of pharmaceuticals in healthcare because of the growth in the world's population has contributed to the release of these unutilized or dissolved compounds into the environment. For that reason, it is required to mineralize, eliminate, transform and reduce these molecules of pollutants from the aquatic habitat. Apart from that, fossil fuels like coal, gas, and petroleum have serious effects on climate change. Many conventional techniques have been developed in this regard for the purification of water. These techniques involve biological, chemical, physical, coagulation, adsorption, sedimentation, flotation, filtration methods, gravitational separation, and reverse osmosis. However, due to the movement of

contaminants from one stage to another stage or partial removal, the performance of these methods is insignificant to exhaustively clean contaminated water. This section presents an advanced technique for dealing with environmental concerns (Asadzadeh-Khaneghah and Habibi-Yangjeh, 2020).

Advanced Oxidation Processes (AOPs) are a category of chemical processes examined to be among the most effective and desirable solutions for the above-mentioned problems. In the past few decades, numerous groundbreaking examinations have been conducted to explore the application of these processes in areas of environmental and wastewater treatment (Asadzadeh-Khaneghah and Habibi-Yangjeh, 2020). These processes do not transfer contaminants from one stage to another, but rather manipulate environmental crises and prevent the production of toxic sludge. This ability made them superior to sedimentation, filtration, physical, and biological processes. These processes are particularly useful as an efficient purification method with high mineralization ability for the non-reactive and rapid degradation of a wide range of highly stable and nonbiodegradable organic chemicals into harmless and environmentally friendly compounds like water, SO_4^- ,

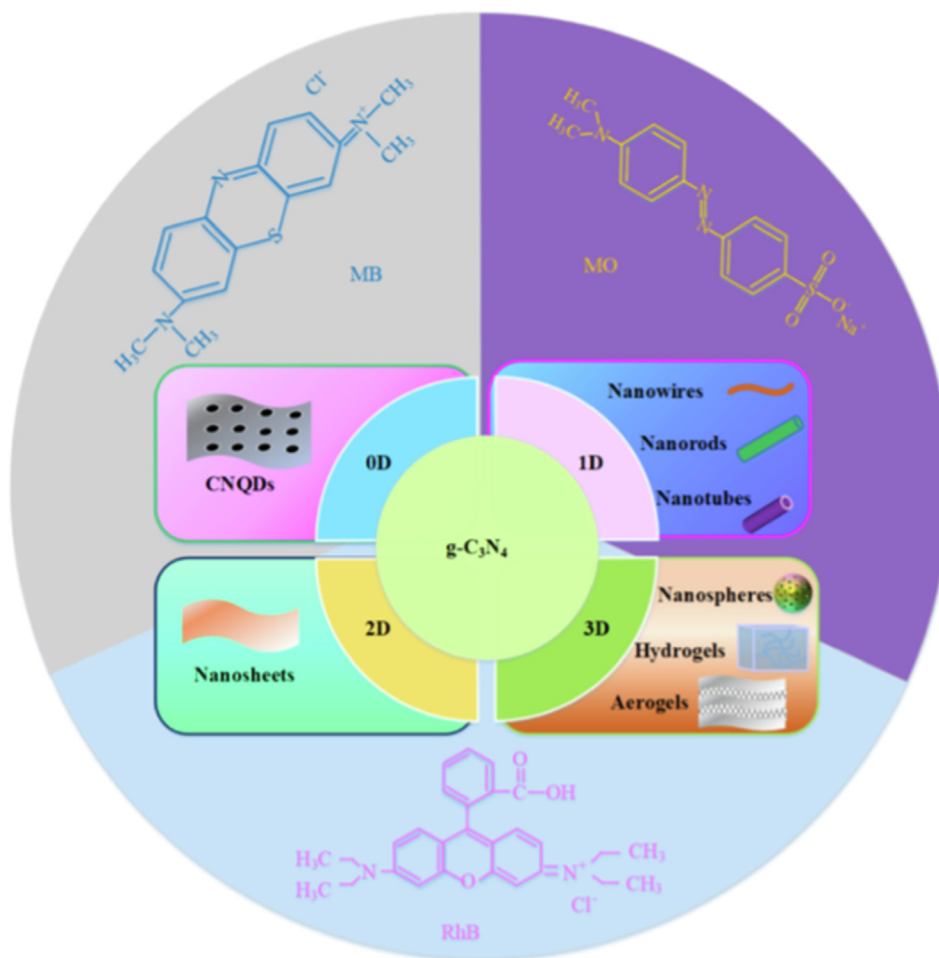


Fig. 3 The applications of $g\text{-C}_3\text{N}_4$ with varying dimensions. (). Adapted from Xie et al., 2022

PO_4^{3-} , and carbon dioxide via reactive species such as SO_4 , O_2 , and h^+ .

Various AOPs are stated in Fig. 5. The most cost-effective provides the ideal solution to remediating energy crisis and environmental contamination among the various AOPs is the heterogeneous photocatalysis mediated by semiconductors (Tseng et al., 2022; Lin et al., 2022). The following indicated the characteristics that made heterogeneous photocatalysis appealing: i) The accomplishment of the process in ambient situations. ii) The feasibility of the process to support the photocatalyst on various forms of inert matrices for example, graphene oxides, carbon nanotubes, glasses, and polymers and in general, the utilized catalysts are non-toxic, affordable, and can be recycled. Furthermore, iii) It is the cheapest method that is eco-friendly when it comes to air and water treatment.

Moreover, heterogeneous photocatalysis mediated by semiconductors can be employed for various applications among which are the production of hydrogen via splitting of water, degradation of water pollutants, reduction of carbon dioxide for fuel production, disinfection of different microorganisms, and nitrogen photofixation, as shown in Fig. 5.

A photocatalyst under light illumination for activation is schematically displayed in Fig. 6. Four fundamental steps explained the process of heterogeneous photocatalysis. Gener-

ally, photocatalysis mediated by semiconductors starts off to absorb proper photon energy that is the same or greater than that of the energy gap (E_g) of the desired photocatalyst to produce e^-/h^+ pairs which then produce few reactive species and thereby leads to various redox reactions on the surface of the heterogeneous photocatalyst. However, the reverse process of this phase is that absorbed energy is released in form of heat at the time scale of nanoseconds as a result of the recombination of a large portion of the photoinduced charges.

3. Selection of appropriate semiconductors

Numerous semiconductors are applied as photocatalysts to produce energy and facilitate environmental purification (Fronczak et al., 2022; Meng et al., 2022; Zhang et al., 2022; Schirmer et al., 2022; Tan et al., 2022; Nguyen et al., 2022; Liu et al., 2022). Among these photocatalysts used are Fe_2O_3 , NaTaO_3 , WO_3 , BiPO_4 , TiO_2 , ZnS , SrTiO_3 , ZnO , and SnO_2 . Despite several pieces of literature, poor harvesting of visible light by the chosen photocatalysts has made the conventional utilization of this process a great challenge. The UV light spectrum of sunlight radiations can only be harvested by photocatalysts that have a wide energy gap and UV light requires protective support for its application, and UV sources are not

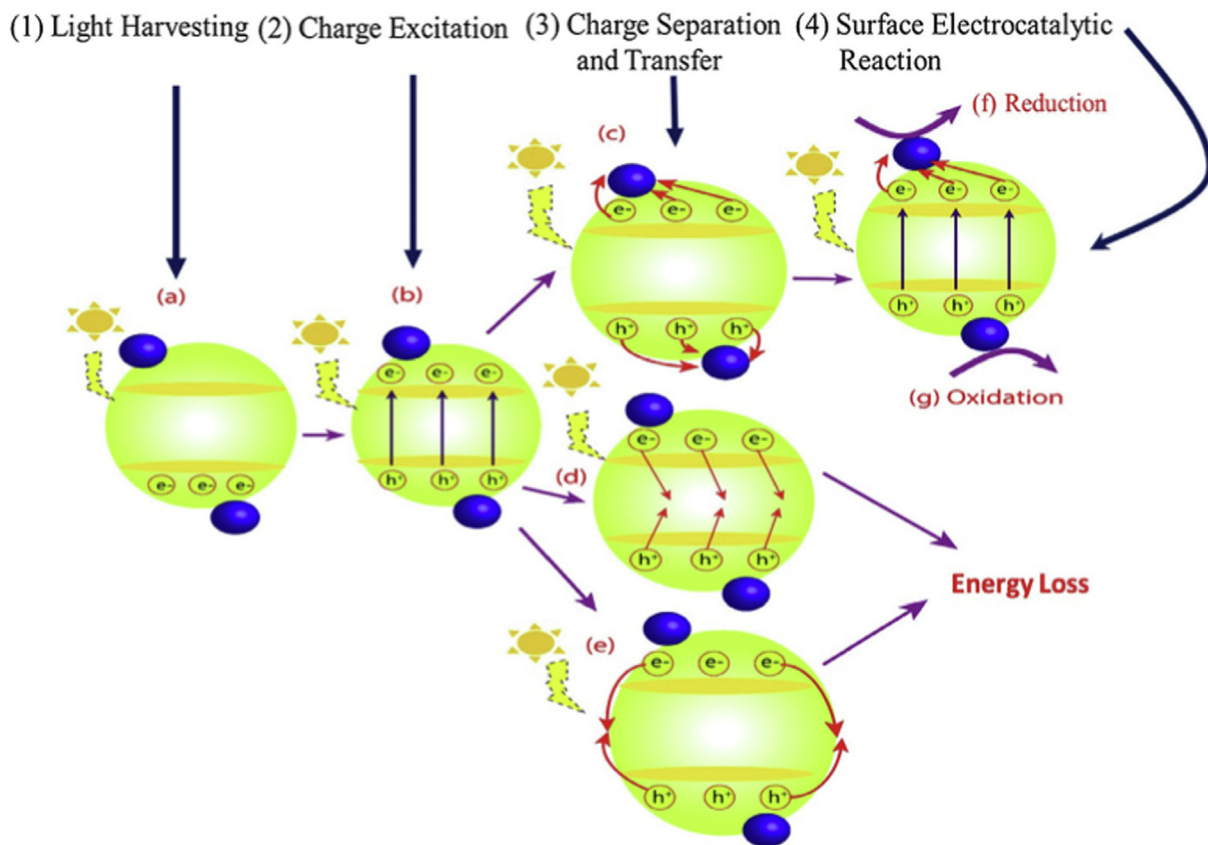


Fig. 4 Fundamental principles of photocatalysis depicting (a) Harvesting of light (b) Charge carrier excitation (c) separation of charges and transfer (d) recombination of charges (e) surface charge recombination, (f) surface reduction reactions, and (g) surface oxidation reactions. (). Adapted from Khan and Tahir, 2019

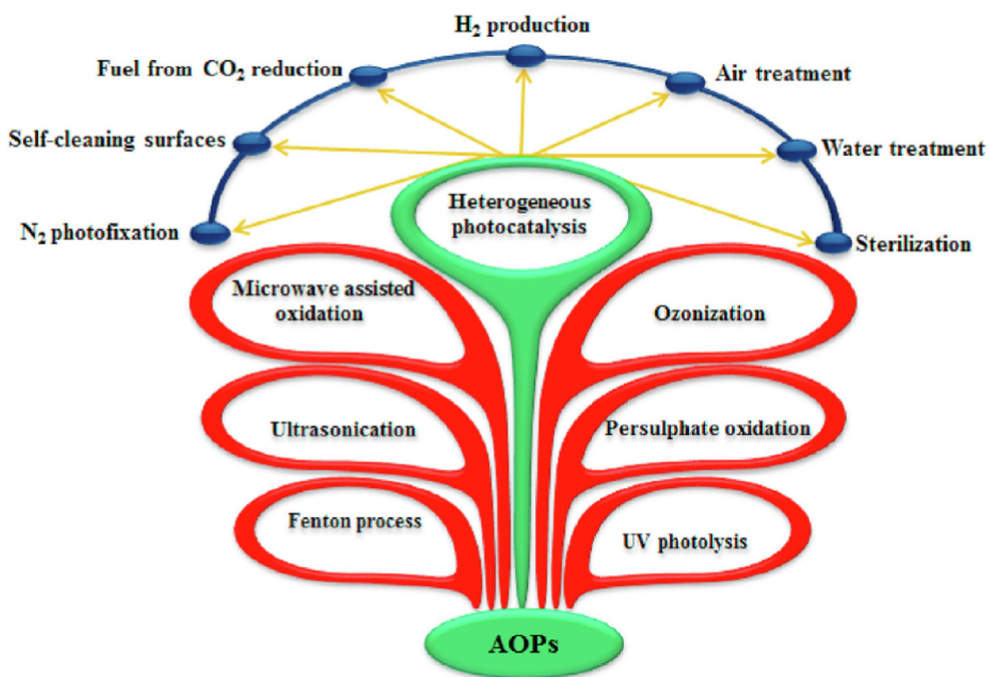


Fig. 5 A general representation of the advanced oxidation processes and the potential applications of semiconductor-mediated photocatalysis. (). Adapted from Li et al., 2019

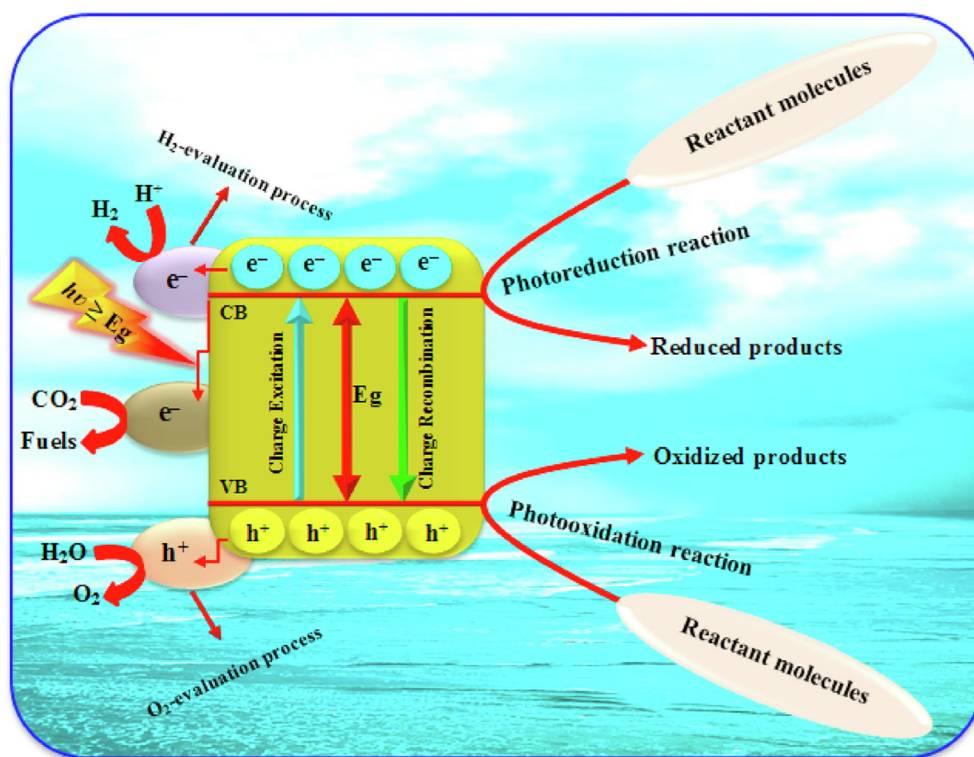


Fig. 6 A schematic diagram demonstrating semiconductor-mediated photocatalytic processes. (). Adapted from Asadzadeh-Khaneghah and Habibi-Yangjeh, 2020

cheap (Xu et al., 2022; Pattappan et al., 2022; Shang et al., 2022). Therefore, photocatalysts that are visible-light-induced can be considered appropriate materials for the utilization of the visible fraction of solar energy. Furthermore, an ideal photocatalyst should possess certain characteristics such as slow recombination of charges, appropriate bandgap potential, suitable bandgap, and high surface area (Wang et al., 2022; Xue et al., 2022; Ding et al., 2021). These are the fundamental reasons that made the designation and fabrication of visible-light-induced photocatalysts a hot area of research.

In summary, Graphitic carbon nitride ($g\text{-C}_3\text{N}_4$) has been largely employed in different photocatalytic applications (Li et al., 2022; Li et al., 2019). This is due to its great advantages like cheap precursors, high stability, and preparation methods that are easy. This is the reason why it is among the most favorable materials that can be applied as an important semiconductor in heterogeneous photocatalysis. Nevertheless, characteristics such as low specific surface area, fast recombination of charges, and inefficient absorption of visible light have hindered the extensive and practical deployment of $g\text{-C}_3\text{N}_4$ (Rajan and Neppolian, 2022; Wan et al., 2022; Shi et al., 2022; Guo et al., 2022; Zhang et al., 2022; Cheng et al., 2022). For that reason, the engineering of $g\text{-C}_3\text{N}_4$ has been performed by numerous research efforts to increase the migration of charges, improve the specific surface area, and boost its absorption efficiency. Fig. 7 presents a SWOT (Strengths, Weaknesses, Opportunities, and Threats) analysis of using graphitic carbon nitride as a photocatalytic material in terms of socioeconomic, technical, and environmental sustainability perspectives.

4. $g\text{-C}_3\text{N}_4$ preparation and structure-dependent performance

4.1. Design of $g\text{-C}_3\text{N}_4$ -based photocatalyst

The preparation of $g\text{-C}_3\text{N}_4$ can be simply carried out by the thermal condensation of several inexpensive nitrogen-rich precursors like melamine, cyanamide, dicyandiamide, urea, thiourea, or combinations thereof (Wang et al., 2022). The typical method for figuring out the phase of carbon nitrides is to employ X-ray powder diffraction (XRD) patterns. There are two distinct diffraction peaks in the $g\text{-C}_3\text{N}_4$ XRD patterns, located at approximately 27.4° and 13.0° (Cao et al., 2015). The former can be indexed for graphitic materials as the 002-peak indicative of interlayer stacking of aromatic systems, and the latter as the 100-peak corresponding to the interplanar separation. Measurements are made using X-ray photoelectron spectroscopy (XPS) to determine the status of nitrogen and carbon elements in $g\text{-C}_3\text{N}_4$. The molecular structure of the polymeric $g\text{-C}_3\text{N}_4$ derived from nitrogen-rich precursors enables the electronic structure to be adjusted by a modest modification of the molecular structure in the copolymerization process of the precursors, along with structure-matching organic additives.

There are several reports on bandgaps and unique surface areas of typical $g\text{-C}_3\text{N}_4$ samples made under various reaction conditions and precursors. These studies imply that an effective method for maximizing the unique surface area and electronic structure of $g\text{-C}_3\text{N}_4$ depends on the choice of various

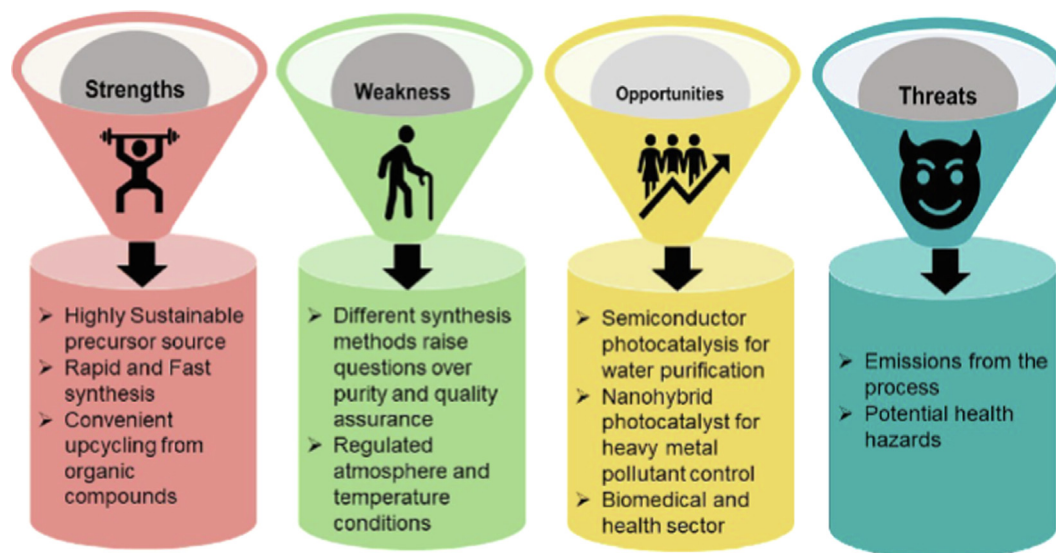


Fig. 7 Strengths, weaknesses, opportunities, and threats of using $g\text{-C}_3\text{N}_4$ as an efficient photocatalyst. (). Adapted from [Sharma et al., 2022](#)

precursors in conjunction with appropriate control over the reaction parameters, such as the time and temperature of the thermal treatment ([Vaya et al., 2022](#)). Urea is one of the several precursors that can be utilized to generate thin-layer $g\text{-C}_3\text{N}_4$ with a lot of specific surface area. However, a variety of precursors and experimental circumstances should be investigated, such as the recently described exfoliation procedures, to streamline the synthesis of $g\text{-C}_3\text{N}_4$ materials and enhance their properties.

4.2. Nanostructure design of $g\text{-C}_3\text{N}_4$

$g\text{-C}_3\text{N}_4$ is a polymer with a flexible structure which makes it suitable for forming various morphologies with the aid of various templates. Several common $g\text{-C}_3\text{N}_4$ nanostructures have been made, including 1D nanostructures, hollow spheres, and porous $g\text{-C}_3\text{N}_4$; a brief description of each of these structures is given below.

The unique optical, chemical, and electrical properties that may be obtained by adjusting the length, diameter, and aspect ratio of 1D nanostructured photocatalysts like nanorods, nanowires, nanobelts, and nanotubes are advantageous for enhancing their photocatalytic activity. By thermally condensing cyanamide in the presence of anodic aluminum oxide (AAO) template, [Li et al. \(Li et al., 2011\)](#) created condensed $g\text{-C}$ nanorods with an average diameter of 260 nm. The AAO template's confinement effect was essential for enhancing the crystallinity and orientation of the $g\text{-C}$ to increase charge-carrier mobility. Additionally, the resulting $g\text{-C}_3\text{N}_4$ nanorods had a more positive VB state, which is necessary for a greater oxidation power.

Hollow sphere photocatalysts are also appealing because they can generate more photoinduced charge carriers and can harvest more incident light through subsequent reflections inside the hollow structure ([Chen et al., 2022](#)). Due to the polymeric $g\text{-C}_3\text{N}_4$ layered structure, which is prone to collapsing during processing, it is difficult to manufacture hollow $g\text{-C}_3\text{N}_4$ spheres. However, several attempts to produce hollow

$g\text{-C}_3\text{N}_4$ spheres have been successful. Monodisperse silica nanoparticles were covered with thin mesoporous silica shells by [Sun et al. \(Sun et al., 2012\)](#). The preparation of $g\text{-C}_3\text{N}_4$ hollow nanospheres was subsequently carried out using these core-shell structures as hard templates. Recently, it was shown that the supramolecular chemistry of triazine molecules makes $g\text{-C}_3\text{N}_4$ hollow structures easier to manufacture. A precursor hydrogen-bonded supramolecular network, like the cyanuric acid-melamine complex, was created in this instance because of the molecular cooperative assembly of the triazine molecules ([Cao et al., 2015](#)). Depending on the solvent used, this complex can be synthesized in a variety of morphological forms. For instance, 3D macro assemblies, flower-like layered spherical aggregates, and an organized pancake-like structure have all been produced in dimethyl sulfoxide and ethanol, respectively.

Porous photocatalysts are incredibly exciting due to their porous structure, which can offer a significant surface area and a huge number of channels to support mass diffusion, charge migration, and separation ([Al-Ahmed, 2022](#)). Because they enable customization of the porosity structure of $g\text{-C}_3\text{N}_4$ by selecting different templates, soft and hard templating methods are frequently utilized. Mesoporous $g\text{-C}_3\text{N}_4$ has been produced successfully using a variety of precursors, including ammonium thiocyanate, cyanamide, urea, and thiourea in the presence of silica nanoparticles used as a hard template, the removal of which produced a 3D interconnected structure of $g\text{-C}_3\text{N}_4$ with a large surface area of up to $373\text{ m}^2\text{ g}^{-1}$. The pore size that was produced matched the dimensions of the silica nanoparticles utilized as the template.

These studies show that distinct $g\text{-C}_3\text{N}_4$ nanostructures can be created utilizing various templating or non-templating techniques. These nanostructures have several benefits and could make a great foundation for the creation of unique photocatalytic systems. Large surface areas are typically attained for $g\text{-C}_3\text{N}_4$ using porous materials, which might result in an abundance of reactive sites. Porous structures can act as efficient channels to enhance interactions between $g\text{-C}_3\text{N}_4$ and the tar-

get reactants in the meantime. Additionally, the requisite specific surface area and charge carrier mobility may both be present in 1D nanostructures of g-C₃N₄.

5. g-C₃N₄ as a promising photocatalyst

The C₃N₄ materials traced back to the time when Berzelius and Liebig produced and reported in 1834 a melon embryonic shape (Scopus - Document details - null | Signed in, (n.d.). <https://www.scopus.com/record/display.uri?id=2-s2.0-7995330>, 2022). This is introduced as the first synthetic polymer in the form of interconnected tri-s-triazine through secondary nitrogen which is a linear polymer. For over 150 years, research on this polymer stopped because of its inability to dissolve in most solvents and its chemical inertness.

Eventually, in the nineties, Liu and Cohen (Cohen, 1993) predicted a diamond-like structure from the fabrication of really hard carbon nitride. Subsequently, bulk hardness and great modulus values were achieved from β-C₃N₄ and then followed by the discovery of various allotropes of C₃N₄ that have several properties, for example, g-C₃N₄, α-C₃N₄, cubic C₃N₄, and pseudocubic C₃N₄. The most resistant among the stated carbon nitrides (C_xN_y) under surrounding conditions is g-C₃N₄ and this is because it has a graphene structured layer. The allotropes g-C₃N₄ have two fundamental tectonic units which are triazine C₃N₃ known as ‘melam’ and heptazine / tri-s-triazane C₆N₇ ‘melem’. At ambient conditions, the latter is the one with the most resistant phase.

The field of heterogeneous photocatalysis witnessed the first application of g-C₃N₄ about a decade ago. It was reported that Wang and his coworkers (Wang et al., 2009) have employed g-C₃N₄ as a conjugated stable to efficiently produce H₂ or O₂ from water splitting, as shown in Fig. 8. This was carried out upon visible light illumination because of its supreme optical features, high stability in basic/acidic systems, good physical–chemical stability, and environmentally friendly nature. In the next session, we discussed in more detail the excellent physicochemical characteristics of g-C₃N₄ which is a result of

the great number of publications on the Web of Science that guarantees the material’s popularity. The elemental composition of g-C₃N₄ as a semiconductor is carbon and nitrogen which are very abundant in the earth (Huang et al., 2022; Pham et al., 2022; Zhong et al., 2022; Che et al., 2022). Fabrication of this organic semiconductor is primarily done with nitrogen-organic precursors which include melamine, urea, cyanamide, dicyanamide, and thiourea among others. Even though, several publications have reported various methods to synthesize g-C₃N₄. The surface chemical features, electronic band structure, and morphology of the as-synthesized g-C₃N₄ are strikingly affected by the choice of precursor, reaction temperature, and reaction environment (Chen et al., 2022; Wu et al., 2022; Chu et al., 2022; Altan and Kalay, 2022; Tang et al., 2022; Zhong et al., 2022; Cheng et al., 2022). Many reviews have also thoroughly reported the comprehensive procedures for the preparation of g-C₃N₄ taking into consideration of the reaction condition and choice of precursor. A thermal polymerization process is a strategy employed on various precursors with nitrogen units (Fig. 9) to fully fabricate g-C₃N₄. It is described as a ‘bottom-up method’. The bottom-up method is the formation of fairly larger and more complex systems from the self-assembly of any smaller units (for example, atoms, molecules, and nanoparticles). This is achieved by the interactions between the building units utilizing hydrogen bonding, Van der Waals force, and/or electrostatic adsorption.

In short, the carbonization and pyrolysis of some organic precursors (containing in general –OH, –COOH, –NH₂, and –C = O) have made the bottom-up method an efficient process to prepare g-C₃N₄ on a large scale.

6. Limitations of g-C₃N₄ and remedy to the obstacles

In the past few years, g-C₃N₄ has been preferred over other semiconductors in different photocatalytic processes. This is due to its superior advantages such as abundance, nontoxicity, inexpensive, high thermal and photochemical stability, biocompatibility, and moderation of activity in visible light (due

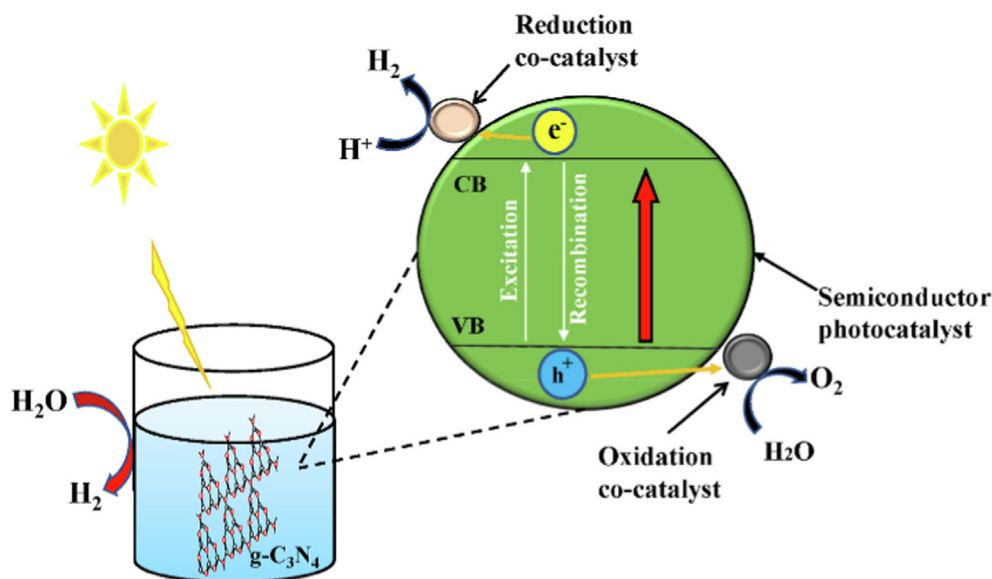


Fig. 8 A schematic representation of hydrogen production via water splitting. (). Adapted from Vaya et al., 2022

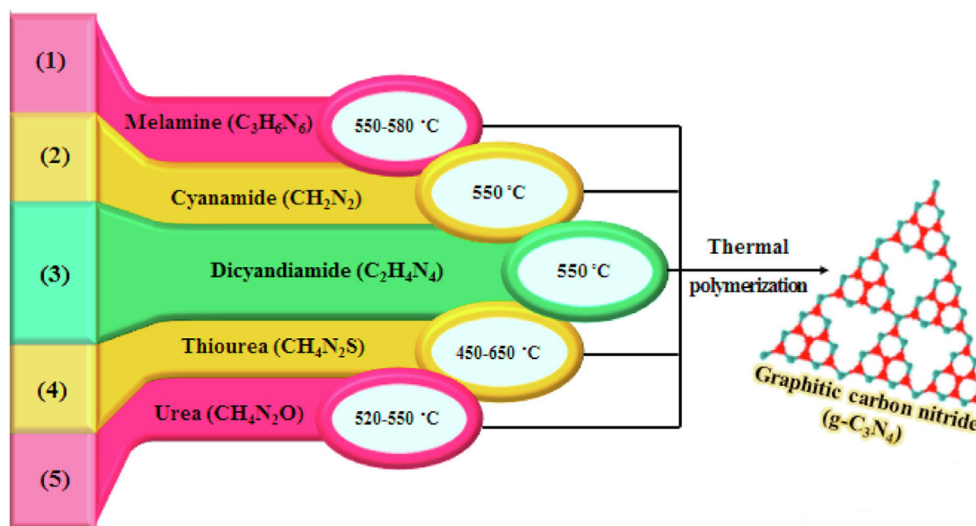


Fig. 9 The $g\text{-C}_3\text{N}_4$ synthesis route via thermal polymerization of different precursors. (). Adapted from Li et al., 2019

to low bandgap) (Mao et al., 2022; Li et al., 2022; Ye et al., 2022; Zhu et al., 2022; Liu et al., 2022). In addition, the CB of $g\text{-C}_3\text{N}_4$ is severely more negative than the potentials needed for the generation of H_2 and O_2 , CO_2 photoreduction processes, and other semiconductors (Swedha et al., 2022). Furthermore, the CB of $g\text{-C}_3\text{N}_4$ can reduce different compounds such as H_2O and O_2 since the photogenerated electrons have high thermodynamic energy. However, $g\text{-C}_3\text{N}_4$ has some intrinsic drawbacks which include electron-hole rapid recombination rate, low quantum yield, inefficient visible-light absorption (below 460 nm), low charge conductivity, negligible electrical mobility, and inefficient specific surface area (about $10\text{ m}^2\text{g}^{-1}$) that result in poor photocatalytic efficiency receiving visible light (Cao et al., 2022; Zeng et al., 2022). In the subsequent paragraphs, we, therefore, discussed the numerous modifications that have been suggested to reduce these problems and enhance the photocatalytic potential of $g\text{-C}_3\text{N}_4$ by utilizing several strategies.

The design of perfect-activity $g\text{-C}_3\text{N}_4$ has been established to largely depend on the surface area, plentiful reactive sites, morphology size, and predominantly extended light-harvesting capability (Wang et al., 2022; Xu et al., 2022; Gholipour et al., 2022; Gao et al., 2022). As it is known, $g\text{-C}_3\text{N}_4$ has the characteristics of a 2D polymer and also possesses a unique layered structure. The delocalized π -conjugated system in the $g\text{-C}_3\text{N}_4$ is made up of C and N with sp^2 hybridization. The rapid recombination of the charges is a result of the random movement of the charge carriers in the plane caused by the inherent graphite π -conjugated structure that leads to chemical sluggishness. To modify and construct $g\text{-C}_3\text{N}_4$ -based systems and defects engineering method is adopted among the various methods of surface modification. The defect generally occurs from the breakage and disturbance of the ideal periodic arrangement of the fundamental unit in $g\text{-C}_3\text{N}_4$ and that affects its photoactivity. Recombination of charges is prevented by broadening its visible-light absorption area as a result of surface defects engineered on $g\text{-C}_3\text{N}_4$ containing C and N defects. In general, the electronic structure and features of photocatalytic materials are affected by these defects. Several studies have been carried out to increase $g\text{-C}_3\text{N}_4$

visible-light activity through defects engineering. Usually, the defects could create molecules' reaction sites of the reactants and transform the features of photocatalysis. Recently, there have been several suggestions to improve the defect-induced photoactivity in $g\text{-C}_3\text{N}_4$. For instance, the N -defected $g\text{-C}_3\text{N}_x$ was constructed by Yu et al. (Yu et al., 2017) with an adjustable band structure that is controlled via surface cyano groups and N vacancies. The N -defective $g\text{-C}_3\text{N}_x$ harvests visible light more impressively than the pristine $g\text{-C}_3\text{N}_4$ due to its ability to separate photoexcited charges. Boosting the activity of $g\text{-C}_3\text{N}_4$ can also be carried out by another procedure and that is to morphologically and texturally fabricate the controlled $g\text{-C}_3\text{N}_4$. Consequently, structural engineering (such as size controlling, shapes, and dimensions) is a great approach to increasing the performance of $g\text{-C}_3\text{N}_4$. This in turn enlarges the surface area with different morphologies such as nanobelts, nanorods, nanowires tubes, porous/mesoporous microspheres, and nanosheets via several methods. The construction of nano-scale structures is interestingly governed by two-dimensional (2D) structures labeled as well-defined building blocks. Thus, $g\text{-C}_3\text{N}_4$ with various morphologies has leading photocatalytic capability when compared to a conventional bulk structure, because of its efficiency, and simplicity, and has more reactive parts as well as a higher specific surface area. Excellent photocatalytic proficiency and boosted optical characteristics can be achieved by open mesoporous morphology (Fig. 10) with tabular nanostructures to strikingly transmit photoinduced charges along the 2D route. This consist of fast electronic immigration and direct route. Based on numerous established literature, the second strategy to improve photocatalytic performance is the preparation of nanocomposites/heterojunction with various semiconductors that contain suitable band energies. This makes the procedure outstanding in impressively slowing down the electron-hole pairs recombination rate. The third strategy is to dope $g\text{-C}_3\text{N}_4$ with metal and non-metal elements. Recently, energy gap engineering of $g\text{-C}_3\text{N}_4$ via doping with different elements yielded excellent results that leads to tuning the redox band potentials, distinctly modulation of the light-receiving ability, as well as changing luminescent and electronic features of $g\text{-C}_3\text{N}_4$

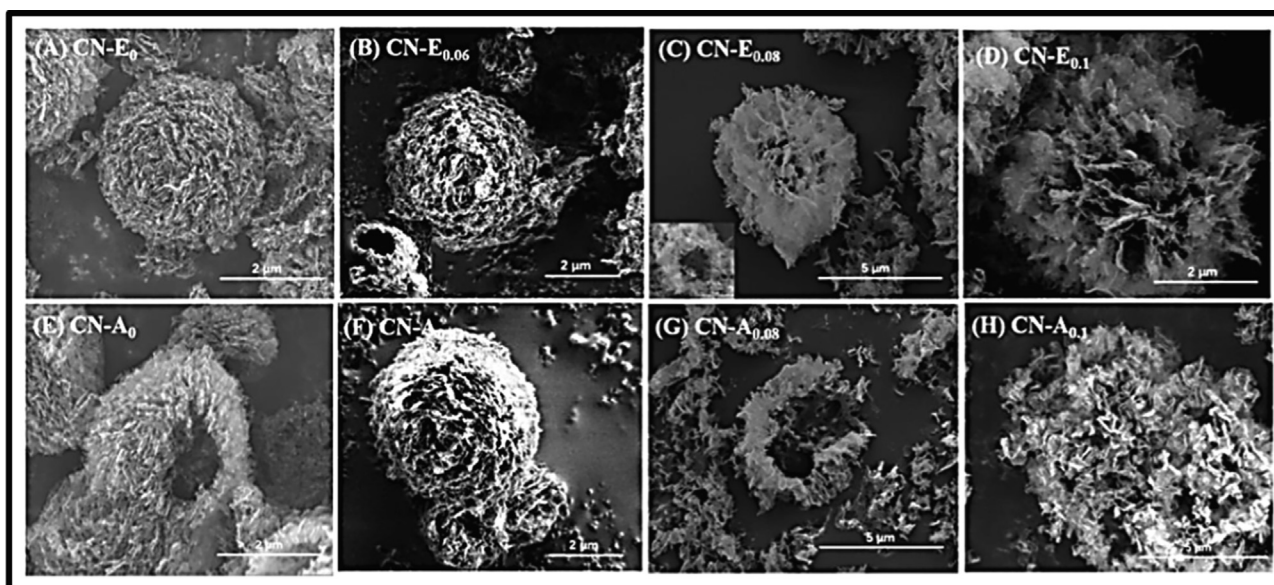


Fig. 10 SEM images of hollow mesoporous carbon nitride. (). Adapted from Al-Ahmed, 2022

C_3N_4 (Yu et al., 2022; Xia et al., 2022; Wang et al., 2022; Alejandra Quintana et al., 298 (2022)). Finally, the simplistic procedure adopted to enhance the photocatalytic performance of $g-C_3N_4$ is to couple it with carbon nanomaterials. Carbon materials that have unique properties such as excellent chemical stability, appropriate electrical conductivity, and large surface area are nowadays employed for various applications. Fabricating heterojunctions with various carbon-rich materials not only compensates for the drawbacks of single semiconductors by increasing visible light utilization, improving charge separation, and increasing photo durability, but also induces synergetic effects that lead to faster electron transition from the surface of a nanocomposite due to carbon's electron transport capability. The photocatalytic ability of the hybrids is successfully enhanced when the carbonaceous materials are coupled with $g-C_3N_4$. Carbon dots (CDs) among different types of carbonaceous materials (for example activated carbon, graphene, fullerene, and carbon nanotubes) have attracted substantial attention calling for the enhancement of their photocatalytic performance. This is because CDs have properties such as good physicochemical durability, water-solubility, nontoxicity, and ultrasound small dimension. In addition, CDs are excellent material when it comes to utilization with regards to application in photocatalysis because they have emissive traps and excellent electron reservoir/transfer. The former is because of the quantum size effect with conjugated π structure. Moreover, multi-photon activation brings about the famous feature of CDs which is known as the up-conversion photoluminescence (UCPL) feature. Considering the drawbacks highlighted for $g-C_3N_4$, the photoactivity of the system can be enhanced by employing CDs for bandgap engineering. Also, CDs give an avenue for excess orbitals for e^- by sp^2 that which slows down the recombination of charges. The utilization of metal-free CDs as a magnificent cocatalyst produces a fundamental basis for interface engineering $g-C_3N_4$ semiconductors for various applications.

Hence, given the substantial state of this review, we focused our study on the global survey of utilizing $g-C_3N_4$ /CDs-based

nanocomposite for energy production technology and treatment of photocatalytic pollutants. Around November 2019, the world witnessed almost 100 published research articles that explored the photocatalytic capability of $g-C_3N_4$ /CDs-based nanocomposite with enormous research interest and broad significance. The increase in popularity of $g-C_3N_4$ /CDs nanocomposite is confirmed by the rapid increase in relevant research papers that have been published in the field of $g-C_3N_4$ /CDs nanocomposite within the last 5 years. Gao et al. (Gao et al., 2015) presented for the first time in 2015; the use of the first principal calculation in the photocatalytic term to explore the interaction between the electronic and optical properties of $g-C_3N_4$ and CDs. They illustrated that through the process of water splitting, hybrid $g-C_3N_4$ /CDs favored the production of hydrogen gas. Consequently, the development of $g-C_3N_4$ /CDs-based materials and diverse synthesis techniques, as well as the application of these photocatalysts to the degradation of various pollutants and antibiotics, water splitting, CO_2 photocatalytic reduction, and other applications, has been significant.

7. Multiple strategies to improve the photocatalytic efficiency of $g-C_3N_4$

Here, the different strategies for improving the photocatalytic efficiency of $g-C_3N_4$ is discussed.

7.1. Metal doping

Essentially, the injection of metallic impurity creates more binding functions which provide the semiconducting material with enhanced photocatalytic activity by minimizing the bandgap and improving visible light absorption (Adegoke and Maxakato, 2022; Hoang et al., 2022; Lin et al., 2023). To incorporate metallic ions into the matrix of the material, the precursor of $g-C_3N_4$ is uniformly mixed with the corresponding soluble salt of the metal, thereby paving way for doping

the metallic impurity into the framework of g-C₃N₄ during the precursor's thermal condensation.

7.1.1. Transition metal

Transition metals such as Zr, W, Cu, Fe, and Pd have been widely used to tune the electronic and optical behavior of g-C₃N₄. Specifically, they prolong carrier lifetime, accelerate carrier mobility, reduce bandgap, and increased light absorption which is critical for enhanced photocatalytic performance. Elsewhere, Pan et al. (Pan et al., 2011) employed first-principles simulations to design novel g-C₃N₄-based nanotubes. Their investigations revealed that the optical and electronic properties of the compound can easily improve by functionalization using metallic elements such as palladium and platinum. These results indicate that metal-functionalization could enhance absorption in the visible region, narrow the bandgap and increase carrier mobility. Despite the remarkable potential of noble metals in enhancing the photocatalytic activity of g-C₃N₄, their practical applications are limited by their high price.

Several reports suggested that introducing a transition metal such as Zr, Mo, Zn, W, Cu, and Fe as a dopant into the matrix of g-C₃N₄ improves its photocatalytic efficiency (Le et al., 2016). For example, Tonda and his team (Tonda et al., 2014) used a simple, cost-effective synthesis technique to fabricate Fe-doped g-C₃N₄ nanosheets. They observed that the Fe-doped g-C₃N₄ nanosheets exhibited redshifts and the Fe-doping has tremendously increased the light absorption in the visible region and improved the photocatalytic activity. The developed Fe-species serve as photo-generated electrons as they were found to exist in a +3-oxidation state, also making them a potential hole-trapping site. The holes existing in the valence band can oxidize OH⁻ while O₂ can be reduced to O₂⁻ by the trapped electrons. Furthermore, Wang et al. (Wang et al., 2016) employed a simple pyrolysis technique using common precursors to fabricate molybdenum-doped g-C₃N₄. Their results suggested that Mo-doping narrows the bandgap, extends the visible light response, enlarges surface area, and reduces the rate of the photogenerated charge carriers. Hence, Mo-doped g-C₃N₄ demonstrated high performance in the reduction of CO₂. Similarly, Li et al. (Wang et al., 2016) used a facile pyrolysis method to introduce the rare earth element yttrium on g-C₃N₄ using urea as a precursor. They reported an enhanced degradation of Rhb.

7.1.2. Alkali metal

Apart from the transition metals, Alkali metals like sodium and potassium were also introduced into the framework of g-C₃N₄ to enhance their photocatalytic activity. Recently, Xiong and his colleagues employed density functional theory to investigate the role of the atoms (Na and K) in the increased photocatalytic performance of the doped g-C₃N₄ (Xiong et al., 2016). They observed that while both dopants narrow the bandgap of the material, however, they exhibit varying impacts on the photocatalytic performance and electronic structure of g-C₃N₄. They observed that while Na atoms were doped into the conjugated planes, K atoms existed in the interlayers of g-C₃N₄. Interestingly, K atoms can form a bond with the neighboring two layers thus they could bridge the layers and form the channel of charge delivery, hence facilitating charge transfer and reducing the chances of carrier recombina-

tion as depicted in Fig. 11. Moreover, Hu et al. (Hu et al., 2014) used potassium hydrate and dicyandiamide as precursors to prepare K-doped g-C₃N₄. They observed that the valence band and conduction band potentials of the material could be controlled by altering the concentration of the dopant. Therefore, both O₂ and OH could be generated, thus yielding a greater photodegradation rate. In a similar work by Zhang et al. (Zhang et al., 2014), where they fabricated Na-doped g-C₃N₄, using sodium hydrate and dicyandiamide as precursors, they observed that both VB and CB potentials could be controlled by changing the dopant's concentration. In general, as reported in the work of Hu et al. (Hu et al., 2014), although both Na and K are suitable for photocatalytic performance enhancement of g-C₃N₄, the degradation rate is higher with K-doped compound, thus making it more suitable for photocatalytic activity improvement.

In summary, metals have been extensively used as dopants on g-C₃N₄ for photocatalytic applications. Mostly, their incorporation can suppress the charge carrier recombination rate, extend the visible light response, and create a new energy level in the bandgap of the parent compound. Despite the successful experimentations of metal doping on g-C₃N₄, there exist a few drawbacks halting the practical applications of the developed material such as poor thermal stability. Also, their newly created energy levels within the bandgap might serve recombination centers, thus resulting in low quantum efficiency.

7.2. Non-metal doping

The doping of non-metallic species on g-C₃N₄ has also attracted widespread attention in the photocatalysis community. Several non-metals such as halogens, boron, oxygen, nitrogen, carbon, sulfur, and phosphorus have been reported as dopants on g-C₃N₄ material (Lin et al., 2023; Alcantara et al., 2022; Wang et al., 2022). Apart from conserving the metal-free characteristic, non-metals often possess higher electronegativity and ionization energies. They easily form covalent bonds with other materials by gaining electrons. Furthermore, non-metal doping can serve to reduce the impact of thermal variation of chemical states.

7.2.1. Phosphorus doping

The first phosphorus-doped g-C₃N₄ was fabricated by Zhang and his team (Zhang et al., 2010) using a simple polycondensation of a mixture containing phosphorus-containing ionic liquid and dicyandiamide as the g-C₃N₄ precursor. The PF₆ reacts with the amine group with increasing temperature resulting in joining the C N matrix. NMR, XPS, and FTIR investigations demonstrated that the P heteratoms substitute the bay or corner C in the framework to create a P—N bond in the C₃N₄ structure. Their findings revealed that doping with a controlled amount of phosphorus heteratoms could significantly increase the electrical conductivity, lower the optical bandgap and change the electronic structure of g-C₃N₄. They concluded that P-doped g-C₃N₄ possesses a remarkable potential for photovoltaic applications. On the other hand, Zhang et al. (Zhang et al., 2013) used the same precursors to prepare P-doped g-C₃N₄. They observed a significant enhancement of the photocatalytic activity with MO and RhB as pollutants. The phosphorus source influences the P doping site and this may affect the photocatalytic behavior of the developed mate-

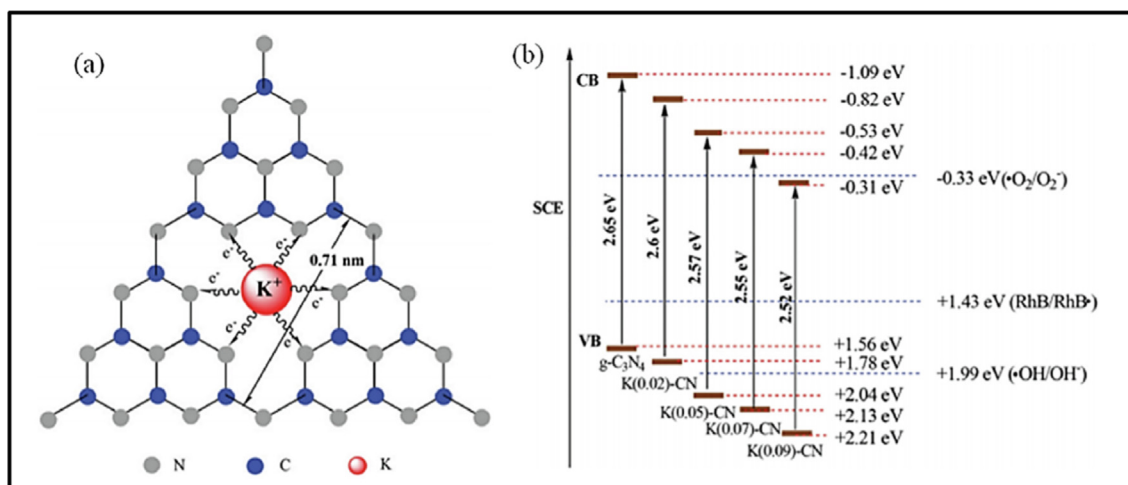


Fig. 11 (a) Possible doping sites for potassium ions in K-doped g-C₃N₄ (b) Band gap structures of as-prepared g-C₃N₄ and K-doped g-C₃N₄. (). Adapted from [Asadzadeh-Khaneghah and Habibi-Yangjeh, 2020](#)

rial. Consequently, different phosphorus sources such as phosphorous acid, ammonium hexafluorophosphate, hexachlorocyclotriphosphazene (HCCP), (hydroxy ethylidene) diphosphonic acid, 2-aminoethylphosphonic acid, diammonium hydrogen phosphate, etc. have been employed to prepare P-doped g-C₃N₄.

Zhou and his team ([Zhou et al., 2015](#)) used a thermal polymerization route to fabricate phosphorus-doped g-C₃N₄ using guanidinium hydrochloride as a precursor and HCCP as a phosphorus source. Their results revealed that phosphorus atoms preferentially occupy the bay-carbon and corner carbon sites, and their incorporation into the lattice of g-C₃N₄ becomes seamless, thereby modulating the electronic structure and consequently reducing the rate of recombination of charge carriers. Finally, they recorded an excellent increase in the photocatalytic activity both in RhB degradation and generation of H₂. Elsewhere, Hu et al. ([Hu et al., 2014](#)) utilized diammonium hydrogen phosphate as the P-source and dicyandiamide as the precursor to synthesize g-C₃N₄. They observed that phosphorus incorporation improves the separation efficiency of charge carriers, narrows the bandgap, and inhibits the crystal growth of g-C₃N₄. Their work also suggested that P atoms were interstitially doped into the lattice of g-C₃N₄ to create the P—N bond. This contradicts the work of Zhou et al. ([Zhou et al., 2015](#)) which states that phosphorus atoms would preferentially occupy substitutional bay-carbon and corner carbon sites. In summary, it can be inferred that the phosphorus precursor used can strongly influence the P-doping site either substitutional or interstitial.

On the other hand, nanostructured materials with certain morphology have been used as active ingredients to provide active sites for photocatalytic activity and accelerate mass transfer ([Wang et al., 2022](#); [Ou et al., 2022](#)). They also facilitate the mobility of the photogenerated carriers and help in their separation. Recently several forms of nanostructured g-C₃N₄ with improved photocatalytic performance such as nanofibers, nanorods, mesostructures, nanotubes, and nanosheets have been employed. Moreover, some researchers combined the structural engineering of g-C₃N₄ with phospho-

rus doping to achieve higher degradation efficiency. For example, Zhu et al. ([Zhu et al., 2015](#)) used the co-condensation of melamine to prepare g-C₃N₄ nanoflowers. They noted that phosphorus atoms could bond chemically with neighboring carbon and nitrogen and exhibit planar coordination in the C₃N₄ structure. The designed flower-shaped morphology together with phosphorus inclusion yielded higher charge separation and transfer, and superior trapping of light for enhanced hydrogen production under the visible region. The specific surface area was also found to increase due to increased mass transfer of molecules as well as high porosity.

For an insightful understanding of the phosphorus doping on the photocatalytic performance and the bandgap, Qiao and his team ([Ran et al., 2015](#)) used a combination of thermal exfoliation and p-doping to prepare porous p-doped g-C₃N₄ nanosheet using 2-aminoethylphosphonic acid as the P-source. X-ray photoelectron spectroscopy investigations revealed that phosphorus preferential substituted carbon to create a P—N bond in the g-C₃N₄ framework. Although past reports indicated a preference for the exfoliated g-C₃N₄ over the bulk one, there remains the challenge of a large bandgap in the thermally exfoliated nanosheets, which impedes its full utilization of the wide solar spectrum. However, with the presence of strong tail absorption, the bandgap of P-doped g-C₃N₄ can be decreased, and this leads to the creation of midgap states within the bandgap.

7.2.2. Sulfur doping

The electronic structure of g-C₃N₄ has also been modified by doping Sulfur atoms to improve carrier mobility, redox potential, light absorbance, and ultimately, photocatalytic activity ([He et al., 2014](#); [Wang et al., 2015](#); [Lu et al., 2017](#)). Liu and his colleagues ([Liu et al., 2010](#)) first fabricated sulfur-doped g-C₃N₄ by heating the powdered g-C₃N₄ in a gaseous H₂S atmosphere. The S-doped system demonstrated an elevation in the conduction band minimum in combination with an increase in the valence band width and a slight decrease in absorbance. The concomitant quantum confinement effect plus the homogeneous substitution of Sulfur for Nitrogen led

to the evolution of a unique electronic structure which made the S-doped system promising for the photooxidation of phenol and photoreduction of hydrogen evolution.

In a study by Feng and coworkers (Feng et al., 2014), thermal condensation was utilized to synthesize microrods of S-doped g-C₃N₄. Their investigations revealed that the S-doped system exhibited improved visible light absorption, satisfactory stability, and a larger surface area. They also observed an activity more than 9 times higher than the pristine system for H₂ production. Similarly, Fan and his team (Fan et al., 2016) fabricated porous rods of S-doped g-C₃N₄. They also observed faster degradation of RhB under visible radiation. The synergistic roles of S-doping and the creation of unique structures led to an S-doped g-C₃N₄ system with narrower bandgaps, a broader light absorption range, and larger surface areas than the pristine system, thus yielding enhanced photoreactivity.

The photocatalytic efficiency of the S-doped g-C₃N₄ system was found to improve with both the in situ and ex situ sulfur doping with a small percentage of the dopant (less than 1.0 wt%). The use of thiourea (TU) as an efficient precursor for the construction of an S-doped g-C₃N₄ system has recently been reported (Hong et al., 2012; Cao et al., 2015). Hong and his colleagues (Hong et al., 2012) first fabricated in situ S-doped g-C₃N₄ systems using a unit of TU. X-ray photoelectron spectroscopy analysis revealed the possibility of the dopant to substitute C with a likely downshift of 0.25 eV in the CB. Remarkably, the prepared S-doped g-C₃N₄ system performed 30 times more than the pristine system for H₂ production. The excellent photo reactivity was attributed to extended and stronger light absorbance by S-doping and increased charge and mass transfer in the mesoporous system.

Some research works proposed sulfur doping to replace the lattice nitrogen atoms instead of the carbon atoms in the g-C₃N₄ framework to form an S—C bond. Considering the similarity of the electronegativities of nitrogen and sulfur, the substitution seems to be favorable. This notion has been substantiated by first-principles density functional theory calculations in the work of Ma et al (Ma et al., 2012). The DFT works demonstrated the presence of impurity states as a consequence of sulfur doping. However, the bandgap was not significantly affected. Therefore, this makes it easy for the photogenerated electrons to jump from the valence band to the impurity states and then to the conduction band. In summary, both theoretical and experimental works revealed that sulfur incorporation into the framework of g-C₃N₄ modified the electronic properties of the materials leading to enhanced carrier mobility, efficient charge separation, and narrowed bandgap.

7.2.3. Oxygen doping

Li and coworkers first fabricated O-doped g-C₃N₄ via a simple H₂O₂ hydrothermal route (Li et al., 2012). X-ray photoelectron spectroscopy studies revealed that O was transmitted directly into the lattice forming N—C—O, thus indicating that oxygen atoms bonded with Sp² hybridized C. Interestingly, while the oxygen doping does not alter the valence band maximum, the conduction band minimum exhibited a downshift by 0.21 eV. Hence, the oxygen-doping on g-C₃N₄ could trigger band and electronic structure modifications, which in turn lead

to improved separation efficiency of the photogenerated carriers, extended visible light response, and improved surface area.

Elsewhere, Huang et al. (Huang et al., 2015) fabricated oxygen-doped g-C₃N₄ with a porous network (MCN). XPS investigations revealed a new peak at 531.4 binding energy which has been attributed to the presence of N—C—O and C—O species within the lattice. First principles simulations showed that the bandgap reduced slightly due to oxygen incorporation, in line with the absorption band edge redshift. Similarly, differential charge density calculations showed a dramatic reduction in the electron density at the surrounding carbon atoms of oxygen dopant as well as a remarkable increase at the surrounding nitrogen atoms. Hence, based on DFT and experimental observations, they reported that oxygen-doping preferentially takes place on 2-coordinated nitrogen positions, and together with a porous network, oxygen-doping promotes charge separation and extended light trapping.

In another study, She and coworkers employed a facile calcination process to prepare two-dimensional porous ultra-thin nanosheets of oxygen-doped g-C₃N₄ (She et al., 2016). They simultaneously modulated the morphology, band positions of the bulk material, and intrinsic electronic structure. The synthesized ultra-thin O-doped g-C₃N₄ system demonstrated 5.2 times photocatalytic activity for hydrogen evolution and 71 times higher for MO degradation than that of the bulk system. The photocatalytic performance enhancement is attributed to the synergistic effects of increased bandgaps, the introduction of the electrophilic groups, and the 2D porous ultra-thin framework. Guo et al. (Guo et al., 2016) employed a photo-Fenton reaction to design holey-structured g-C₃N₄ sheets with O-doping. The prepared oxygen-doped holey nanosheet structure yielded efficient photocatalytic performance for RhB degradation and H₂ generation under visible light irradiation due to increased surface area and reduced bandgap. Fig. 12 represents the fabrication route of the 3D holey g-C₃N₄ using the mixture of dicyandiamide and water heat-treated to get the melamine-cyanaurate complex.

7.2.4. Carbon, nitrogen, or boron doping

Through the density functional theory investigations g-C₃N₄ system, Dong and coworkers (Dong et al., 2012) observed that the substitution of bridging nitrogen atoms with carbon atoms leads to the creation of delocalized π -bonds among the substituted C atoms and the hexatomic ring, thereby enhancing the electrical conductivity of the material. Moreover, the bandgap of the material would be reduced by the carbon self-doping thereby enhancing light absorption in the visible spectrum. In agreement with the theoretical findings, the fabricated C-doped g-C₃N₄ exhibited improved absorption in the visible region and demonstrated higher surface area and electrical conductivity, thereby improving the photocatalytic activity. In a similar study by Zhao and colleagues (Zhao et al., 2015), C self-doped g-C₃N₄ material was prepared for the purification of NO in air. Their study revealed that the developed photocatalyst showed enhanced carrier separation, extended light absorption, and more surface area. Zhang and his team (Zhang et al., 2015) used glucose and melamine as precursors to prepare nanosheets of C-doped g-C₃N₄ using a facile hydrothermal approach. The introduction of C into

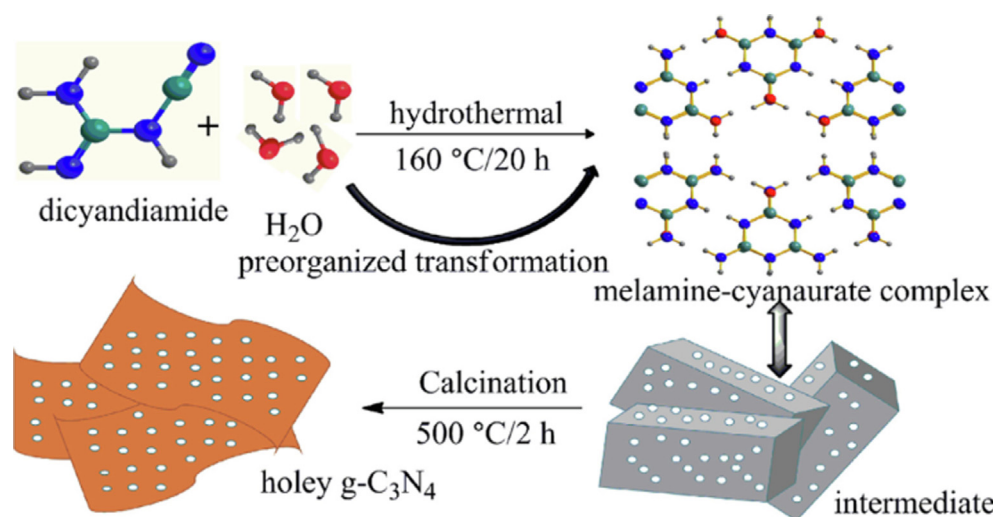


Fig. 12 Representation of synthesis of 3D holey $g\text{-C}_3\text{N}_4$ nanosheets. (). Adapted from Liu et al., 2018

the CN framework led to improved absorption of light due to reduced bandgap, and also enhance the electrical conductivity because electron transfer was favored by the delocalized big π -bonds.

Elsewhere (Fang et al., 2015), nitrogen self-doped $g\text{-C}_3\text{N}_4$ was fabricated from melamine and hydrazine via the thermal condensation route. X-ray photoelectron spectroscopy investigations demonstrated that nitrogen substituted the sp^2 carbon atom. The UV-vis spectroscopic studies revealed that nitrogen doping decreases the bandgap of the material and weakens the red-shift of the light adsorption band edge of the photocatalyst. The EPR results confirmed that nitrogen self-doping has successfully modified the electronic structure of $g\text{-C}_3\text{N}_4$. Interestingly, nitrogen incorporation significantly improves charge carrier mobility and promoted the separation of photogenerated electrons and holes. Consequently, nitrogen-doped $g\text{-C}_3\text{N}_4$ demonstrated more capacity in photocatalytic hydrogen production under visible light than pure $g\text{-C}_3\text{N}_4$ material.

Yan et al. (Yan et al., 2010) prepared the first boron-doped $g\text{-C}_3\text{N}_4$ by heat-treating the mixture of boron oxide and melamine. Typically, they heat-treated the precursors in a furnace to 500 °C temperature for 2 h and further heated the mixture at increased temperature for another 2 h. The pristine $g\text{-C}_3\text{N}_4$ powder was synthesized using simple pyrolysis. Several other starting materials were used to synthesize B-doped $g\text{-C}_3\text{N}_4$ for effective B incorporation. For example, an enhancement in CO_2 reduction was achieved by Sagara and coworkers (Sagara et al., 2016) when they used BH_3NH_3 as the boron source. Lu and coworkers (Lu et al., 2016) employed copolycondensation H_3BO_3 and thiourea to fabricate boron-doped $g\text{-C}_3\text{N}_4$ photocatalytic material. They observed a significant enhancement in visible light absorption and a simultaneous reduction in the bandgap. Therefore, carbon, nitrogen, and boron are essential elements that can be used to improve the photocatalytic performance of graphitic carbon nitride-based compounds.

7.2.5. Halogen doping

The photocatalytic performance of $g\text{-C}_3\text{N}_4$ was enhanced by incorporating several halogen species as dopants. For example, Wang and colleagues (Wang et al., 2010), fabricated

fluorine-doped $g\text{-C}_3\text{N}_4$ using ammonium fluoride as the fluorine source. Owing to the difference in electronegativity of fluorine and nitrogen, the incorporated F binds easily with C instead of N thereby causing C-sp^2 to sp^3 . They observed a decrease in the energy gap from 2.69 to 2.63 eV. On the other hand, first principles investigations revealed that the introduction of fluorine at the bay C site shifts both the conduction band and valence band to upper energy levels. The fluorine-doped $g\text{-C}_3\text{N}_4$ photocatalyst exhibit 2.7 times more performance than the pristine material for hydrogen evolution application.

In another work, Zhang and his team (Zhang et al., 2014) used ammonium iodide and dicyandiamide to fabricate iodine-doped $g\text{-C}_3\text{N}_4$ via the co-condensation route. Their results indicated that iodine incorporation enhances the separation of photogenerated electrons and holes, increased optical absorption, broadens the surface area, and consequently stimulated hydrogen evolution. First principles investigations revealed that iodine preferentially substitutes the sp^2 -bonded nitrogen in the C-N framework. The π -conjugated system was extended by the interaction between carbon nitride and iodine, this could be helpful for the transfer of generated charge electrons and holes. In another fascinating work by Han and colleagues (Han et al., 2015), a simple ball milling of bulk $g\text{-C}_3\text{N}_4$ catalyst with iodine yields nanosheets of I-doped $g\text{-C}_3\text{N}_4$. They observed an upshift of both the conduction band minimum and valence band maximum depicting a reduction in bandgap and alignment of energy levels. The I-modified $g\text{-C}_3\text{N}_4$ demonstrated a significant increase in photocatalytic H_2 evolution under visible light due to the enhanced charge separation, increased light absorption, enlarged specific surface area, and better-aligned energy levels.

Elsewhere, Lan et al. (Lan et al., 2016) prepared a bromine-doped $g\text{-C}_3\text{N}_4$ photocatalyst using ammonium bromine and urea as precursors via a co-condensation route. Their work showed that bromine incorporation into the framework of $g\text{-C}_3\text{N}_4$ has indeed modulated the carrier separation efficiency, electron conductivity, optical absorption, and texture. They also achieved high stability under visible light and recorded twice the H_2 production rate with the optimal sample compared to the unmodified catalyst.

7.3. Codoping

The method of cooping combines the advantages of individual dopants to yield a better photocatalyst. The technique has recently generated widespread interest among researchers working on the $g\text{-C}_3\text{N}_4$ photocatalyst because of the positive impacts it showed on the optical and structural properties. For example, Hu and coworkers (Hu et al., 2014) conducted a metal/non-metal doping on $g\text{-C}_3\text{N}_4$ material using diammonium hydrogen phosphate, ferric nitrate, and dicyandiamide as precursors to yield phosphorus and iron co-doped $g\text{-C}_3\text{N}_4$. It was observed that iron atoms coordinated with the nitrogen atoms at the interstitial sites of the N pots of the material. Meanwhile, P atoms formed a P—N bond at the interstitial position of the $g\text{-C}_3\text{N}_4$. The enhanced photocatalytic performance was ascribed to the combined effects of P and Fe doping which halted the crystal growth of $g\text{-C}_3\text{N}_4$, improved carrier separation, narrowed the bandgap, and enhance the surface area of the photocatalyst.

Furthermore, Zeng and coworkers (Zhang et al., 2014) prepared a $g\text{-C}_3\text{N}_4$ co-doped with Fe and C to reduce the bandgap and extend visible light absorption with a more positive valence band. Their results showed that the developed photocatalyst displayed improved photocatalytic activity under visible light irradiation for the degradation of RhB compared with the pristine and single-specie-doped $g\text{-C}_3\text{N}_4$. The significant improvement could be ascribed to an increase in electrical conductivity and a more positive valence band, increased surface area and charge separation, and reduction in bandgap which ultimately facilitated visible light absorption.

Apart from the metal/non-metal co-dopants, some works also reported non-metal/non-metal co-dopants as a substitute. For instance, Ma and colleagues (Ma et al., 2015) fabricated oxygen and phosphorus co-doped $g\text{-C}_3\text{N}_4$ for improved photocatalytic performance under anoxic conditions. Their performance enhancement was also attributed to features similar to the work of Zeng et al. (Zhang et al., 2014). In another paper by Wang and Lin (Lin and Wang, 2014), boron/fluorine codoped $g\text{-C}_3\text{N}_4$ was prepared by polymerizing urea with an ionic liquid. XPS analysis showed that both F and B heteroatoms have been incorporated into the material's matrix by the formation of B-F and B-N bonds. They attributed the enhanced hydrogen production rate to higher electron-hole separation and enhanced optical harvesting.

Recently, some works reported the doping of $g\text{-C}_3\text{N}_4$ with three different heteroatoms. For example, Ma and coworkers (Ma et al., 2015) developed a novel S-Co-O tri-doped $g\text{-C}_3\text{N}_4$ through a hydrothermal approach in the absence of H_2O_2 . They first synthesized S and Co codoped $g\text{-C}_3\text{N}_4$ by annealing the mixture of $\text{Co}(\text{NO}_3)_2 \cdot 6\text{H}_2\text{O}$ and thiourea and then conducted hydrothermal treatment to acquire S-Co-O tri-doped photocatalyst. They observed a modification of the bandgap, separation efficiency of charge carriers, and the surface area of the photocatalyst.

Noteworthy, apart from improving the adsorption ability of $g\text{-C}_3\text{N}_4$, oxygen doping creates photogenerated holes for the degradation of RhB by capturing the generated electrons. In summary, while cooping and tridoping improve the photocatalytic activity of the developed catalyst, it is remarkable to note that excessive doping of these materials on the $g\text{-C}_3\text{N}_4$

may degrade the photocatalytic performance due to the creation of more defects for charge carrier recombination.

7.4. Heterojunction based on doped $g\text{-C}_3\text{N}_4$

In general, elemental doping of $g\text{-C}_3\text{N}_4$ has been considered a remarkable way to enhance its photocatalytic activity by modifying its surface area and modulating its electronic properties (Koutsouroubi et al., 2022; Chen et al., 2022; Mo et al., 2022; Xu et al., 2022; Ma et al., 2022; Saeed et al., 2022; Choudhury et al., 2022; Che et al., 2022; Verma et al., 2022). The heterojunction development has always been adopted to facilitate the separation of charge carriers to prevent carrier recombination. The simultaneous effect of employing doping and heterojunction engineering is expected to yield excellent photocatalytic performance by reducing the bandgap, improving carrier separation, and widening the surface area for effective visible light harvesting.

Many research works have reported on the heterojunction engineering of $g\text{-C}_3\text{N}_4$ (Kong et al., 2022; Altan et al., 2022; Ma et al., 2022). Wide bandgap inorganic semiconducting oxides have been useful in the heterojunction engineering of $g\text{-C}_3\text{N}_4$ catalysts based on their band energy levels. They would promote the separation of photogenerated electrons and holes. Titanium dioxide is one of the deeply studied photocatalysts owing to its low-cost, chemical stability, and suitable conduction and valence band positions for redox reactions. However, its employability is halted by its relatively large bandgap that does not utilize the visible portion of the light. Bu et al. (Bu and Chen, 2014) synthesized nanostructured-oxygen-doped $\text{C}_3\text{N}_4@ \text{TiO}_2$ composites. They found that a significant reduction in carrier recombination can be achieved due to the formation of interfacial chemical bonds between TiO_2 and $\text{O-C}_3\text{N}_4$ which serves as a medium for the transfer of photogenerated electrons.

Elsewhere, Raziq and colleagues (Raziq et al., 2016) fabricated nanosheets of B-doped $g\text{-C}_3\text{N}_4$ and its composite with nanostructured TiO_2 . The resulting nanocomposite exhibited superior photocatalytic performance compared to the pristine and B-doped $g\text{-C}_3\text{N}_4$. They ascribed this to the improved separation of electrons and holes following B incorporation and subsequent TiO_2 coupling. The boron-induced states close to the top of the valence band trapped holes, and they created heterojunctions to channel electrons from boron to CN to TiO_2 . Al_2O_3 is yet another semiconducting material that has been used as catalyst support owing to its broad bandgap, good thermal stability, high specific surface area, and chemical stability. Wang and his team (Wang et al., 2016) combined H_2O_2 -treated $g\text{-C}_3\text{N}_4$ ($\text{O-g-C}_3\text{N}_4$) using the hydrothermal technique. Their investigations revealed that the defects sites in Al_2O_3 led to a dramatic enhancement in charge separation which consequently increased the photocatalytic performance for water splitting. In addition, Luo and colleagues (Luo et al., 2015) developed $\text{CeO}_2/\text{P-C}_3\text{N}_4$ photocatalyst by incorporating phosphorus and then coupling it with cerium dioxide. Their study found that the developed catalyst performed 7.9 times higher than pristine $g\text{-C}_3\text{N}_4$ and 12.2 times higher than pure cerium dioxide. They ascribed the improvement to the extended absorption of light from the visible range and increased separation efficiency of the photogenerated electrons and holes.

Li and coworkers (Li et al., 2016) fabricated DyVO₄/g-C₃N₄I composite semiconducting material using a facile hating process. They utilized the advantage of the narrow bandgap of DyVO₄ (2.3 eV) and the fact that it exhibits strong absorption in the visible region. The evolution of hydrogen was 1.7, 4.7, and 10.6 times higher than that of g-C₃N₄I, g-C₃N₄, and DyVO₄ respectively. The notable photocatalytic activity enhancement was attributed to enhanced separation efficiency, improved visible light absorption, reduced bandgap, and increased specific surface area.

Apart from wide bandgap semiconductors, several semiconducting materials have been utilized to modify g-C₃N₄ for improved photocatalytic activity. These materials include zinc phthalocyanine (Liang et al., 2016); Zn_{0.8}Cd_{0.2}S (Tian et al., 2016); BiPO₄ (Yuan et al., 2014), BiVO₄ (Kong et al., 2016), ZnIn₂S₄ (Chen et al., 2016), and many others.

7.5. Carbon dots modified g-C₃N₄

Firstly, we introduced the various functions carbon dots (CDs) can adhere to on g-C₃N₄ surface in the field of photocatalysis applications which contain spectra converter, electron acceptor and mediator, and photosensitizer. Fast generation of charge carriers is one of the key subjects in photocatalysis after the absorption of suitable photons over photocatalysts. For this reason, overpowering the recombination of these charges is among the significant parameters to enhance photocatalytic capability. An increase in photocatalytic ability in g-C₃N₄/CDs-based nanocomposite is achieved using CDs to slow down the recombination of electron-hole pairs. Therefore, the applications of CDs as spectral converters are on the principle of their extraordinary feature of multi-photon irradiation. The UCPL is a feature that the applied excitation wavelength is greater than the PL emission wavelength. That is to say, the lights with high wavelengths can be transformed into lights with low wavelengths to generate charge carriers, increase photocatalytic ability, and enable the utilization of CDs for various purposes. Moreover, the CDs can serve as an electron mediator when the arrangement of electrons between the semiconductors is a Z-scheme photocatalytic system or a type-II heterojunction. CDs function as suitable electron conduction mediation in such mechanisms to impressively enhance the photocatalytic ability and this is due to their best electron acceptor/donor feature.

As a result of the foregoing, g-C₃N₄/CDs-based nanocomposites can contribute significantly to photocatalytic activities in a variety of applications. Linked CDs with g-C₃N₄ play a key role in the degradation of different pollutants, generation of H₂, and reduction of CO₂, as will be explored in greater depth in the following sections.

7.6. Degradation of contaminant by g-C₃N₄/CDs-based photocatalysts

Rapid population increase and major industrialization have resulted in the introduction of hazardous, toxic, and limitless contaminants into the environment that not only exacerbates environmental issues but poses a risk to human life and health (Singh et al., 2022; Guo et al., 2022; Ni et al., 2022; Praus, 2022). Therefore, photocatalytic degradation of contaminants is globally recognized as a popular research topic for environ-

mental preservation and societal sustainable growth. In this respect, the use of g-C₃N₄/CDs-based nanocomposites used as novel hybrid photocatalysis has in recent times attracted a lot of attention because of their potential for removing a wide range of contaminants (Li et al., 2018; Xiang et al., 2020). Considering this, Zhang et al. (Zhang et al., 2016) fabricated a binary g-C₃N₄/CDs-based nanocomposites using a simple impregnation thermal technique via coupling of various fractions of CDs mole with g-C₃N₄. The photocatalyst that contains 0.5 % of CDs resulted has displayed the most superior photodegradation ability of phenol compared to other photocatalysts. The phenol elimination in this photocatalyst had a 3.7-folds premier rate in comparison with g-C₃N₄. The activity of photocatalyst can be finally improved through excitation of the up-converted light in g-C₃N₄ since CDs has the UCPL feature that could convert long wavelengths into short wavelengths of light that is less than 460 nm. As a result, electrons migrate from the CB of g-C₃N₄ to CDs, facilitating charge separation. The stability of the g-C₃N₄/CDs photocatalyst was also significantly improved, with the nanocomposite's photocatalytic ability remaining great following five consecutive photocatalytic recoveries under visible light. In another work, Fang et al. (Fang et al., 2016) studied the photoactivity of g-C₃N₄ reformed with CDs that were produced using dicyandiamide and CDs as precursors in a new process and used to eliminate RhB and create H₂, respectively, in the presence of UV and visible light. The findings of this study showed the performance of CDs (0.25 wt%)/g-C₃N₄ was approximately 3-folds larger than the single g-C₃N₄. Also, Zhang et al. (Zhang et al., 2017) integrated carbon quantum dots (CQDs) with g-C₃N₄ nanosheets with the exceptional ability for evaluating the photoelectrocatalytic characteristics of the nanocomposites stated in the removal of MB under visible light. The results showed that the photo-electrocatalytic performance is significantly affected by the surface hybrid heterojunction structures between g-C₃N₄ nanosheets and CQDs.

In other work, urea and sugarcane juice were used as precursors by Sim et al. (Sim et al., 2018) to fabricate g-C₃N₄/CDs nanocomposite via the hydrothermal method. Bisphenol A (BPA) degradation showed enhanced photocatalytic performance in comparison to g-C₃N₄ under irradiation from natural sunlight. Furthermore, a superior BPA elimination rate was displayed by this binary photocatalyst, and this was 3.87-fold premier more than that of g-C₃N₄. Eventually, a carbon precursor specifically human fingernails serving as low-cost organic waste was used by Tai et al 2018 to prepare CQDs/g-C₃N₄ through the hydrothermal method. High performance for 2, 4-dichlorophenol (2, 4-DCP) degradation which is relative to the sample of immaculate g-C₃N₄ was displayed by the fabricated CQDs/g-C₃N₄. Therefore, it can be deduced that the stated outstanding efficiency obtained by research workers was because of CDs' ability to serve as electron sinks, also slowing down the recombination rate of e⁻/h⁺ pairs and improving their separation rate. CDs also operate as a photosensitizer to sharpen g-C₃N₄, as evidenced by UV-vis DRS results, resulting in a broad absorption spectrum from the light source. More electrons are produced because of this broad spectral absorption, which boosts photocatalytic activity.

A research group of Habibi-Yangajeh (Asadzadeh-Khaneghah et al., 2018) conducted a study that proved the degradation of pollutants like MB, MO fuchsine, RhB, and

unexpectedly Cr (VI) photoreduction, as a typical heavy metal ion pollutant, applying g-C₃N₄ nanosheet/CDs (CNNs/CDs) linked to BiOX (X: Br, I), were superior to that of g-C₃N₄ under visible light. The presence of the formation of an interface between the components of BiOX, CDs, and CNNs was confirmed. The improved activity relative to the sample of g-C₃N₄ is about 129 times from the photodegradation of RhB by the best composite that contains CNNs/CDs/BiOBr (20 %). Electrons are excited to the CBS of CNNs and BiOBr by the utilized light in the sample of CNNs/CDs/BiOBr (20 %). Subsequently, by satisfying the Z-scheme mechanism, the electrons from CB are transmitted to CDs, thereafter to the VB of BiOBr. Hence, a dramatic reduction in the recombination rate is caused by electrons that gather in the holes in the VB of BiOBr and CB of CNNs as presented (Fig. 13).

The preparation of graphene oxide/g-C₃N₄/CDs was also carried out by Prakash et al. (Prakash et al., 2019) to study its effectiveness via hydrothermal technique on the photodegradation of crystal violet (CV) and RhB. Maximum photoactivity was shown by the GO/g-C₃N₄/CDs nanocomposite under the illumination of visible light. Apart from that, a Z-scheme photocatalyst was formed from the addition of CDs that is doped with nitrogen over the g-C₃N₄/Ag₃PO₄ nanocomposite. When compared with binary g-C₃N₄/Ag₃PO₄ under visible light, the ternary-prepared heterojunction photocatalyst showed an enhanced photoelectrocatalytic performance for phenol, RhB, and MB degradations. The rise in light-harvesting capacity, acceleration of electron transfer, and activation of molecular oxygen is more significantly achieved by the presence of NCDs and the impressive amelioration in the ability of g-C₃N₄/Ag₃PO₄/NCDs photocatalyst was given to the Z-scheme. The rate of charge recombination

and the transfer of interfacial charges of the stated nanocomposites has exhibited a more powerful photocurrent response than those of the binary and pure ones. A superior photoactivity by the ternary photocatalyst over the binary ones was displayed due to the subsequent addition of NCDs that improve the performance of visible-light absorption.

In a study by Dadigala et al. (Dadigala et al., 2017), a photochemical reduction technique was used to integrate g-C₃N₄ nanosheet/CDs nanocomposite with Ag nanoparticles (Fig. 14). The stated photocatalyst displayed superior ability when the visible light efficiency of the optimized sample of AgNPs/CDs/CNNs that has 2 wt% of CDs was evaluated for p-nitrophenol (PNP) and MO degradation when compared to that of the single counterpart. This was 5.8 and 11.5 -folds premier than that of the degradation of PNP and MO respectively for CNNs. Broad visible-light absorption was a result of the sensitization of CDs and also the recombination of e⁻/h⁺ pairs, which was caused by the movement of electrons in the AgNPs/CDs/CNNs nanocomposite from CNNs approaching AgNPs and CDs.

Jian et al. (Jian et al., 2016) used an electrostatic adsorption approach with positively charged HpCN and negatively charged CQDs to remove MB under visible-light irradiation using CQDs and proton functionalized g-C₃N₄ (CQDs/HpCN). The electrostatic self-assembly approach, according to this study group, is a good way to make a well-dispersed HpCN/CQDs heterojunction. The heterostructure was used to accelerate the decomposition of MB in this study, which took 90 min. The enhancement was attributed to a strong absorption peak in the visible region between 400 and 800 nm, indicating that CQDs/HpCN can absorb more energy from visible light, resulting in increased photocatalytic activity.

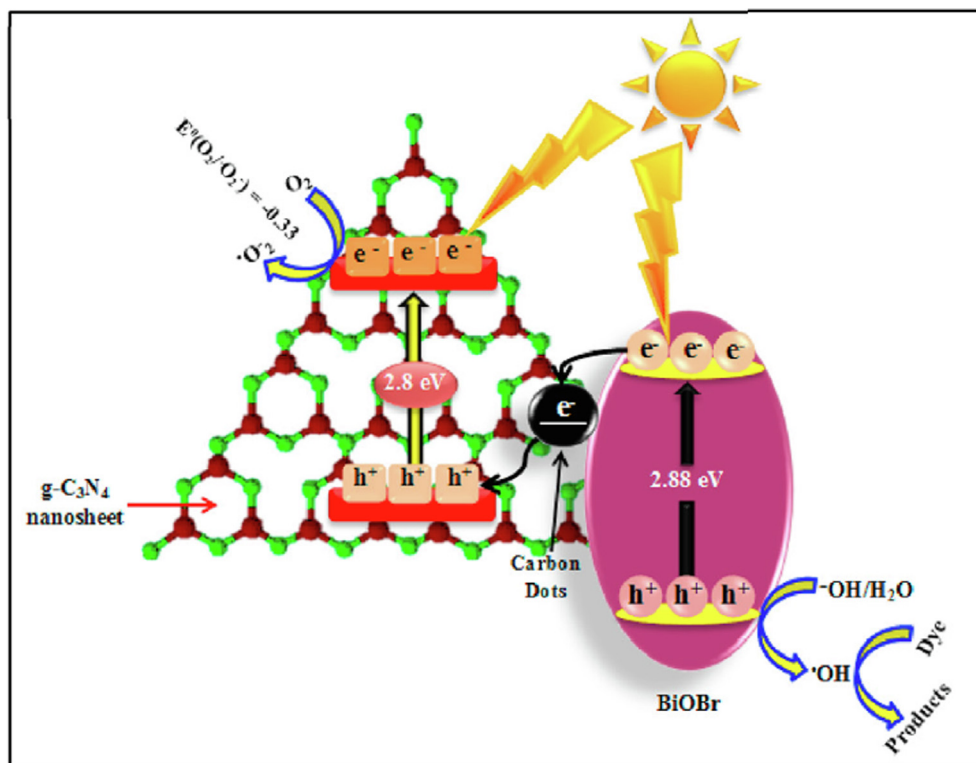


Fig. 13 Proposed mechanism in the form of Z-scheme for the CNNs/CDs/BiOBr photocatalysts. (). Adapted from Asadzadeh-Khaneghah et al., 2018

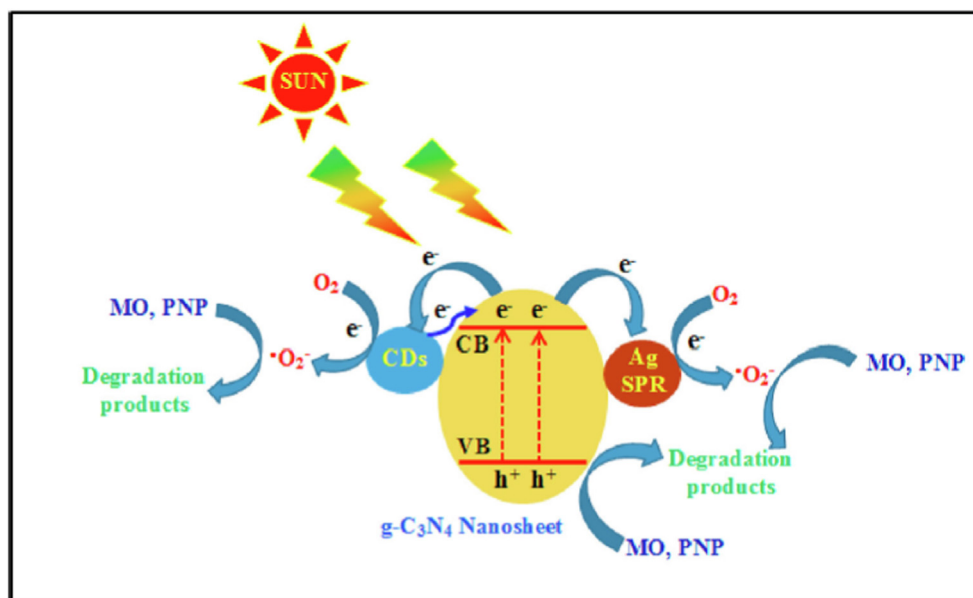


Fig. 14 Schematic diagram of the photocatalytic process over the AgNPs/CDs/CNNs. (). Adapted from Dadigala et al., 2017

In related work, Jiang et al. (Jiang et al., 2018) suggested a technique to raise the effectiveness of the visible-light harvesting performance of a fabricated hybrid photocatalyst hybrid (i.e., utilizing CdS quantum dots (CdS QDs), g-C₃N₄, and CQDs). This was achieved by integrating the CDs with CdS/g-C₃N₄ and the occurrence of a red shift due to the light absorption trait of CdS QDs and CDs. The CDs conductivity, in addition to the diversity in CB energy levels of the introduced nanomaterials, is the most important factor that enhances the performance of the ternary photocatalysts. The conductivity of the CDs serves as an electron-transfer mediator for the electron that moves from g-C₃N₄ to the surface of the components. Here, an appropriate pathway was promoted and produced by the systematic movement between the components using CDs and the separation of charges. Due to the cohabitation of CDs and CdS QDs on the g-C₃N₄, these major improvements also resulted in rectified visible-light harvesting and, as a result, premier photoactivity of ternary nanocomposites for organic pollutants destruction.

In another example, Liu et al. (Liu et al., 2017) applied a simple impregnation technique to fabricate a Fe(III)/CDQs/Fe-doped with g-C₃N₄ (Fe(III)/CDQs/Fe-g-C₃N₄) which has been used for several environmental purification purposes. These developed nanocomposites were created using a simple impregnation process. Over the Fe-g-C₃N₄, the presence of CQDs with a size of 2–5 nm was well-recognized. The phenol and MO removal ability by the Fe(III)/CQDs/Fe-CN photocatalyst showed good photoactivity when compared to g-C₃N₄ Fe-doped g-C₃N₄, CQDs/Fe-g-C₃N₄, and Fe(III)/Fe-g-C₃N₄. This increase was attributed to improved light absorption, shorter e⁻/h⁺ pair movement distances, and OH being confirmed as a main active component.

7.7. g-C₃N₄/CDs-based photocatalysts in degradation of different antibiotics

Human health and the environment are at risk due to the presence of antibiotics and other surfacing contaminants in drink-

ing and surface waters. This is a result of their non-biodegradable nature and their ability to remain in the environment for a long time. Thus, several research works have been published that resulted in several growing pieces of literature with regard to the removal of antibiotics. Wang et al. (Wang et al., 2017) investigated the removal of antibiotics by the utilization of g-C₃N₄/CDs-based nanocomposite. This was achieved via the fabrication of N-doped CDS(NCDs)/g-C₃N₄ nanocomposite. A small amount of NCDs (1.0 wt%) was introduced to raise the degradation ability of indomethacin (IDM) under visible light illumination. The ability of the photocatalyst to respond to visible light is enhanced as a result of the effect that NCDs have, which has been established extraordinarily by UV-vis DRS. A decrease in the energy gap was remarkably illustrated by the NCDs/g-C₃N₄ (i.e., after the addition of NCDs) when compared with g-C₃N₄. Furthermore, this substantial progress is a result of the premier duty of the nanocomposite that has been formed in the migration of charges and boosted absorption in the visible area. A diagram of the simplified energy band of the NCDs/g-C₃N₄ photocatalyst is demonstrated in Fig. 15. The probability to recombine charge carriers was slowed down and the photocatalytic ability in the degradation of IDM remarkably improved according to the described mechanism.

To increase the degradation ability for tetracycline (TC) treatment, the fabrication of hybrid CDs/g-C₃N₄/ZnO was carried out by Guo and coworkers (Guo et al., 2017) via an easy thermal impregnation process. The preparation of the CDs/g-C₃N₄/ZnO photocatalyst was done and compared with other species. As the ideal photocatalyst, superior ability in the removal of this pollutant was particularly shown by CDs/g-C₃N₄/ZnO with the solution of CDs. After 30 min of visible light illumination, the ideal nanocomposite can make TC fully decomposed. The CDs on the g-C₃N₄/ZnO photocatalyst are the major driver of excellent ability. It also not only boosts the ability to respond to visible light but also makes the e⁻/h⁺ pair separation ability efficient and this is due to its feature of electron migrations. Likewise, Xie et al. (Xie et al., 2018)

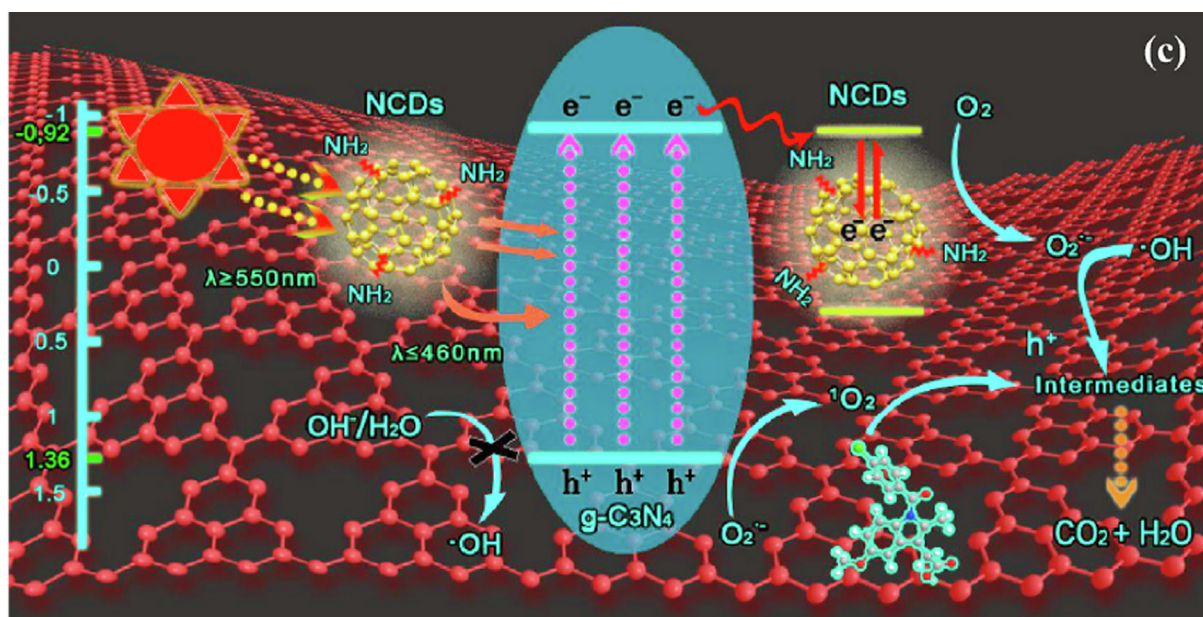


Fig. 15 The proposed photocatalytic mechanism in the Nitrogen-doped CDs/g-C₃N₄. (). Adapted from Wang et al., 2017

reported that the TC photodegradation rate was improved over the CDs/g-C₃N₄/ZnO nanocomposites. The Z scheme heterojunction structure, the high separation capacity of e⁻/h⁺ pairs, and the superior ability of UCPL are the synergistic effect behind this improvement. The literature demonstrated an excellent photocatalytic efficiency for TC degradation by the CDs/g-C₃N₄/MoO₃ photocatalyst when compared with MoO₃/g-C₃N₄ nanocomposite and the original g-C₃N₄ under UV–vis irradiation. The Proposed mechanisms for the photocatalytic elimination of TC under visible light over the CDs/g-C₃N₄/MoO₃ composites are presented in Fig. 16.

Similarly, the Z-scheme system is responsible for the enhanced photocatalytic process after the irradiation of UV–vis. Because of the UCPL properties of CDs, long-wavelength lights can be converted to short-wavelength lights, allowing MoO₃ and g-C₃N₄ semiconductors to be effectively stimulated by the absorption of the up-converted lights. The separation of charges is afterward improved due to the Z-scheme heterojunction produced as a result of the migration of generated electrons from CB of MoO₃ to VB of g-C₃N₄. Furthermore, the photocatalytic ability is raised by the transfer of electrons gathered in g-C₃N₄ following the slowing down of the charges from recombination.

In another study, the extraordinary photocatalytic ability was witnessed in the company of 1.0 wt% CDs by Su and colleagues (Su et al., 2017) via the fabrication of CDs/TiO₂/g-C₃N₄ nanocomposites. This photocatalyst is substantially better at degrading enrofloxacin (ENF) because of its efficiency in separating the CDs charges, efficiency in migration of electrons, and distinctive UCPL feature. The up-converted emissions were strikingly seen within the 350 nm to 600 nm region and CDs are excited from 600 nm to 900 nm are the premier UCPL feature. These occurrences show that CDs can step up the photocatalytic activity by converting wavelengths of light that are near infra-red (NIR) to wavelengths that are of visible light, and this remarkably improves the nanocomposite's light utilization. The stated UCPL feature of CDs can also

be used by TiO₂/g-C₃N₄ photocatalyst nanocomposite to convert lights with NIR wavelengths to lights in the visible-light region following the direct introduction of the Z-scheme mechanism. In this place, CDs exist to facilitate the mechanism of Z-scheme movement. The active components in the common mechanism that is heterostructured can convert ENX into some ultimate materials (like CO₂ and H₂O) or significantly get rid of it to form inorganic compounds. In other research work, combined calcination of silica colloid, CQDs, and cyanamide was performed by Wang and coworkers (Wang et al., 2018) to prepare g-C₃N₄/CQDs composite that is mesoporous. For photodegradation of fluoroquinolone antibiotics, the stated composite in this literature presented a degradation efficiency of about 1.7 and 2.7- folds superior to the mpg-C₃N₄ under visible light with a wavelength greater than 420 nm and simulated sunlight with a wavelength greater than 290 nm illuminations, respectively and this is the most superior photocatalytic performance. The unique UCPL features of the CDs, the effective charge separation, and the high surface area of mpg-C₃N₄ are the major reasons behind the enhancement of this photoactivity. Similarly, Zhang et al. (Zhang and De Zhang, 2019) showed that the removal of CIP by g-C₃N₄ photocatalyst which has a deficiency of CDs@nitrogen (CDs@ND-g-C₃N₄) has a photocatalytic ability that is superior to that of fresh g-C₃N₄. They associated the addition of nitrogen defects and CDs reduce the recombination of the e⁻/h⁺ pairs as well as incense the nanocomposite's absorption capacity to visible light which are responsible for boosting the photocatalytic ability of CDs@nitrogen-g-C₃N₄ photocatalyst.

7.8. g-C₃N₄/CDs-based nanocomposite in H₂ generation

As a favorable energy source, the use of a photocatalyst and solar energy is introduced to generate H₂ as another fuel from H₂O. This will also reduce the over-dependence on fossil fuel reserves (Fattahimoghaddam et al., 2022; Shahsavandi et al., 2022; Zhao et al., 2022; Zhang et al., 2022; Cao et al., 2022;

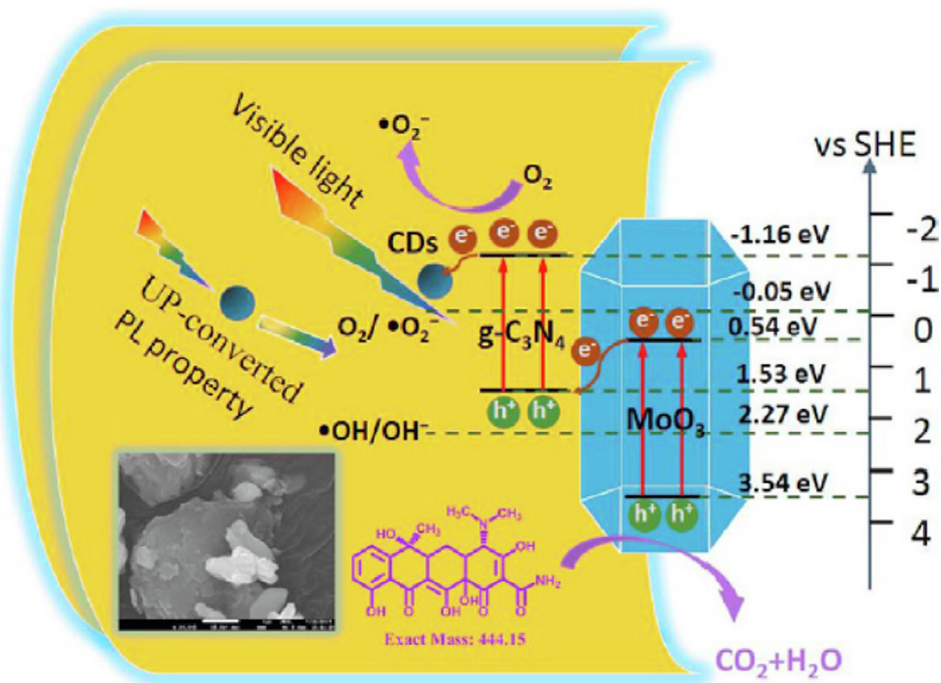


Fig. 16 Proposed mechanisms for the photocatalytic elimination of TC under visible light over the CDs/g-C₃N₄/MoO₃ composites. (). Adapted from Xie et al., 2018

Martinez et al., 2022; Alaghmandfard and Ghandi, 2022; Huang et al., 2022; Hao et al., 2022). The amount of energy density of H₂ is significantly higher in comparison to that of petrol and diesel (hydrocarbons). In the past few years, there has been a large number of increased expansions in the performance of g-C₃N₄-based photocatalysts for water-splitting applications. The electron-hole pairs are transferred towards the surface reaction area on the CDs or g-C₃N₄ in photocatalytic water splitting to generate H₂ and O₂ under the illumination of light over the g-C₃N₄/CDs photocatalyst without recombination. This can change the adsorbed H₂O molecules to gaseous O₂ and H₂. By introducing 7 mL of CQDs ethanol solution to g-C₃N₄ nanosheets (CNNS), Li et al. (Li et al., 2016) found that the rate of H₂ production was 116.1 μmol h⁻¹, which was three times higher than that of plain CNNS (37.8 μmol h⁻¹). The increased photocatalytic ability is because of the discovered CQDs PL spectra to appropriately quench electrons which leads to promoting charge separation of the e⁻/h⁺ pairs in CNNS. The construction of heterojunctions was demonstrated in a research work by Qin et al. (Qin et al., 2017) to produce Ag NPs/CQDs/g-C₃N₄ heterostructures of CQDs/g-C₃N₄ and Ag NPs. The fabricated photocatalyst was analyzed using SEM and it confirmed the attachment of Ag NPs and CQDs nanoparticles over the g-C₃N₄ a. The UV-vis DRS of the 6 mL CQDs/g-C₃N₄ (6CCN) and 3 wt% Ag NPs/6 mL CQDs/g-C₃N₄ (3S6CCN) nanocomposite showed a redshift to visible light, indicating excellent coupling of CQDs with g-C₃N₄ and Ag NPs, as well as the presence of surface plasmon resonance from silver nanoparticles. Furthermore, in the interface regions, the synergistic action of CQDs, Ag NPs, and g-C₃N₄ can ease electron production, separation, and transfer, hence increasing photoactivity.

In comparison to the binary photocatalyst g-C₃N₄/TiO₂, the ternary CDs/g-C₃N₄/TiO₂ (CGT) nanocomposite likewise was used to generate H₂ and the investigators reported that the positive effects of CDs, as well as the formation of heterojunction between TiO₂ nanosheets and g-C₃N₄, are the fundamental reasons behind the improved photoactivity. Thereby, face-to-face orientation and strong integration of TiO₂ and g-C₃N₄ nanosheets can be provided by the well-defined heterojunction and application CDs as electron traps (electron reservoirs). This improves the photocatalytic ability to generate H₂ because of the slowing down of the recombination of charges. One more interesting ternary photocatalyst that demonstrated an impact on H₂ generation is the g-C₃N₄ which is doped with CDs/MoS₂ quantum dots (g-C₃N₄/NCDs/MoS₂QDs). This is because of the formation of the Z-scheme mechanism among g-C₃N₄ and NCDs, which remarkably facilitate the separation and migration of charge carriers.

7.9. H₂O₂ production using g-C₃N₄ photocatalyst

Hydrogen peroxide has been extensively employed in the paper industry, chemical synthesis, disinfection, textile bleaching, and production of rocket fuel (Pattappan et al., 2022). More than 95 % of the H₂O₂ produced industrially is produced via the anthraquinone method, namely the Riedl-Pfleiderer process. Utilizing catalysts made of precious metals, this procedure is carried out in organic solvents. Nevertheless, it has a lot of shortcomings: (i) The hazardous nature of the organic solvents utilized in preparation. (ii) The price of precious metal catalysts is high. (iii) Both hydrogenation and oxidation require a significant amount of energy. (iv) The industrial process produces a large amount of waste, which causes environ-

mental damage (Yang et al., 2019). Thus, it is necessary to look for alternative effective, clean, and secure H_2O_2 preparation techniques. H_2O_2 was said to be produced directly from oxygen and hydrogen in literature. The explosive risk associated with this technique, which involves the direct interaction of hydrogen and oxygen, makes it challenging to use in large-scale industrial manufacturing. Another method is to use ultrasonic chemistry to prepare H_2O_2 by separating oxygen and water. However, the long sonochemical exposure duration could result in H_2O_2 decay and lower the yield. Recently, solar-powered photocatalysis for the creation of H_2O_2 has garnered a lot of interest. This method uses plentiful water and oxygen as raw materials to create H_2O_2 using semiconductor photocatalysts, as opposed to employing an explosive mixture of hydrogen and oxygen. Throughout the entire production process, no pollutants are produced. Consequently, it is thought that photocatalytic H_2O_2 production is a potential technique.

With water and oxygen as the raw materials, photocatalytic H_2O_2 synthesis is an upward process, and the associated Gibbs free energy is 117 kJ mol^{-1} (Wang et al., 2016). One-step two-electron reduction and two-step single-electron reduction are the two primary processes used in the synthesis of H_2O_2 via photocatalysis. Numerous studies demonstrated the potential of $\text{g-C}_3\text{N}_4$ for photocatalytic H_2O_2 generation, but their activity is severely constrained by the unfavorable recombination of photoinduced excitons. To improve the separation and transfer of photoinduced carriers, numerous efforts have been made. For instance, Yang et al. (Yang et al., 2019) used a chemical etching technique to create Ti_3C_2 and $\text{g-C}_3\text{N}_4$ nanosheets by protonating bulk $\text{g-C}_3\text{N}_4$ with hydrochloric acid and supplementing it with ultrasound exfoliation. Finally, they used electrostatic self-assembly to create a mixture of Ti_3C_2 and $\text{g-C}_3\text{N}_4$. The combination of $\text{g-C}_3\text{N}_4$ and of Ti_3C_2 is seen in the TEM image. The $\text{Ti}_3\text{C}_2/\text{g-C}_3\text{N}_4$ composite's ability to absorb light was greatly enhanced by Ti_3C_2 . Additionally, the Schottky connection between Ti_3C_2 and $\text{g-C}_3\text{N}_4$ considerably aided in exciton dissociation and molecular oxygen activation, which was advantageous for the production of H_2O_2 . Therefore, the most active sample's H_2O_2 generation rate reached $2.20 \mu\text{mol/L min}^{-1}$ or about 2.1 times that of $\text{g-C}_3\text{N}_4$.

8. CO_2 mitigation using $\text{g-C}_3\text{N}_4$ -based nanocomposite

Among the assured byproducts resulting from the combustion of fossil fuels is carbon dioxide (CO_2), which is one of the major greenhouse gases present in the atmosphere due to its constant increase in concentration. It is one of the most fundamental problems that lead to climate change and global warming (Liang et al., 2022; Tseng et al., 2022; Mahdavi et al., 2022; Zhou et al., 2022; Sudhaik et al., 2022; Al-Hajji et al., 2022; Li et al., 2022; Sakuna et al., 2022). Because of the stated environmental problems, numerous research works have been focused to improve societal and industrial standards via the reduction of inorganic compounds, particularly CO_2 . Its photoreduction to organic fuels and value-added chemicals has been proposed as a means of not only reducing greenhouse gas emissions but also increasing demand for renewable fuels. The developing interest in the photocatalytic conversion of CO_2 is notably due to the schematic and feasible nature of the process, and in addition, only light, H_2O , CO_2 , and the right photocatalyst are needed in the process. Therefore, the photoreduction of CO_2

in the generation of chemical fuels has been ideally chosen to solve energy and environmental crises. The emergence of a range of products can be possible from the photoreduction of CO_2 under light irradiation employed on various photocatalysts, like CO , CH_4 , CH_3OH , and HCOOH which incorporate multi-electron processes. Thus, various semiconductors have been investigated for the photocatalytic reduction of CO_2 by several researchers (Liu et al., 2022; Zhang et al., 2022; Li et al., 2022; Liu et al., 2022; Gorai and Kundu, 2022). Because of the specific properties of CDs, such as photosensitization, increased electrical conductivity, and electron-withdrawing effects, $\text{g-C}_3\text{N}_4$ sensitized by CDs has been used to simplify the photocatalytic CO_2 transformation in the last six years. Zhao et al. (Zhao et al., 2018) used a photochemical one-step approach to synthesize $\text{Au/CDs/g-C}_3\text{N}_4$ electrocatalysts for CO_2 photoreduction. At 0.5 V, the improved electrocatalyst had a significant CO faradic efficiency of 79.8 %. The synergetic effect between Au, CDs and $\text{g-C}_3\text{N}_4$ nanoparticles is the major reason behind the improved photocatalytic ability. Also, the simplified transformation of CO from CO_2 can be achieved through the coupling of CDs with $\text{g-C}_3\text{N}_4$, which is a result of its superior ability to adsorb H^+ and CO_2 and the impressive conductivity of the CDs. The photocatalyst was very active in the photoreduction of CO from CO_2 because it has a particularly high surface area (S_{BET}) of $117 \text{ m}^2 \text{ g}^{-1}$. Protonated $\text{g-C}_3\text{N}_4$ and CDs obtained respectively from glucose and urea precursors were hybridized by Ong et al. (Ong et al., 2016) to derive a better performance. The fabrication of the photocatalyst was carried out for 8 h and in the presence of water, vapors produced CH_4 and CO with respectively 29.23 and $58.82 \mu\text{mol} \cdot \text{g}_{\text{catalyst}}^{-1}$ as the total amount. Also, the outstanding ability of the photocatalyst ability to separate e^-/h^+ pairs is confirmed by the considerable trapping intensity presented by the PL spectra, and this was found to have a significant effect on the photocatalyst's performance. Feng et al. (Scopus - Document details - null | Signed in, (n.d.). <https://www.scopus.com/record/display.uri?id=2-s2.0-8506987>, 2022) investigated the reactivity of CO_2 reduction products using a $\text{CQDs/g-C}_3\text{N}_4$ nanocomposite with CQDs with an average size of 2.5 nm. Under the same conditions as the single $\text{g-C}_3\text{N}_4$ nanocomposite, which produced H_2 , CO, and O_2 , the $\text{CQDs/g-C}_3\text{N}_4$ nanocomposite produced 6 times more O_2 , CO and comparable CH_4 in the absence of detectable H_2 . The Nyquist plots depicted effective e^-/h^+ pairs transfer among the improved photocatalyst components. As a result, electron migration significantly reduced the recombination of charge carriers. The most effective photocatalyst with 2 wt% CQDs had elevated rates of O_2 , CH_4 , and CO evolution, as well as a yield greater than $\text{g-C}_3\text{N}_4$. Thus, $\text{g-C}_3\text{N}_4/\text{CDs}$ systems displayed extremely interesting methods that can be employed for photocatalytic CO_2 reduction and provided critical feedback for future advancements.

9. Conclusion and future perspective

The distinguishing properties of graphitic carbon nitride such as suitable bandgap, thermal and chemical stability, visible light absorption, less hazardous, excellent redox ability, polymeric structure, and easy fabrication make it an attractive material for different photocatalytic applications like hydrogen production, CO_2 reduction, water splitting and degradation of organic pollutants in wastewater. This review reported the recent advancements and lingering challenges hindering the large-scale utilization of $\text{g-C}_3\text{N}_4$ semiconductor as an efficient vis-

ible light-responsive photocatalytic material. Various methodologies used to improve the photocatalytic performance of the compound such as metal and non-metal doping, co-doping, and heterojunction engineering have been discussed in detail. The paper has also highlighted some of the hitherto weaknesses and limitations of the material that requires attention in future works. In summary, metal doping creates a new energy level within the bandgap and enhances the spectral response which can reduce the charge carrier recombination. However, the newly created energy levels serve as recombination centers, thereby decreasing quantum efficiency. The doped ions also exhibit poor thermal stability. On the other hand, non-metal doping serves as an effective technique to modulate the mobility of photogenerated charge carriers and enhance absorbance and redox potentials. Meanwhile, codoping or tridoping combines the advantages of these single dopants and has led to improved photocatalytic activity. Despite the many successes achieved, some challenges need to be addressed in future works. For instance, the mechanism of photocatalytic enhancement by elemental doping, how the defect influences the electronic structure, the nature of the chemical states, and the role and site of the metal ion in heteroatom are not fully understood.

Some aspects in which future research works could be directed include codoping and tridoping as a strategy to integrate the benefits of single dopants. Also, heterojunction and simultaneous doping could improve charge carrier separation for enhanced photocatalytic performance. Furthermore, combining elemental doping with nanostructuring to obtain different morphologies such as nanofibers, nanosheets, nanorods, and nanotubes could be a new direction of research. Finally, innovative doping strategies should be employed to modulate the higher occupied molecular orbital and lower unoccupied molecular orbital with orientation for high oxidation and reduction potential.

Declaration of Competing Interest

The authors declare that they have no known competing financial interests or personal relationships that could have appeared to influence the work reported in this paper.

Acknowledgment

The authors acknowledge the support received from the Deanship of Research, Oversight and Coordination (DROC), King Fahd University of Petroleum & Minerals (KFUPM), Dhahran, Saudi Arabia under project # INCB2216. We are also thankful to Physics Department and Interdisciplinary Research Center for Construction and Building Materials, KFUPM for supporting this work. M.A. Gondal and Y.S. Wudil are thankful to the DROC, KFUPM for the support received through project # DF201018.

References

- Adegoke, K.A., Maxakato, N.W., 2022. Efficient strategies for boosting the performance of 2D graphitic carbon nitride nanomaterials during photoreduction of carbon dioxide to energy-rich chemicals. *Mater. Today Chem.* 23,. <https://doi.org/10.1016/J.MTCHEM.2021.100605> 100605.
- Ahmed, S., Rasul, M.G., Martens, W.N., Brown, R., Hashib, M.A., 2010. Heterogeneous photocatalytic degradation of phenols in wastewater: A review on current status and developments. *Desalination* 261, 3–18. <https://doi.org/10.1016/J.DESAL.2010.04.062>.
- A. Alaghmandfard, K. Ghandi, A Comprehensive Review of Graphitic Carbon Nitride (g-C₃N₄)–Metal Oxide-Based Nanocomposites: Potential for Photocatalysis and Sensing. *Nanomater.* 2022, Vol. 12, Page 294. 12 (2022) 294. <https://doi.org/10.3390/NANO12020294>.
- Al-Ahmed, A., 2022. Photocatalytic properties of graphitic carbon nitrides (g-C₃N₄) for sustainable green hydrogen production: recent advancement. *Fuel* 316,. <https://doi.org/10.1016/J.FUEL.2022.123381> 123381.
- R. Alcántara, J. Qian, Y. Liu, W. Zheng, B. Zhou, X. Dong, Covalent Modification of Iron Phthalocyanine into Skeleton of Graphitic Carbon Nitride and Its Visible-Light-Driven Photocatalytic Reduction of Nitroaromatic Compounds, *Catal.* 2022, Vol. 12, Page 752. 12 (2022) 752. <https://doi.org/10.3390/CATAL12070752>.
- M. Alejandra Quintana, R.R. Solís, M. Ángeles Martín-Lara, G. Blázquez, F. Mónica Calero, M.J. Muñoz-Batista, Enhanced boron modified graphitic carbon nitride for the selective photocatalytic production of benzaldehyde, *Sep. Purif. Technol.* 298 (2022) 121613. <https://doi.org/10.1016/J.SEPPUR.2022.121613>.
- Al-Hajji, L.A., Alshareef, F.M., Ismail, A.A., Mahmoud, M.H.H., 2022. RuO₂ nanoparticles-accommodated graphitic carbon nitride for significant enhancement in photocatalytic oxidation of trichloroethylene. *Opt. Mater. (Amst)*. 125,. <https://doi.org/10.1016/J.OPTMAT.2022.112086> 112086.
- Almessiere, M.A., Slimani, Y., Sertkol, M., Gungunes, H., Wudil, Y. S., Korkmaz, A.D., Baykal, A., 2021. Impact of Gd substitution on the structure, hyperfine interactions, and magnetic properties of Sr hexaferrites. *Ceram. Int.* 47, 33853–33864. <https://doi.org/10.1016/J.CERAMINT.2021.08.297>.
- O.A. Al-Najjar, Y.S. Wudil, U.F. Ahmad, O.S.B. Al-Amoudi, M.A. Al-Osta, M.A. Gondal, Applications of laser induced breakdown spectroscopy in geotechnical engineering: a critical review of recent developments, perspectives and challenges, <https://doi.org/10.1080/05704928.2022.2136192>. (2022) 1–37. <https://doi.org/10.1080/05704928.2022.2136192>.
- Alrebd, T.A., Wudil, Y.S., Ahmad, U.F., Yakasai, F.A., Mohammed, J., Kallas, F.H., 2022. Predicting the thermal conductivity of Bi₂Te₃-based thermoelectric energy materials: a machine learning approach. *Int. J. Therm. Sci.* 181,. <https://doi.org/10.1016/J.IJTHEMALSCI.2022.107784> 107784.
- Altan, O., Kalay, E., 2022. The influence of band bending phenomenon on photocatalytic Suzuki-Miyaura coupling reaction: the case of AgPd alloy nanoparticles supported on graphitic carbon nitride. *Appl. Surf. Sci.* 580. <https://doi.org/10.1016/J.APSUSC.2021.152287> 152287.
- Altan, O., Altintas, E., Alemdar, S., Metin, Ö., 2022. The rational design of a graphitic carbon nitride-based dual S-scheme heterojunction with energy storage ability as a day/night photocatalyst for formic acid dehydrogenation. *Chem. Eng. J.* 441. <https://doi.org/10.1016/J.CEJ.2022.136047> 136047.
- Asadzadeh-Khaneghah, S., Habibi-Yangjeh, A., Nakata, K., 2018. Graphitic carbon nitride nanosheets anchored with BiOBr and carbon dots: exceptional visible-light-driven photocatalytic performances for oxidation and reduction reactions. *J. Colloid Interface Sci.* 530, 642–657. <https://doi.org/10.1016/J.JCIS.2018.07.024>.
- Asadzadeh-Khaneghah, S., Habibi-Yangjeh, A., 2020. g-C₃N₄/carbon dot-based nanocomposites serve as efficacious photocatalysts for environmental purification and energy generation: a review. *J. Clean. Prod.* 276,. <https://doi.org/10.1016/J.JCLEPRO.2020.124319> 124319.
- Azami, M.S., Jalil, A.A., Aziz, F.F.A., Hassan, N.S., Mamat, C.R., Fauzi, A.A., Izzudin, N.M., 2022. Exploiting the potential of silver oxo-salts with graphitic carbon nitride/fibrous silica-titania in designing a new dual Z-scheme photocatalyst for photodegradation of 2-chlorophenol. *Sep. Purif. Technol.* 292. <https://doi.org/10.1016/J.SEPPUR.2022.120984> 120984.
- Boumeriam, H., Machado, B.F., Moura, N.M.M., Serp, P., Andrade, L., Lopes, T., Mendes, A., Chafik, T., Da Silva, E.S., Faria, J.L., 2022. Graphitic carbon nitride/few-layer graphene heterostructures for enhanced visible-LED photocatalytic hydrogen generation. *Int. J. Hydrogen Energy* 47, 25555–25570. <https://doi.org/10.1016/J.IJHYDENE.2022.05.285>.

- Bu, Y., Chen, Z., 2014. Effect of oxygen-doped C₃N₄ on the separation capability of the photoinduced electron-hole pairs generated by O-C₃N₄@TiO₂ with quasi-shell-core nanostructure. *Electrochim. Acta* 144, 42–49. <https://doi.org/10.1016/J.ELECTACTA.2014.08.095>.
- Cao, S., Low, J., Yu, J., Jaroniec, M., 2015. Polymeric photocatalysts based on graphitic carbon nitride. *Adv. Mater.* 27, 2150–2176. <https://doi.org/10.1002/ADMA.201500033>.
- Cao, L., Wang, R., Wang, D., 2015. Synthesis and characterization of sulfur self-doped g-C₃N₄ with efficient visible-light photocatalytic activity. *Mater. Lett.* 149, 50–53. <https://doi.org/10.1016/J.MATLET.2015.02.119>.
- Cao, S., Zhang, Y., Ding, K., Xu, J., Zhao, Y., Wang, Y., Xie, X., Wang, H., 2022. Efficient visible light driven degradation of antibiotic pollutants by oxygen-doped graphitic carbon nitride via the homogeneous supramolecular assembly of urea. *Environ. Res.* 210, <https://doi.org/10.1016/J.ENVRES.2022.112920> 112920.
- Cao, A., Zhang, M., Su, X., Romanovski, V., Chu, S., 2022. In situ fabrication of NiS₂-decorated graphitic carbon nitride/metal-organic framework nanostructures for photocatalytic H₂ evolution. *ACS Appl. Nano Mater.* 5, 5416–5424. https://doi.org/10.1021/ACSANM.2C00417/ASSET/IMAGES/LARGE/AN2C00417_0008.JPEG.
- Che, S., Zhou, X., Zhang, L., Su, D., Wang, T., Wang, C., 2022. Construction of a 2D layered phosphorus-doped graphitic carbon Nitride/BiOBr heterojunction for highly efficient photocatalytic disinfection. *Chem. – An Asian J.* 17, e202200095. <https://doi.org/10.1002/ASIA.202200095>.
- Che, S., Zhang, L., Wang, T., Su, D., Wang, C., 2022. Graphitic carbon nitride-based photocatalysts for biological applications. *Adv. Sustain. Syst.* 6, 2100294. <https://doi.org/10.1002/ADSU.202100294>.
- Chen, W., Liu, T.Y., Huang, T., Liu, X.H., Yang, X.J., 2016. Novel mesoporous P-doped graphitic carbon nitride nanosheets coupled with ZnIn₂S₄ nanosheets as efficient visible light driven heterostructures with remarkably enhanced photo-reduction activity. *Nanoscale* 8, 3711–3719. <https://doi.org/10.1039/C5NR07695A>.
- Chen, L., Ning, S., Liang, R., Xia, Y., Huang, R., Yan, G., Wang, X., 2022. Potassium doped and nitrogen defect modified graphitic carbon nitride for boosted photocatalytic hydrogen production. *Int. J. Hydrogen Energy* 47, 14044–14052. <https://doi.org/10.1016/J.IJHYDENE.2022.02.147>.
- Chen, X., Xu, Y., Xu, G., 2022. Modification of graphite carbon nitride by adding an ultra-micro amount of triaminotriphenylamine for superior photocatalytic hydrogen evolution. *New J. Chem.* 46, 9057–9063. <https://doi.org/10.1039/D2NJ00393G>.
- Cheng, C., Chen, D., Li, N., Li, H., Xu, Q., He, J., Lu, J., 2022. NH₂-MIL-125(Ti) modified graphitic carbon nitride with carbon vacancy for efficient photocatalytic NO removal. *Chemosphere* 307, <https://doi.org/10.1016/J.CHEMOSPHERE.2022.135660> 135660.
- Cheng, C., Dong, C.L., Shi, J., Mao, L., Huang, Y.C., Kang, X., Zong, S., Shen, S., 2022. Regulation on polymerization degree and surface feature in graphitic carbon nitride towards efficient photocatalytic H₂ evolution under visible-light irradiation. *J. Mater. Sci. Technol.* 98, 160–168. <https://doi.org/10.1016/J.JMST.2021.05.019>.
- Cheng, C.Q., Feng, Y., Shi, Z.Z., Zhou, Y.L., Kang, W.J., Li, Z., Mao, J., Shen, G.R., Dong, C.K., Liu, H., Du, X.W., 2022. Highly conjugated graphitic carbon nitride nanofoam for photocatalytic hydrogen evolution. *Langmuir* 38, 1471–1478. https://doi.org/10.1021/ACS.LANGMUIR.1C02716/ASSET/IMAGES/LARGE/LA1C02716_0005.JPEG.
- Cheng, L., Zhang, P., Wen, Q., Fan, J., Xiang, Q., 2022. Copper and platinum dual-single-atoms supported on crystalline graphitic carbon nitride for enhanced photocatalytic CO₂ reduction. *Chinese J. Catal.* 43, 451–460. [https://doi.org/10.1016/S1872-2067\(21\)63879-2](https://doi.org/10.1016/S1872-2067(21)63879-2).
- Choong, C.E., Park, C.M., Chang, Y.Y., kyu Yang, J., Kim, J.R., Oh, S.E., Jeon, B.H., Choi, E.H., Yoon, Y., Jang, M., 2022. Interfacial coupling perovskite CeFeO₃ on layered graphitic carbon nitride as a multifunctional Z-scheme photocatalyst for boosting nitrogen fixation and organic pollutants demineralization. *Chem. Eng. J.* 427, <https://doi.org/10.1016/J.CEJ.2021.131406> 131406.
- Choudhury, S., Sahoo, U., Pattnayak, S., Padhiari, S., Tripathy, M., Hota, G., 2022. Hematite nanoparticles decorated nitrogen-doped reduced graphene oxide/graphitic carbon nitride multifunctional heterostructure photocatalyst towards environmental applications. *New J. Chem.* 46, 13100–13116. <https://doi.org/10.1039/D2NJ01301K>.
- Chu, Y., Zheng, X., Fan, J., 2022. Preparation of sodium and boron co-doped graphitic carbon nitride for the enhanced production of H₂O₂ via two-electron oxygen reduction and the degradation of 2,4-DCP via photocatalytic oxidation coupled with Fenton oxidation. *Chem. Eng. J.* 431, <https://doi.org/10.1016/J.CEJ.2021.134020> 134020.
- M.L. Cohen, Predicting useful materials, *Science* (80-). 261 (1993) 307–308. <https://doi.org/10.1126/SCIENCE.261.5119.307/ASSET/A3111EC4-4183-4A1D-ADE2-ABFAD03DB4CC/ASSETS/SCIENCE.261.5119.307.FP.PNG>.
- Dadigala, R., Bandi, R.K., Gangapuram, B.R., Guttena, V., 2017. Carbon dots and Ag nanoparticles decorated g-C₃N₄ nanosheets for enhanced organic pollutants degradation under sunlight irradiation. *J. Photochem. Photobiol. A Chem.* 342, 42–52. <https://doi.org/10.1016/J.JPHOTOCHEM.2017.03.032>.
- Ding, J., Tang, Q., Fu, Y., Zhang, Y., Hu, J., Li, T., Zhong, Q., Fan, M., Kung, H.H., 2021. Core-shell covalently linked graphitic carbon nitride-melamine-resorcinol-formaldehyde microsphere polymers for efficient photocatalytic CO₂ reduction to methanol. *J. Am. Chem. Soc.* https://doi.org/10.1021/JACS.1C13301/ASSET/IMAGES/MEDIUM/JA1C13301_M010.GIF.
- Dong, Q., Chen, Z., Zhao, B., Zhang, Y., Lu, Z., Wang, X., Li, J., Chen, W., 2022. In situ fabrication of niobium pentoxide/graphitic carbon nitride type-II heterojunctions for enhanced photocatalytic hydrogen evolution reaction. *J. Colloid Interface Sci.* 608, 1951–1959. <https://doi.org/10.1016/J.JCIS.2021.10.161>.
- Dong, G., Zhao, K., Zhang, L., 2012. Carbon self-doping induced high electronic conductivity and photoreactivity of g-C₃N₄. *Chem. Commun.* 48, 6178–6180. <https://doi.org/10.1039/C2CC32181E>.
- W. Fan, B.K. Lok, F.K. Lai, Evaluation of printed heating elements for continuous flow PCR application, *Proc. 2016 IEEE 18th Electron. Packag. Technol. Conf. EPTC 2016.* (2017) 360–364. <https://doi.org/10.1109/EPTC.2016.7861505>.
- Fang, J., Fan, H., Li, M., Long, C., 2015. Nitrogen self-doped graphitic carbon nitride as efficient visible light photocatalyst for hydrogen evolution. *J. Mater. Chem. A* 3, 13819–13826. <https://doi.org/10.1039/C5TA02257F>.
- Fang, S., Xia, Y., Lv, K., Li, Q., Sun, J., Li, M., 2016. Effect of carbon-dots modification on the structure and photocatalytic activity of g-C₃N₄. *Appl. Catal. B Environ.* 185, 225–232. <https://doi.org/10.1016/J.APCATB.2015.12.025>.
- Fattahimoghaddam, H., Mahvelati-Shamsabadi, T., Jeong, C.S., Lee, B.K., 2022. Coral-like potassium and phosphorous doped graphitic carbon nitride structures with enhanced charge and mass transfer dynamics toward photocatalytic hydrogen peroxide production and microbial disinfection. *J. Colloid Interface Sci.* 617, 326–340. <https://doi.org/10.1016/J.JCIS.2022.03.027>.
- Feng, L.L., Zou, Y., Li, C., Gao, S., Zhou, L.J., Sun, Q., Fan, M., Wang, H., Wang, D., Li, G.D., Zou, X., 2014. Nanoporous sulfur-doped graphitic carbon nitride microrods: a durable catalyst for visible-light-driven H₂ evolution. *Int. J. Hydrogen Energy* 39, 15373–15379. <https://doi.org/10.1016/J.IJHYDENE.2014.07.160>.

- Fronczak, M., Tálás, E., Pászti, Z., Szijjártó, G.P., Mihály, J., Tompos, A., Baranowski, P., Tiwari, S.K., Bystrzejewski, M., 2022. Photocatalytic performance of alkali metal doped graphitic carbon nitrides and Pd-alkali metal doped graphitic carbon nitride composites. *Diam. Relat. Mater.* 125, <https://doi.org/10.1016/j.DIAMOND.2022.109006> 109006.
- A. Fujishima, K. Honda, Electrochemical Photolysis of Water at a Semiconductor Electrode, *Nat.* 1972 2385358. 238 (1972) 37–38. <https://doi.org/10.1038/238037a0>.
- Gao, X., Ai, L., Wang, L., Ju, Y., Liu, S., Wang, J., Fan, H., 2022. The stable and elastic graphitic carbon nitride/polyvinyl alcohol photocatalytic composite sponge: simple synthesis and application for wastewater treatment. *J. Environ. Chem. Eng.* 10, <https://doi.org/10.1016/j.JECE.2022.107814> 107814.
- Gao, G., Jiao, Y., Ma, F., Jiao, Y., Waclawik, E., Du, A., 2015. Carbon nanodot decorated graphitic carbon nitride: New insights into the enhanced photocatalytic water splitting from ab initio studies. *Phys. Chem. Chem. Phys.* 17, 31140–31144. <https://doi.org/10.1039/C5CP05512A>.
- Gao, Q., Lei, Q., Miao, R., Gao, M., Liu, H., Yang, Q., Liu, Y., Song, F., Yu, Y., Yang, W., 2022. Bi-doped graphitic carbon nitride nanotubes boost the photocatalytic degradation of Rhodamine B. *New J. Chem.* 46, 3588–3594. <https://doi.org/10.1039/D1NJ05569K>.
- B. Gholipour, A. Zonouzi, M. Shokouhimehr, S. Rostamnia, Integration of plasmonic AgPd alloy nanoparticles with single-layer graphitic carbon nitride as Mott-Schottky junction toward photo-promoted H₂ evolution, *Sci. Reports* 2022 121. 12 (2022) 1–13. <https://doi.org/10.1038/s41598-022-17238-4>.
- Gorai, D.K., Kundu, T.K., 2022. Platinum-silicon doped graphitic carbon nitride: a first principle calculation. *Phys. B Condens. Matter.* 627, <https://doi.org/10.1016/j.PHYSB.2021.413547> 413547.
- Guo, F., Shi, W., Guan, W., Huang, H., Liu, Y., 2017. Carbon dots/g-C₃N₄/ZnO nanocomposite as efficient visible-light driven photocatalyst for tetracycline total degradation. *Sep. Purif. Technol.* 173, 295–303. <https://doi.org/10.1016/j.SEPUR.2016.09.040>.
- Guo, F., Shi, C., Sun, W., Liu, Y., Shi, W., Lin, X., 2022. Pomelo biochar as an electron acceptor to modify graphitic carbon nitride for boosting visible-light-driven photocatalytic degradation of tetracycline, *Chinese J. Chem. Eng.* 48, 1–11. <https://doi.org/10.1016/j.CJCHE.2021.06.027>.
- Guo, L., Xu, F., Liu, Z., Zhang, M., Ma, D., Lai, C., Liu, S., Li, L., Fu, Y., Qin, L., 2022. Constructing benzene ring modified graphitic carbon nitride with narrowed bandgap and enhanced molecular oxygen activation for efficient photocatalytic degradation of oxytetracycline. *Sep. Purif. Technol.* 294, <https://doi.org/10.1016/j.SEPUR.2022.121170> 121170.
- Guo, S.N., Zhu, Y., Yan, Y.Y., Min, Y.L., Fan, J.C., Xu, Q.J., 2016. Holey structured graphitic carbon nitride thin sheets with edge oxygen doping via photo-Fenton reaction with enhanced photocatalytic activity. *Appl. Catal. B Environ.* 185, 315–321. <https://doi.org/10.1016/j.APCATB.2015.11.030>.
- Han, Q., Hu, C., Zhao, F., Zhang, Z., Chen, N., Qu, L., 2015. One-step preparation of iodine-doped graphitic carbon nitride nanosheets as efficient photocatalysts for visible light water splitting. *J. Mater. Chem. A* 3, 4612–4619. <https://doi.org/10.1039/C4TA06093H>.
- Y. Hao, Y.C. Hou, D. Song, W.M. Yin, X.Y. Chen, C. Wang, Y. R. Guo, L. Li, Q.J. Pan, Interfacial coupling enhanced photocatalytic activity: an experimental/DFT combined study of porous graphitic carbon nitride/carbon composite material, *Cellul.* 2022 297. 29 (2022) 3759–3772. <https://doi.org/10.1007/S10570-022-04529-2>.
- He, F., Chen, G., Yu, Y., Zhou, Y., Zheng, Y., Hao, S., 2014. The sulfur-bubble template-mediated synthesis of uniform porous g-C₃N₄ with superior photocatalytic performance. *Chem. Commun.* 51, 425–427. <https://doi.org/10.1039/C4CC07106A>.
- T.V.A. Hoang, E.W. Shin, T.K.A. Nguyen, D.Q. Dao, P.A. Nguyen, D.H. Jeong, Solvent Etching Process for Graphitic Carbon Nitride Photocatalysts Containing Platinum Cocatalyst: Effects of Water Hydrolysis on Photocatalytic Properties and Hydrogen Evolution Behaviors, *Nanomater.* 2022, Vol. 12, Page 1188. 12 (2022) 1188. <https://doi.org/10.3390/NANO12071188>.
- Hong, J., Xia, X., Wang, Y., Xu, R., 2012. Mesoporous carbon nitride with in situ sulfur doping for enhanced photocatalytic hydrogen evolution from water under visible light. *J. Mater. Chem.* 22, 15006–15012. <https://doi.org/10.1039/C2JM32053C>.
- Hrahsheh, F., Sani Wudil, Y., Wilemski, G., 2017. Confined phase separation of aqueous-organic nanodroplets. *Phys. Chem. Phys.* 19, 26839–26845. <https://doi.org/10.1039/C7CP04531J>.
- Hu, S., Ma, L., You, J., Li, F., Fan, Z., Wang, F., Liu, D., Gui, J., 2014. A simple and efficient method to prepare a phosphorus modified g-C₃N₄ visible light photocatalyst. *RSC Adv.* 4, 21657–21663. <https://doi.org/10.1039/C4RA02284J>.
- Hu, S., Ma, L., You, J., Li, F., Fan, Z., Lu, G., Liu, D., Gui, J., 2014. Enhanced visible light photocatalytic performance of g-C₃N₄ photocatalysts co-doped with iron and phosphorus. *Appl. Surf. Sci.* 311, 164–171. <https://doi.org/10.1016/j.APSUSC.2014.05.036>.
- Hu, S., Li, F., Fan, Z., Wang, F., Zhao, Y., Lv, Z., 2014. Band gap-tunable potassium doped graphitic carbon nitride with enhanced mineralization ability. *Dalt. Trans.* 44, 1084–1092. <https://doi.org/10.1039/C4DT02658F>.
- Huang, M., Chen, C., Wang, T., Sui, Q., Zhang, K., Li, B., 2022. Cadmium-sulfide/gold/graphitic-carbon-nitride sandwich hetero-junction photocatalyst with regulated electron transfer for boosting carbon-dioxide reduction to hydrocarbon. *J. Colloid Interface Sci.* 613, 575–586. <https://doi.org/10.1016/j.JCIS.2022.01.065>.
- Huang, T., Chen, J., Zhang, L., Khataee, A., Han, Q., Liu, X., Sun, J., Zhu, J., Pan, S., Wang, X., Fu, Y., 2022. Precursor-modified strategy to synthesize thin porous amino-rich graphitic carbon nitride with enhanced photocatalytic degradation of RhB and hydrogen evolution performances. *Chinese J. Catal.* 43, 497–506. [https://doi.org/10.1016/S1872-2067\(21\)63873-1](https://doi.org/10.1016/S1872-2067(21)63873-1).
- Huang, Z.F., Song, J., Pan, L., Wang, Z., Zhang, X., Zou, J.J., Mi, W., Zhang, X., Wang, L., 2015. Carbon nitride with simultaneous porous network and O-doping for efficient solar-energy-driven hydrogen evolution. *Nano Energy.* 12, 646–656. <https://doi.org/10.1016/j.NANOEN.2015.01.043>.
- Jian, X., Liu, X., Yang, H.M., Li, J.G., Song, X.L., Dai, H.Y., Liang, Z.H., 2016. Construction of carbon quantum dots/proton-functionalized graphitic carbon nitride nanocomposite via electrostatic self-assembly strategy and its application. *Appl. Surf. Sci.* 370, 514–521. <https://doi.org/10.1016/j.APSUSC.2016.02.119>.
- W. Jiang, H. Wang, X. Zhang, Y. Zhu, Y. Xie, Two-dimensional polymeric carbon nitride: structural engineering for optimizing photocatalysis, *Sci. China Chem.* 2018 6110. 61 (2018) 1205–1213. <https://doi.org/10.1007/S11426-018-9292-7>.
- E. Kanimba, Z. Tian, H. Choi, Y.J. Kim, J. Song, C.S. Kim, G.S. Lee, S.S. Kim, J. Park, S.H. Yim, S.H. Park, H.R. Hwang, M. Hong, P. Veluswamy, B.J. Cho, P.M. Rodrigo, A. Valera, E.F. Fernández, F.M. Almonacid, K. Yang, K. Cho, S. Yang, Y. Park, S.S. Kim, D. Kong, W. Zhu, Z. Guo, Y. Deng, Y. Zhou, S.S. Zhang, X. Xu, W. Liu, S.S. Zhang, G. Li, J. He, S.M. Pourkiaei, M.H. Ahmadi, M. Sadeghzadeh, S. Moosavi, F. Pourfayaz, L. Chen, M.A. Pour Yazdi, R. Kumar, K. Karthick, S. Suresh, H. Singh, G.C. Joy, R. Dhanuskodi, H.M. Elmoughni, A.K. Menon, R.M.W. Wolfe, S.K. Yee, A.A. Angeline, L.G. Asirvatham, D.J. Hemanth, J. Jayakumar, S. Wongwises, M. Marefati, M. Mehrpooya, Z. Yuan, X. Tang, Y. Liu, Z. Xu, K. Liu, J. Li, Z. Zhang, H. Wang, K. Karthick, S. Suresh, M.M.M.D. Hussain, H.M. Ali, C.S.S. Kumar, X. Zhao, W. Han, C. Zhao, S. Wang, F. Kong, X. Ji, Z. Li, X. Shen, L.K. Allison, T.L. Andrew, Y.J. Cui, B.L. Wang, K.F. Wang, L. Zheng, E. Houshfar, A. Mohammadnia, B.M. Ziapour, F. Sedaghati, L.A. Rosendahl, A. Rezaia, S. Mahmoudezhad, P.A. Cotfas, D.T. Cotfas, L.A. Rosendahl, A.

- Rezania, Y.S., Wudil, M.A., Gondal, S.G., Rao, S., Kunwar, Thermal conductivity of PLD-grown thermoelectric Bi₂Te_{2.7}Se_{0.3} films using temperature-dependent Raman spectroscopy technique, *Appl. Therm. Eng.* 4 (2019) 25–43. <https://doi.org/10.1016/j.seta.2019.02.008>.
- Khan, A.A., Tahir, M., 2019. Recent advancements in engineering approach towards design of photo-reactors for selective photocatalytic CO₂ reduction to renewable fuels. *J. CO₂ Util.* 29, 205–239. <https://doi.org/10.1016/J.JCOU.2018.12.008>.
- Kong, H.J., Won, D.H., Kim, J., Woo, S.I., 2016. Sulfur-doped g-C₃N₄/BiVO₄ composite photocatalyst for water oxidation under visible light. *Chem. Mater.* 28, 1318–1324. https://doi.org/10.1021/ACS.CHEMMATER.5B04178/ASSET/IMAGES/LARGE/CM-2015-04178G_0008.JPEG.
- Kong, W., Xing, Z., Fang, B., Cui, Y., Li, Z., Zhou, W., 2022. Plasmon Ag/Na-doped defective graphite carbon nitride/NiFe layered double hydroxides Z-scheme heterojunctions toward optimized photothermal-photocatalytic-Fenton performance. *Appl. Catal. B Environ.* 304, <https://doi.org/10.1016/J.APCATB.2021.120969> 120969.
- Koutsouroubi, E.D., Vamvasakis, I., Drivas, C., Kennou, S., Armatas, G.S., 2022. Photochemical deposition of SnS₂ on graphitic carbon nitride for photocatalytic aqueous Cr(VI) reduction. *Chem. Eng. J. Adv.* 9, <https://doi.org/10.1016/J.CEJA.2021.100224> 100224.
- Kumar, A., Kashyap, S., Sharma, M., Krishnan, V., 2022. Tuning the surface and optical properties of graphitic carbon nitride by incorporation of alkali metals (Na, K, Cs and Rb): effect on photocatalytic removal of organic pollutants. *Chemosphere* 287, <https://doi.org/10.1016/J.CHEMOSPHERE.2021.131988> 131988.
- Lan, Z.A., Zhang, G., Wang, X., 2016. A facile synthesis of Br-modified g-C₃N₄ semiconductors for photoredox water splitting. *Appl. Catal. B Environ.* 192, 116–125. <https://doi.org/10.1016/J.APCATB.2016.03.062>.
- Le, S., Jiang, T., Zhao, Q., Liu, X.F., Li, Y., Fang, B., Gong, M., 2016. Cu-doped mesoporous graphitic carbon nitride for enhanced visible-light driven photocatalysis. *RSC Adv.* 6, 38811–38819. <https://doi.org/10.1039/C6RA03982K>.
- Li, X., Cong, H., Wang, R., Wang, Y., Nie, Z., Jing, Q., Zhao, Y., Song, H., Wang, H., 2022. Ascorbic acid-induced structural defect in photocatalytic graphitic carbon nitride to boost H₂O₂ fuel cell performance. *J. Power Sources* 532, <https://doi.org/10.1016/J.JPOWSOUR.2022.231368> 231368.
- Li, H., Liu, Y., Cui, Y., Zhang, W., Fu, C., Wang, X., 2016. Facile synthesis and enhanced visible-light photoactivity of DyVO₄/g-C₃N₄ composite semiconductors. *Appl. Catal. B Environ.* 183, 426–432. <https://doi.org/10.1016/J.APCATB.2015.11.012>.
- Li, Y., Liu, X., Tan, L., Cui, Z., Yang, X., Zheng, Y., Yeung, K.W.K., Chu, P.K., Wu, S., 2018. Rapid sterilization and accelerated wound healing using Zn²⁺ and graphene oxide modified g-C₃N₄ under dual light irradiation. *Adv. Funct. Mater.* 28, 1800299. <https://doi.org/10.1002/ADFM.201800299>.
- Li, Y., Liu, X., Tan, L., Cui, Z., Jing, D., Yang, X., Liang, Y., Li, Z., Zhu, S., Zheng, Y., Yeung, K.W.K., Zheng, D., Wang, X., Wu, S., 2019. Eradicating multidrug-resistant bacteria rapidly using a multi functional g-C₃N₄@ Bi₂S₃ nanorod heterojunction with or without antibiotics. *Adv. Funct. Mater.* 29, 1900946. <https://doi.org/10.1002/ADFM.201900946>.
- Li, F., Lu, Z., Zhang, P., Jin, Y., Li, T., Hu, C., 2022. Boosting the extra generation of superoxide radicals on graphitic carbon nitride with carbon vacancies by the modification of pollutant adsorption for high-performance photocatalytic degradation. *ACS ES&T Eng.* <https://doi.org/10.1021/ACSESTENGG.1C00459>.
- Li, B., Luo, Y., Zheng, Y., Liu, X., Tan, L., Wu, S., 2022. Two-dimensional antibacterial materials. *Prog. Mater. Sci.* 130, <https://doi.org/10.1016/J.PMATSCI.2022.100976> 100976.
- Li, K., Su, F.Y., De Zhang, W., 2016. Modification of g-C₃N₄ nanosheets by carbon quantum dots for highly efficient photocatalytic generation of hydrogen. *Appl. Surf. Sci.* 375, 110–117. <https://doi.org/10.1016/J.APSUSC.2016.03.025>.
- Li, D., Wen, C., Huang, J., Zhong, J., Chen, P., Liu, H., Wang, Z., Liu, Y., Lv, W., Liu, G., 2022. High-efficiency ultrathin porous phosphorus-doped graphitic carbon nitride nanosheet photocatalyst for energy production and environmental remediation. *Appl. Catal. B Environ.* 307, <https://doi.org/10.1016/J.APCATB.2022.121099> 121099.
- Li, D., Liu, Y., Wen, C., Huang, J., Li, R., Liu, H., Zhong, J., Chen, P., Lv, W., Liu, G., 2022. Construction of dual transfer channels in graphitic carbon nitride photocatalyst for high-efficiency environmental pollution remediation: Enhanced exciton dissociation and carrier migration. *J. Hazard. Mater.* 436, <https://doi.org/10.1016/J.JHAZMAT.2022.129171> 129171.
- Li, J., Safarzadeh, M.S., Moats, M.S., Miller, J.D., Levier, K.M., Dietrich, M., Wan, R.Y., 2012. Thiocyanate hydrometallurgy for the recovery of gold. part I: chemical and thermodynamic considerations. *Hydrometallurgy* 113–114, 1–9. <https://doi.org/10.1016/J.HYDROMET.2011.11.005>.
- Li, L., Xiaoxue, S., Yuchong, Z., Jin, W., Zilong, L., Yuxi, G., Shuai, C., Youjun, J., Jinying, C., 2022. Application in photocatalytic degradation of zearalenone based on graphitic carbon nitride. *Luminescence* 37, 190–198. <https://doi.org/10.1002/BIO.4160>.
- Li, X., Xiong, J., Gao, X., Huang, J., Feng, Z., Chen, Z., Zhu, Y., 2019. Recent advances in 3D g-C₃N₄ composite photocatalysts for photocatalytic water splitting, degradation of pollutants and CO₂ reduction. *J. Alloys Compd.* 802, 196–209. <https://doi.org/10.1016/J.JALLCOM.2019.06.185>.
- Li, X.H., Zhang, J., Chen, X., Fischer, A., Thomas, A., Antonietti, M., Wang, X., 2011. Condensed graphitic carbon nitride nanorods by nanoconfinement: promotion of crystallinity on photocatalytic conversion. *Chem. Mater.* 23, 4344–4348. https://doi.org/10.1021/CM201688V/SUPPL_FILE/CM201688V_SI_001.PDF.
- Liang, Z., Xue, Y., Wang, X., Zhang, X., Tian, J., Cui, H., 2022. The incorporation of cocatalyst cobalt sulfide into graphitic carbon nitride: boosted photocatalytic hydrogen evolution performance and mechanism exploration. *Nano Mater. Sci.* <https://doi.org/10.1016/J.NANOMS.2022.03.001>.
- Liang, Q., Zhang, M., Liu, C., Xu, S., Li, Z., 2016. Sulfur-doped graphitic carbon nitride decorated with zinc phthalocyanines towards highly stable and efficient photocatalysis. *Appl. Catal. A Gen.* 519, 107–115. <https://doi.org/10.1016/J.APCATA.2016.03.033>.
- Lin, Y.Y., Hung, J.T., Chou, Y.C., Shen, S.J., Wu, W.T., Liu, F.Y., Lin, J.H., Chen, C.C., 2022. Synthesis of bismuth oxybromochloroiodide/graphitic carbon nitride quaternary composites (BiOxCly/BiOmBrn/BiOpIq/g-C₃N₄) enhances visible-light-driven photocatalytic activity. *Catal. Commun.* 163, <https://doi.org/10.1016/J.CATCOM.2022.106418> 106418.
- Lin, Y.Y., Hung, K.Y., Liu, F.Y., Dai, Y.M., Lin, J.H., Chen, C.C., 2022. Photocatalysts of quaternary composite, bismuth oxyfluoride/bismuth oxyiodide/ graphitic carbon nitride: synthesis, characterization, and photocatalytic activity. *Mol. Catal.* 528, <https://doi.org/10.1016/J.MCAT.2022.112463> 112463.
- Lin, Z., Wang, X., 2014. Ionic liquid promoted synthesis of conjugated carbon nitride photocatalysts from urea. *ChemSusChem.* 7, 1547–1550. <https://doi.org/10.1002/CSSC.201400016>.
- Lin, H., Wu, J., Zhou, F., Zhao, X., Lu, P., Sun, G., Song, Y., Li, Y., Liu, X., Dai, H., 2023. Graphitic carbon nitride-based photocatalysts in the applications of environmental catalysis. *J. Environ. Sci.* 124, 570–590. <https://doi.org/10.1016/J.JES.2021.11.017>.
- Liu, J., 2016. Effect of phosphorus doping on electronic structure and photocatalytic performance of g-C₃N₄: Insights from hybrid density functional calculation. *J. Alloys Compd.* 672, 271–276. <https://doi.org/10.1016/J.JALLCOM.2016.02.094>.
- Liu, Q., Chen, T., Guo, Y., Zhang, Z., Fang, X., 2017. Grafting Fe (III) species on carbon nanodots/Fe-doped g-C₃N₄ via interfacial charge transfer effect for highly improved photocatalytic perfor-

- mance. *Appl. Catal. B Environ.* 205, 173–181. <https://doi.org/10.1016/J.APCATB.2016.12.028>.
- Liu, X., Cui, M., Cui, K., Ding, Y., Chen, X., Chen, C., Nie, X., 2022. Construction of Li/K dopants and cyano defects in graphitic carbon nitride for highly efficient peroxymonosulfate activation towards organic contaminants degradation. *Chemosphere* 294, <https://doi.org/10.1016/J.CHEMOSPHERE.2022.133700> 133700.
- Liu, J., Liang, H., Li, C., Bai, J., 2022. Construction of V-doped graphitic carbon nitride with nanotube structure for sustainable photodegradation of tetracycline. *Vacuum* 204, <https://doi.org/10.1016/J.VACUUM.2022.111342> 111342.
- Liu, Y., Liu, Y., Xu, Y., He, Q., Yin, R., Sun, P., Dong, X., 2022. Phenanthroline bridging graphitic carbon nitride framework and Fe (II) ions to promote transfer of photogenerated electrons for selective photocatalytic reduction of Nitrophenols. *J. Colloid Interface Sci.* 608, 2088–2099. <https://doi.org/10.1016/J.JCIS.2021.10.146>.
- Liu, G., Niu, P., Sun, C., Smith, S.C., Chen, Z., Lu, G.Q., Cheng, H. M., 2010. Unique electronic structure induced high photoreactivity of sulfur-doped graphitic C₃N₄. *J. Am. Chem. Soc.* 132, 11642–11648. https://doi.org/10.1021/JA103798K/SUPPL_FILE/JA103798K_SI_001.PDF.
- Liu, G., Tang, Z., Gu, X., Li, N., Lv, H., Huang, Y., Zeng, Y., Yuan, M., Meng, Q., Zhou, Y., Wang, C., 2022. Boosting photocatalytic nitrogen reduction to ammonia by dual defective -CN and K-doping sites on graphitic carbon nitride nanorod arrays. *Appl. Catal. B Environ.* 317, <https://doi.org/10.1016/J.APCATB.2022.121752> 121752.
- Liu, Q., Wang, X., Yang, Q., Zhang, Z., Fang, X., 2018. Mesoporous g-C₃N₄ nanosheets prepared by calcining a novel supramolecular precursor for high-efficiency photocatalytic hydrogen evolution. *Appl. Surf. Sci.* 450, 46–56. <https://doi.org/10.1016/J.APSUSC.2018.04.175>.
- Liu, W., Wen, F., Wang, J., 2022. Construction of chlorine doped graphitic carbon nitride nanodisc for enhanced photocatalytic activity and mechanism insight. *Int. J. Hydrogen Energy* 47, 16887–16899. <https://doi.org/10.1016/J.IJHYDENE.2022.03.178>.
- X. Long, C. Feng, S. Yang, D. Ding, J. Feng, M. Liu, Y. Chen, J. Tan, xingjie Peng, J. Shi, R. Chen, Oxygen doped graphitic carbon nitride with regulatable local electron density and band structure for improved photocatalytic degradation of bisphenol A, *Chem. Eng. J.* 435 (2022) 134835. <https://doi.org/10.1016/J.CEJ.2022.134835>
- Lu, C., Chen, R., Wu, X., Fan, M., Liu, Y., Le, Z., Jiang, S., Song, S., 2016. Boron doped g-C₃N₄ with enhanced photocatalytic UO₂²⁺ reduction performance. *Appl. Surf. Sci.* 360, 1016–1022. <https://doi.org/10.1016/J.APSUSC.2015.11.112>.
- Lu, Y., Wang, W., Cheng, H., Qiu, H., Sun, W., Fang, X., Zhu, J., Zheng, Y., 2022. Bamboo-charcoal-loaded graphitic carbon nitride for photocatalytic hydrogen evolution. *Int. J. Hydrogen Energy* 47, 3733–3740. <https://doi.org/10.1016/J.IJHYDENE.2021.10.267>.
- Lu, C., Zhang, P., Jiang, S., Wu, X., Song, S., Zhu, M., Lou, Z., Li, Z., Liu, F., Liu, Y., Wang, Y., Le, Z., 2017. Photocatalytic reduction elimination of UO₂²⁺ pollutant under visible light with metal-free sulfur doped g-C₃N₄ photocatalyst. *Appl. Catal. B Environ.* 200, 378–385. <https://doi.org/10.1016/J.APCATB.2016.07.036>.
- Luo, J., Zhou, X., Ma, L., Xu, X., 2015. Enhancing visible-light photocatalytic activity of g-C₃N₄ by doping phosphorus and coupling with CeO₂ for the degradation of methyl orange under visible light irradiation. *RSC Adv.* 5, 68728–68735. <https://doi.org/10.1039/C5RA10848A>.
- Ma, H., Li, Y., Li, S., Liu, N., 2015. Novel PO codoped g-C₃N₄ with large specific surface area: Hydrothermal synthesis assisted by dissolution-precipitation process and their visible light activity under anoxic conditions. *Appl. Surf. Sci.* 357, 131–138. <https://doi.org/10.1016/J.APSUSC.2015.09.009>.
- Ma, X., Lv, Y., Xu, J., Liu, Y., Zhang, R., Zhu, Y., 2012. A strategy of enhancing the photoactivity of g-C₃N₄ via doping of nonmetal elements: a first-principles study. *J. Phys. Chem. C* 116, 23485–23493. https://doi.org/10.1021/JP308334X/SUPPL_FILE/JP308334X_SI_001.PDF.
- Ma, Z., Xu, L., Dong, K., Chen, T., Xiong, S.X., Peng, B., Zeng, J., Tang, S., Li, H., Huang, X., Luo, K.W., Wang, L.L., 2022. GaN/Surface-modified graphitic carbon nitride heterojunction: promising photocatalytic hydrogen evolution materials. *Int. J. Hydrogen Energy* 47, 7202–7213. <https://doi.org/10.1016/J.IJHYDENE.2021.12.077>.
- Ma, H., Zhao, S., Li, S., Liu, N., 2015. A facile approach to synthesizing S-Co-O tridoped g-C₃N₄ with enhanced oxygen-free photocatalytic performance via a hydrothermal post-treatment. *RSC Adv.* 5, 79585–79592. <https://doi.org/10.1039/C5RA14081A>.
- Mahdavi, M., Mirmohammadi, M., Baghdadi, M., Mahpishanian, S., 2022. Visible light photocatalytic degradation and pretreatment of lignin using magnetic graphitic carbon nitride for enhancing methane production in anaerobic digestion. *Fuel* 318, <https://doi.org/10.1016/J.FUEL.2022.123600> 123600.
- Mandari, K.K., Son, N., Kang, M., 2022. Synergistic effects of Tin sulfide Nitrogen-doped titania Nanobelt-Modified graphitic carbon nitride nanosheets with outstanding photocatalytic activity. *J. Colloid Interface Sci.* 606, 1767–1778. <https://doi.org/10.1016/J.JCIS.2021.08.120>.
- Mao, L., Lu, B., Shi, J., Zhang, Y., Kang, X., Chen, Y., Jin, H., Guo, L., 2022. Rapid high-temperature hydrothermal post treatment on graphitic carbon nitride for enhanced photocatalytic H₂ evolution. *Catal. Today.* <https://doi.org/10.1016/J.CATTOD.2022.03.035>.
- Martinez, B., Chang, D.N., Huang, Y.C., Dong, C.L., Chiu, T.W., Chiang, M.H., Kuo, C.H., 2022. Formation of a p-n heterojunction photocatalyst by the interfacing of graphitic carbon nitride and delafossite CuGaO₂. *J. Chinese Chem. Soc.* 69, 1042–1050. <https://doi.org/10.1002/JCCS.202200083>.
- Meng, Y., Li, Z., Tan, J., Li, J., Wu, J., Zhang, T., Wang, X., 2022. Oxygen-doped porous graphitic carbon nitride in photocatalytic peroxymonosulfate activation for enhanced carbamazepine removal: performance, influence factors and mechanisms. *Chem. Eng. J.* 429, <https://doi.org/10.1016/J.CEJ.2021.130860> 130860.
- Mo, F., Liu, Y., Xu, Y., He, Q., Sun, P., Dong, X., 2022. Photocatalytic elimination of moxifloxacin by two-dimensional graphitic carbon nitride nanosheets: enhanced activity, degradation mechanism and potential practical application. *Sep. Purif. Technol.* 292, <https://doi.org/10.1016/J.SEPPUR.2022.121067> 121067.
- Mo, Z., Xu, K., Yu, L., Huang, T., Song, Y., Yuan, J., Ding, C., Lei, Y., Li, H., Xu, H., 2022. Activation of Fe species on graphitic carbon nitride nanotubes for efficient photocatalytic ammonia synthesis. *Int. J. Energy Res.* 46, 13453–13462. <https://doi.org/10.1002/ER.8056>.
- Nguyen, M.D., Nguyen, T.B., Thamilselvan, A., Nguyen, T.G., Kuncoro, E.P., an Doong, R., 2022. Fabrication of visible-light-driven tubular F, P-codoped graphitic carbon nitride for enhanced photocatalytic degradation of tetracycline. *J. Environ Chem. Eng.* 10, <https://doi.org/10.1016/J.JECE.2021.106905> 106905.
- Ni, Y., Wang, M., Liu, L., Li, M., Hu, S., Lin, J., Sun, J., Yue, T., Zhu, M.-Q., Wang, J., 2022. Efficient and reusable photocatalytic river water disinfection by additive graphitic carbon nitride/magnesium oxide nano-onions with particular “nano-magnifying glass effect”. *J. Hazard. Mater.* 439, <https://doi.org/10.1016/J.JHAZMAT.2022.129533> 129533.
- Niu, B., Xiao, J., Xu, Z., 2022. Recycling spent LiCoO₂ battery as a high-efficient lithium-doped graphitic carbon nitride/Co₃O₄ composite photocatalyst and its synergistic photocatalytic mechanism. *Energy Environ. Mater.* <https://doi.org/10.1002/EEM2.12312>.
- W.J. Ong, L.K. Putri, Y.C. Tan, L.L. Tan, N. Li, Y.H. Ng, X. Wen, S.P. Chai, Unravelling charge carrier dynamics in protonated g-C₃N₄ interfaced with carbon nanodots as co-catalysts toward enhanced photocatalytic CO₂ reduction: A combined experimental

- and first-principles DFT study, *Nano Res.* 2016 105. 10 (2017) 1673–1696. <https://doi.org/10.1007/S12274-016-1391-4>.
- Ou, H., Ning, S., Zhu, P., Chen, S., Han, A., Kang, Q., Hu, Z., Ye, J., Wang, D., Li, Y., 2022. Carbon nitride photocatalysts with integrated oxidation and reduction atomic active centers for improved CO₂ conversion. *Angew. Chem.* 134, e202206579. <https://doi.org/10.1002/ANGE.202206579>.
- Pan, H., Zhang, Y.W., Shenoy, V.B., Gao, H., 2011. Ab initio study on a novel photocatalyst: Functionalized graphitic carbon nitride nanotube. *ACS Catal.* 1, 99–104. https://doi.org/10.1021/CS100045U/SUPPL_FILE/CS100045U_SI_001.PDF.
- Pattappan, D., Kavya, K.V., Vargheese, S., Kumar, R.T.R., Haldorai, Y., 2022. Graphitic carbon nitride/NH₂-MIL-101(Fe) composite for environmental remediation: visible-light-assisted photocatalytic degradation of acetaminophen and reduction of hexavalent chromium. *Chemosphere* 286,. <https://doi.org/10.1016/J.CHEMOSPHERE.2021.131875> 131875.
- Pham, T.H., Myung, Y., Van Le, Q., Kim, T.Y., 2022. Visible-light photocatalysis of Ag-doped graphitic carbon nitride for photodegradation of micropollutants in wastewater. *Chemosphere* 301,. <https://doi.org/10.1016/J.CHEMOSPHERE.2022.134626> 134626.
- Prakash, K., Kumar, J.V., Latha, P., Kumar, P.S., Karuthapandian, S., 2019. Fruitful fabrication of CDs on GO/g-C₃N₄ sheets layers: a carbon amalgamation for the remediation of carcinogenic pollutants. *J. Photochem. Photobiol. A Chem.* 370, 94–104. <https://doi.org/10.1016/J.JPHOTOCHEM.2018.10.046>.
- P. Praus, A brief review of s-triazine graphitic carbon nitride, *Carbon Lett.* 2022 323. 32 (2022) 703–712. <https://doi.org/10.1007/S42823-022-00319-9>.
- Qin, T., You, Z., Wang, H., Shen, Q., Zhang, F., Yang, H., 2017. Preparation and photocatalytic behavior of carbon-nanodots/graphitic carbon nitride composite photocatalyst. *J. Electrochem. Soc.* 164, H211–H214. <https://doi.org/10.1149/2.1421704JES/XML>.
- Rajan, A., Neppolian, B., 2022. Coordinative integration of amorphous nickel-imidazole framework with graphitic carbon nitride for enhanced photocatalytic hydrogen production. *Appl. Mater. Today* 28,. <https://doi.org/10.1016/J.APMT.2022.101524> 101524.
- Ran, J., Ma, T.Y., Gao, G., Du, X.W., Qiao, S.Z., 2015. Porous P-doped graphitic carbon nitride nanosheets for synergistically enhanced visible-light photocatalytic H₂ production. *Energy Environ. Sci.* 8, 3708–3717. <https://doi.org/10.1039/C5EE02650D>.
- Rana, A., Sudhaik, A., Raizada, P., Nguyen, V.H., Xia, C., Parwaz Khan, A.A., Thakur, S., Nguyen-Tri, P., Nguyen, C.C., Kim, S.Y., Van Le, Q., Singh, P., 2022. Graphitic carbon nitride based immobilized and non-immobilized floating photocatalysts for environmental remediation. *Chemosphere* 297,. <https://doi.org/10.1016/J.CHEMOSPHERE.2022.134229> 134229.
- Raziq, F., Qu, Y., Zhang, X., Humayun, M., Wu, J., Zada, A., Yu, H., Sun, X., Jing, L., 2016. Enhanced cocatalyst-free visible-light activities for photocatalytic fuel production of g-C₃N₄ by trapping holes and transferring electrons. *J. Phys. Chem. C* 120, 98–107. https://doi.org/10.1021/ACS.JPCA.5B10313/ASSET/IMAGES/LARGE/JP-2015-10313M_0008.JPEG.
- Saeed, U., Jilani, A., Iqbal, J., Al-Turaif, H., 2022. Reduced graphene oxide-assisted graphitic carbon nitride@ZnO rods for enhanced physical and photocatalytic degradation. *Inorg. Chem. Commun.* 142,. <https://doi.org/10.1016/J.INOCHE.2022.109623> 109623.
- Sagara, N., Kamimura, S., Tsubota, T., Ohno, T., 2016. Photoelectrochemical CO₂ reduction by a p-type boron-doped g-C₃N₄ electrode under visible light. *Appl. Catal. B Environ.* 192, 193–198. <https://doi.org/10.1016/J.APCATB.2016.03.055>.
- Sakuna, P., Ketwong, P., Ohtani, B., Trakulmututa, J., Kobkeatthawin, T., Luengnaruemitchai, A., Smith, S.M., 2022. The influence of metal-doped graphitic carbon nitride on photocatalytic conversion of acetic acid to carbon dioxide. *Front. Chem.* 10. <https://doi.org/10.3389/FCHEM.2022.825786/FULL>.
- Salhi, B., Wudil, Y.S., Hossain, M.K., Al-Ahmed, A., Al-Sulaiman, F.A., 2018. Review of recent developments and persistent challenges in stability of perovskite solar cells. *Renew. Sustain. Energy Rev.* 90, 210–222. <https://doi.org/10.1016/J.RSER.2018.03.058>.
- Schirmer, T.E., Abdellaoui, M., Savateev, A., Ollivier, C., Antonietti, M., Fensterbank, L., König, B., 2022. Mesoporous graphitic carbon nitride as a heterogeneous organic photocatalyst in the dual catalytic arylation of Alkyl Bis(catecholato)silicates. *Org. Lett.* 24, 2483–2487. https://doi.org/10.1021/ACS.ORGLETT.2C00529/ASSET/IMAGES/LARGE/OL2C00529_0001.JPEG.
- Scopus - Document details - null | Signed in, (n.d.). <https://www.scopus.com/record/display.uri?eid=2-s2.0-79953302537&origin=inward> (accessed August 17, 2022).
- Scopus - Document details - null | Signed in, (n.d.). https://www.scopus.com/record/display.uri?eid=2-s2.0-85069872356&origin=inward&featureToggles=FEATURE_NEW_DOC_DETAILS_EXPORT:1,FEATURE_EXPORT_REDESIGN:0 (accessed August 14, 2022).
- Shahsavandi, F., Amirjani, A., Reza Madaah Hosseini, H., 2022. Plasmon-enhanced photocatalytic activity in the visible range using AgNPs/polydopamine/graphitic carbon nitride nanocomposite. *Appl. Surf. Sci.* 585,. <https://doi.org/10.1016/J.APSUSC.2022.152728> 152728.
- Shang, Y., Wang, Y., Lv, C., Jing, F., Liu, T., Li, W., Liu, S., Chen, G., 2022. A broom-like tube-in-tube bundle O-doped graphitic carbon nitride nanoreactor that promotes photocatalytic hydrogen evolution. *Chem. Eng. J.* 431,. <https://doi.org/10.1016/J.CEJ.2021.133898> 133898.
- Sharma, R., Almáši, M., Nehra, S.P., Rao, V.S., Panchal, P., Paul, D. R., Jain, I.P., Sharma, A., 2022. Photocatalytic hydrogen production using graphitic carbon nitride (GCN): a precise review. *Renew. Sustain. Energy Rev.* 168,. <https://doi.org/10.1016/J.RSER.2022.112776> 112776.
- She, X., Liu, L., Ji, H., Mo, Z., Li, Y., Huang, L., Du, D., Xu, H., Li, H., 2016. Template-free synthesis of 2D porous ultrathin nonmetal-doped g-C₃N₄ nanosheets with highly efficient photocatalytic H₂ evolution from water under visible light. *Appl. Catal. B Environ.* 187, 144–153. <https://doi.org/10.1016/J.APCATB.2015.12.046>.
- Shi, J., Luo, Y., Yang, T., Wang, H., Ju, C., Pu, K., Shi, J., Zhao, T., Xue, J., Li, Y., Li, H., Xu, H., Li, X., Fan, Z., 2022. Enhanced nonsacrificial photocatalytic generation of hydrogen peroxide under visible light using modified graphitic carbon nitride with doped phosphorus and loaded carbon quantum dots: constructing electron transfer channel. *J. Colloid Interface Sci.* 628, 259–272. <https://doi.org/10.1016/J.JCIS.2022.07.137>.
- Shi, Y., Zhao, Q., Li, J., Gao, G., Zhi, J., 2022. Onion-like carbon-embedded graphitic carbon nitride for enhanced photocatalytic hydrogen evolution and dye degradation. *Appl. Catal. B Environ.* 308,. <https://doi.org/10.1016/J.APCATB.2022.121216> 121216.
- Sim, L.C., Wong, J.L., Hak, C.H., Tai, J.Y., Leong, K.H., Saravanan, P., 2018. Sugarcane juice derived carbon dot–graphitic carbon nitride composites for bisphenol A degradation under sunlight irradiation. *Beilstein J. Nanotechnol.* 935 (9), 353–363. <https://doi.org/10.3762/BJNANO.9.35>.
- Singh, S., Yadav, R.K., Kim, T.W., Singh, C., Singh, P., Singh, A.P., Singh, A.K., Singh, A.K., Baeg, J.O., Gupta, S.K., 2022. Rational design of a graphitic carbon nitride catalytic–biocatalytic system as a photocatalytic platform for solar fine chemical production from CO₂. *React. Chem. Eng.* 7, 1566–1572. <https://doi.org/10.1039/D2RE00079B>.
- Song, X., Wang, M., Liu, W., Li, X., Zhu, Z., Huo, P., Yan, Y., 2022. Thickness regulation of graphitic carbon nitride and its influence on the photocatalytic performance towards CO₂ reduction. *Appl. Surf. Sci.* 577,. <https://doi.org/10.1016/J.APSUSC.2021.151810> 151810.
- Su, Y., Chen, P., Wang, F., Zhang, Q., Chen, T., Wang, Y., Yao, K., Lv, W., Liu, G., 2017. Decoration of TiO₂/g-C₃N₄ Z-scheme by carbon dots as a novel photocatalyst with improved visible-light

- photocatalytic performance for the degradation of enrofloxacin. *RSC Adv.* 7, 34096–34103. <https://doi.org/10.1039/C7RA05485H>.
- Sudhaik, A., Raizada, P., Khan, A.A.P., Singh, A., Singh, P., 2022. Graphitic carbon nitride-based upconversion photocatalyst for hydrogen production and water purification. *Nanofabrication* 7, 183–190. <https://doi.org/10.37819/NANOFAB.007.189>.
- J. Sun, J. Zhang, M. Zhang, M. Antonietti, X. Fu, X. Wang, Bioinspired hollow semiconductor nanospheres as photosynthetic nanoparticles, *Nat. Commun.* 2012 31. 3 (2012) 1–7. <https://doi.org/10.1038/ncomms2152>.
- Sun, Z., Wang, H., Wu, Z., Wang, L., 2018. g-C₃N₄ based composite photocatalysts for photocatalytic CO₂ reduction. *Catal. Today* 300, 160–172. <https://doi.org/10.1016/J.CATTOD.2017.05.033>.
- Swedha, M., Alatar, A.A., Okla, M.K., Alaraidh, I.A., Mohebaldin, A., Aufy, M., Raju, L.L., Thomas, A.M., Abdel-Maksoud, M.A., Sudheer Khan, S., 2022. Graphitic carbon nitride embedded Ni₃(VO₄)₂/ZnCr₂O₄ Z-scheme photocatalyst for efficient degradation of p-chlorophenol and 5-fluorouracil, and genotoxic evaluation in *Allium cepa*. *J. Ind. Eng. Chem.* 112, 244–257. <https://doi.org/10.1016/J.JIEC.2022.05.018>.
- Tan, J., Li, Z., Li, J., Meng, Y., Yao, X., Wang, Y., Lu, Y., Zhang, T., 2022. Visible-light-assisted peroxymonosulfate activation by metal-free bifunctional oxygen-doped graphitic carbon nitride for enhanced degradation of imidacloprid: role of non-photochemical and photocatalytic activation pathway. *J. Hazard. Mater.* 423. <https://doi.org/10.1016/J.JHAZMAT.2021.127048> 127048.
- Tang, J.Y., Er, C.C., Tan, L.L., Chew, Y.H., Mohamed, A.R., Chai, S.P., 2022. Uncovering the multifaceted roles of nitrogen defects in graphitic carbon nitride for selective photocatalytic carbon dioxide reduction: a density functional theory study. *Phys. Chem. Chem. Phys.* 24, 11124–11130. <https://doi.org/10.1039/D2CP00466F>.
- Tao, L., Zhang, H., Li, G., Liao, C., Jiang, G., 2022. Photocatalytic degradation of pharmaceuticals by pore-structured graphitic carbon nitride with carbon vacancy in water: identification of intermediate degradants and effects of active species. *Sci. Total Environ.* 824. <https://doi.org/10.1016/J.SCITOTENV.2022.153845> 153845.
- Tian, W., Li, N., Zhou, J., 2016. A novel P-doped g-C₃N₄/Zn_{0.8}Cd_{0.2}S composite photocatalyst for degradation of methylene blue under simulated sunlight. *Appl. Surf. Sci.* 361, 251–258. <https://doi.org/10.1016/J.APSUSC.2015.11.157>.
- Tipplook, M., Panomsuwan, G., Sudare, T., Teshima, K., 2022. Graphitic carbon nitride nanoflakes decorated on multielement-doped carbon as photocatalysts for bacterial disinfection under visible and near-infrared light. *ACS Appl. Nano Mater.* 5, 3422–3433. https://doi.org/10.1021/ACSANM.1C03980/ASSET/IMAGES/LARGE/ANI1C03980_0011.JPEG.
- Tonda, S., Kumar, S., Kandula, S., Shanker, V., 2014. Fe-doped and -mediated graphitic carbon nitride nanosheets for enhanced photocatalytic performance under natural sunlight. *J. Mater. Chem. A* 2, 6772–6780. <https://doi.org/10.1039/C3TA15358D>.
- Tseng, I.H., You, B.J., Chang, P.Y., 2022. Sugarcane bagasse supported graphitic carbon nitride for photocatalytic conversion of carbon dioxide. *Catal. Commun.* 164. <https://doi.org/10.1016/J.CATCOM.2022.106431> 106431.
- Van Thuan, D., Nguyen, T.L., Pham Thi, H.H., Thanh, N.T., Ghotekar, S., Sharma, A.K., Binh, M.T., Nga, T.T., Pham, T.D., Cam, D.P., 2022. Development of Indium vanadate and Silver deposited on graphitic carbon nitride ternary heterojunction for advanced photocatalytic degradation of residual antibiotics in aqueous environment. *Opt. Mater. (Amst)*. 123. <https://doi.org/10.1016/J.OPTMAT.2021.111885> 111885.
- Vaya, D., Kaushik, B., Surolia, P.K., 2022. Recent advances in graphitic carbon nitride semiconductor: structure, synthesis and applications. *Mater. Sci. Semicond. Process.* 137. <https://doi.org/10.1016/J.MSSP.2021.106181>.
- Verma, S.K., Verma, R., Girish, Y.R., Xue, F., Yan, L., Verma, S., Singh, M., Vaishnav, Y., Shaik, A.B., Bhandare, R.R., Rakesh, K. P., Sharath Kumar, K.S., Rangappa, K.S., 2022. Heterogeneous graphitic carbon nitrides in visible-light-initiated organic transformations. *Green Chem.* 24, 438–479. <https://doi.org/10.1039/D1GC03490A>.
- Wan, S., Xu, J., Cao, S., Yu, J., 2022. Promoting intramolecular charge transfer of graphitic carbon nitride by donor–acceptor modulation for visible-light photocatalytic H₂ evolution. *Interdiscip. Mater.* 1, 294–308. <https://doi.org/10.1002/IDM2.12024>.
- Wan, C., Zhou, L., Xu, S., Jin, B., Ge, X., Qian, X., Xu, L., Chen, F., Zhan, X., Yang, Y., guo Cheng, D., 2022. Defect engineered mesoporous graphitic carbon nitride modified with AgPd nanoparticles for enhanced photocatalytic hydrogen evolution from formic acid. *Chem. Eng. J.* 429. <https://doi.org/10.1016/J.CEJ.2021.132388> 132388.
- Wang, B., Bai, C., Wang, Z., She, P., Sun, H., Lu, G., Liang, S., Liu, Z., 2022. Phosphorus-oxygen-codoped graphitic carbon nitride for enhanced hydrogen evolution and photocatalytic degradation under visible light irradiation. *ACS Appl. Energy Mater.* 2022, 5784. https://doi.org/10.1021/ACSAEM.2C00099/ASSET/IMAGES/LARGE/AE2C00099_0008.JPEG.
- Wang, X., Cao, Z., Zhang, Y., Xu, H., Cao, S., Zhang, R., 2020. All-solid-state Z-scheme Pt/ZnS-ZnO heterostructure sheets for photocatalytic simultaneous evolution of H₂ and O₂. *Chem. Eng. J.* 385. <https://doi.org/10.1016/J.CEJ.2019.123782> 123782.
- Wang, F., Chen, P., Feng, Y., Xie, Z., Liu, Y., Su, Y., Zhang, Q., Wang, Y., Yao, K., Lv, W., Liu, G., 2017. Facile synthesis of N-doped carbon dots/g-C₃N₄ photocatalyst with enhanced visible-light photocatalytic activity for the degradation of indomethacin. *Appl. Catal. B Environ.* 207, 103–113. <https://doi.org/10.1016/J.APCATB.2017.02.024>.
- Wang, G., Chen, Z., Wang, T., Wang, D., Mao, J., 2022. P and Cu dual sites on graphitic carbon nitride for photocatalytic CO₂ reduction to hydrocarbon fuels with high C₂H₆ evolution. *Angew. Chemie Int. Ed.* 61, e202210789. <https://doi.org/10.1002/ANIE.202210789>.
- Wang, Y., Di, Y., Antonietti, M., Li, H., Chen, X., Wang, X., 2010. Excellent visible-light photocatalysis of fluorinated polymeric carbon nitride solids. *Chem. Mater.* 22, 5119–5121. https://doi.org/10.1021/CM1019102/SUPPL_FILE/CM1019102_SI_001.PDF.
- X. Wang, K. Maeda, A. Thomas, K. Takanabe, G. Xin, J.M. Carlsson, K. Domen, M. Antonietti, A metal-free polymeric photocatalyst for hydrogen production from water under visible light, *Nat. Mater.* 2009 81. 8 (2008) 76–80. <https://doi.org/10.1038/nmat2317>.
- Wang, K., Li, Q., Liu, B., Cheng, B., Ho, W., Yu, J., 2015. Sulfur-doped g-C₃N₄ with enhanced photocatalytic CO₂-reduction performance. *Appl. Catal. B Environ.* 176–177, 44–52. <https://doi.org/10.1016/J.APCATB.2015.03.045>.
- Wang, X., Li, Q., Gan, L., Ji, X., Chen, F., Peng, X., Zhang, R., 2020. 3D macropore carbon-vacancy g-C₃N₄ constructed using polymethylmethacrylate spheres for enhanced photocatalytic H₂ evolution and CO₂ reduction. *J. Energy Chem.* 53, 139–146. <https://doi.org/10.1016/J.JEACHEM.2020.05.001>.
- Wang, F., Li, W., Zhang, W., Ye, R., Tan, X., 2022. Facile fabrication of the Ag nanoparticles decorated graphitic carbon nitride photocatalyst film for indoor air purification under visible light. *Build. Environ.* 222. <https://doi.org/10.1016/J.BUILDENV.2022.109402> 109402.
- Wang, S., Li, Y., Wang, X., Zi, G., Zhou, C., Liu, B., Liu, G., Wang, L., Huang, W., 2022. One-step supramolecular preorganization constructed crinkly graphitic carbon nitride nanosheets with enhanced photocatalytic activity. *J. Mater. Sci. Technol.* 104, 155–162. <https://doi.org/10.1016/J.JMST.2021.07.014>.
- Wang, X., Li, Q., Lin, Q., Zhang, R., Ding, M., 2022. CdS-sensitized 3D ordered macroporous g-C₃N₄ for enhanced visible-light photocatalytic hydrogen generation. *J. Mater. Sci. Technol.* 111, 204–210. <https://doi.org/10.1016/J.JMST.2021.09.046>.

- Wang, F., Wang, Y., Feng, Y., Zeng, Y., Xie, Z., Zhang, Q., Su, Y., Chen, P., Liu, Y., Yao, K., Lv, W., Liu, G., 2018. Novel ternary photocatalyst of single atom-dispersed silver and carbon quantum dots co-loaded with ultrathin g-C₃N₄ for broad spectrum photocatalytic degradation of naproxen. *Appl. Catal. B Environ.* 221, 510–520. <https://doi.org/10.1016/J.APCATB.2017.09.055>.
- Wang, Q., Xiao, M., Peng, Z., Zhang, C., Du, X., Wang, Z., Wang, W., 2022. Visible LED photocatalysis combined with ultrafiltration driven by metal-free oxygen-doped graphitic carbon nitride for sulfamethazine degradation. *J. Hazard. Mater.* 439, <https://doi.org/10.1016/J.JHAZMAT.2022.129632> 129632.
- Wang, Y., Xu, Y., Wang, Y., Qin, H., Li, X., Zuo, Y., Kang, S., Cui, L., 2016. Synthesis of Mo-doped graphitic carbon nitride catalysts and their photocatalytic activity in the reduction of CO₂ with H₂O. *Catal. Commun.* 74, 75–79. <https://doi.org/10.1016/J.CATCOM.2015.10.029>.
- Wang, J., Xu, M., Tremblay, P.L., Zhang, T., 2022. Improved polyhydroxybutyrate production by Cupriavidus necator and the photocatalyst graphitic carbon nitride from fructose under low light intensity. *Int. J. Biol. Macromol.* 203, 526–534. <https://doi.org/10.1016/J.IJBIOMAC.2022.01.179>.
- Wang, C., Yang, C., Qin, J., Rajendran, S., Zhang, X., 2022. A facile template synthesis of phosphorus-doped graphitic carbon nitride hollow structures with high photocatalytic hydrogen production activity. *Mater. Chem. Phys.* 275, <https://doi.org/10.1016/J.MATCHEMPHYS.2021.125299> 125299.
- Wang, Y., Zeng, Y., Li, B., Li, A., Yang, P., Yang, L., Wang, G., Chen, J., Wang, R., 2016. In-situ hydrothermal synthesized γ -Al₂O₃/O-g-C₃N₄ heterojunctions with enhanced visible-light photocatalytic activity in water splitting for hydrogen. *J. Energy Chem.* 25, 594–600. <https://doi.org/10.1016/J.JEACHEM.2016.03.018>.
- Wang, Y., Li, Y., Bai, X., Cai, Q., Liu, C., Zuo, Y., Kang, S., Cui, L., 2016. Facile synthesis of Y-doped graphitic carbon nitride with enhanced photocatalytic performance. *Catal. Commun.* 84, 179–182. <https://doi.org/10.1016/J.CATCOM.2016.06.020>.
- Q. Wu, D. Lu, B. Zhang, K.K. Kondamareddy, Y. Zeng, Y. Zhang, J. Wang, M. Zhou, N. D. H. Hao, H. Fan, Interfacial optimization of CeO₂ nanoparticles loaded two-dimensional graphite carbon nitride toward synergistic enhancement of visible-light-driven photoelectric and photocatalytic hydrogen evolution, *Int. J. Hydrogen Energy.* 47 (2022) 2313–2326. <https://doi.org/10.1016/J.IJHYDENE.2021.10.221>
- Wudil, Y.S., Gondal, M.A., Rao, S.G., Kunwar, S., Alsayoud, A.Q., 2020. Improved thermoelectric performance of ternary Cu/Ni/Bi₂Te_{2.7}Se_{0.3} nanocomposite prepared by pulsed laser deposition. *Mater. Chem. Phys.* 253, <https://doi.org/10.1016/J.MATCHEMPHYS.2020.123321> 123321.
- Wudil, Y.S., Gondal, M.A., Rao, S.G., Kunwar, S., Alsayoud, A.Q., 2020. Substrate temperature-dependent thermoelectric figure of merit of nanocrystalline Bi₂Te₃ and Bi₂Te_{2.7}Se_{0.3} prepared using pulsed laser deposition supported by DFT study. *Ceram. Int.* <https://doi.org/10.1016/j.ceramint.2020.06.196>.
- Wudil, Y.S., Gondal, M.A., Almessiere, M.A., Alsayoud, A.Q., 2021. The multi-dimensional approach to synergistically improve the performance of inorganic thermoelectric materials: a critical review. *Arab. J. Chem.* 14, <https://doi.org/10.1016/j.arabj.2021.103103> 103103.
- Wudil, Y.S., Peng, Q., Alsayoud, A.Q., Gondal, M.A., 2022. Hydrostatic pressure-tuning of thermoelectric properties of CsSn₃ perovskite by first-principles calculations. *Comput. Mater. Sci.* 201, <https://doi.org/10.1016/J.COMMATSCI.2021.110917> 110917.
- Xia, L., Sun, Z., Wu, Y., Yu, X.F., Cheng, J., Zhang, K., Sarina, S., Zhu, H.Y., Weerathunga, H., Zhang, L., Xia, J., Yu, J., Yang, X., 2022. Leveraging doping and defect engineering to modulate exciton dissociation in graphitic carbon nitride for photocatalytic elimination of marine oil spill. *Chem. Eng. J.* 439, <https://doi.org/10.1016/J.CEJ.2022.135668> 135668.
- Xiang, Y., Zhou, Q., Li, Z., Cui, Z., Liu, X., Liang, Y., Zhu, S., Zheng, Y., Yeung, K.W.K., Wu, S., 2020. A Z-scheme heterojunction of ZnO/CDots/C₃N₄ for strengthened photoresponsive bacteria-killing and acceleration of wound healing. *J. Mater. Sci. Technol.* 57, 1–11. <https://doi.org/10.1016/J.JMST.2020.05.016>.
- Xie, K., Fang, J., Li, L., Deng, J., Chen, F., 2022. Progress of graphite carbon nitride with different dimensions in the photocatalytic degradation of dyes: a review. *J. Alloys Compd.* 901, <https://doi.org/10.1016/J.JALLCOM.2021.163589> 163589.
- Xie, Z., Feng, Y., Wang, F., Chen, D., Zhang, Q., Zeng, Y., Lv, W., Liu, G., 2018. Construction of carbon dots modified MoO₃/g-C₃N₄ Z-scheme photocatalyst with enhanced visible-light photocatalytic activity for the degradation of tetracycline. *Appl. Catal. B Environ.* 229, 96–104. <https://doi.org/10.1016/J.APCATB.2018.02.011>.
- Xiong, T., Cen, W., Zhang, Y., Dong, F., 2016. Bridging the g-C₃N₄ interlayers for enhanced photocatalysis. *ACS Catal.* 6, 2462–2472. https://doi.org/10.1021/ACSCATAL.5B02922/ASSET/IMAGES/LARGE/CS-2015-029222_0014.JPG.
- Xu, F., An, N., Lai, C., Zhang, M., Li, B., Liu, S., Li, L., Qin, L., Fu, Y., Yi, H., Yan, H., 2022. Nitrogen-doping coupled with cerium oxide loading co-modified graphitic carbon nitride for highly enhanced photocatalytic degradation of tetracycline under visible light. *Chemosphere* 293, <https://doi.org/10.1016/J.CHEMOSPHERE.2022.133648> 133648.
- Xu, B., Wang, B., Zhang, H., Yang, P., 2022. Z-scheme Cu₂O nanoparticle/graphite carbon nitride nanosheet heterojunctions for photocatalytic hydrogen evolution. *ACS Appl. Nano Mater.* 5, 8475–8483. <https://doi.org/10.1021/ACSANM.2C01616>.
- Xu, Y., Wang, M., Liu, Y., Yu, R., Xu, Q., Meng, S., Jiang, D., Chen, M., 2022. Efficient charge transfer in Co-doped CeO₂/graphitic carbon nitride with N vacancies heterojunction for photocatalytic hydrogen evolution. *J. Colloid Interface Sci.* 627, 261–269. <https://doi.org/10.1016/J.JCIS.2022.07.042>.
- Xue, Y., Wang, X., Liang, Z., Zhang, X., Tian, J., 2022. The fabrication of graphitic carbon nitride hollow nanocages with semi-metal 1T' phase molybdenum disulfide as co-catalysts for excellent photocatalytic nitrogen fixation. *J. Colloid Interface Sci.* 608, 1229–1237. <https://doi.org/10.1016/J.JCIS.2021.10.153>.
- Yan, S.C., Li, Z.S., Zou, Z.G., 2010. Photodegradation of rhodamine B and methyl orange over boron-doped g-C₃N₄ under visible light irradiation. *Langmuir* 26, 3894–3901. https://doi.org/10.1021/LA904023J/SUPPL_FILE/LA904023J_SI_001.PDF.
- Yang, Y., Zeng, Z., Zeng, G., Huang, D., Xiao, R., Zhang, C., Zhou, C., Xiong, W., Wang, W., Cheng, M., Xue, W., Guo, H., Tang, X., He, D., 2019. Ti₃C₂ Mxene/porous g-C₃N₄ interfacial Schottky junction for boosting spatial charge separation in photocatalytic H₂O₂ production. *Appl. Catal. B Environ.* 258, <https://doi.org/10.1016/J.APCATB.2019.117956> 117956.
- Q. Ye, L. Xu, Y. Xia, R. Gang, C. Xie, Zinc oxide quantum dots/graphitic carbon nitride nanosheets based visible-light photocatalyst for efficient tetracycline hydrochloride degradation, *J. Porous Mater.* 2022 292. 29 (2022) 571–581. <https://doi.org/10.1007/S10934-022-01197-2>.
- You, Q., Zhang, Q., Gu, M., Du, R., Chen, P., Huang, J., Wang, Y., Deng, S., Yu, G., 2022. Self-assembled graphitic carbon nitride regulated by carbon quantum dots with optimized electronic band structure for enhanced photocatalytic degradation of diclofenac. *Chem. Eng. J.* 431, <https://doi.org/10.1016/J.CEJ.2021.133927> 133927.
- D. Yu, T. Jia, Z. Deng, Q. Wei, K. Wang, L. Chen, P. Wang, J. Cui, One-Dimensional P-Doped Graphitic Carbon Nitride Tube: Facile Synthesis, Effect of Doping Concentration, and Enhanced Mechanism for Photocatalytic Hydrogen Evolution, *Nanomater.* 2022, Vol. 12, Page 1759. 12 (2022) 1759. <https://doi.org/10.3390/NANO12101759>.
- Yu, Z., Li, Y., Torres-Pinto, A., LaGrow, A.P., Diaconescu, V.M., Simonelli, L., Sampaio, M.J., Bondarchuk, O., Amorim, I., Araujo,

- A., Silva, A.M.T., Silva, C.G., Faria, J.L., Liu, L., 2022. Single-atom Ir and Ru anchored on graphitic carbon nitride for efficient and stable electrocatalytic/photocatalytic hydrogen evolution. *Appl. Catal. B Environ.* 310, <https://doi.org/10.1016/j.apcatb.2022.121318> 121318.
- Yu, H., Shi, R., Zhao, Y., Bian, T., Zhao, Y., Zhou, C., Waterhouse, G.I.N., Wu, L.-Z., Tung, C.-H., Zhang, T., Yu, H., Shi, R., Zhao, Y., Bian, T., Zhao, C., Wu, L., Tung, C., Zhang, T., Waterhouse, G.I.N., 2017. Alkali-assisted synthesis of nitrogen deficient graphitic carbon nitride with tunable band structures for efficient visible-light-driven hydrogen evolution. *Adv. Mater.* 29, 1605148. <https://doi.org/10.1002/adma.201605148>.
- Yuan, J., Gao, Q., Li, X., Liu, Y., Fang, Y., Yang, S., Peng, F., Zhou, X., 2014. Novel 3-D nanoporous graphitic-C₃N₄ nanosheets with heterostructured modification for efficient visible-light photocatalytic hydrogen production. *RSC Adv.* 4, 52332–52337. <https://doi.org/10.1039/C4RA10038G>.
- Zehab Salmasi, M., Kazemini, M., Sadjadi, S., Nematollahi, R., 2022. Spinel MgAl₂O₄ nanospheres coupled with modified graphitic carbon nitride nanosheets as an efficient Z-scheme photocatalyst for photodegradation of organic contaminants. *Appl. Surf. Sci.* 585, <https://doi.org/10.1016/j.apsusc.2022.152615> 152615.
- Zeng, G., Duan, M., He, J., Ge, F., Wang, W., 2022. Sulfate doped graphitic carbon nitride with enhanced photocatalytic activity towards degradation of methylene blue. *Mater. Lett.* 309, <https://doi.org/10.1016/j.matlet.2021.131310> 131310.
- Zhang, L., Chen, X., Guan, J., Jiang, Y., Hou, T., Mu, X., 2013. Facile synthesis of phosphorus doped graphitic carbon nitride polymers with enhanced visible-light photocatalytic activity. *Mater. Res. Bull.* 48, 3485–3491. <https://doi.org/10.1016/j.materresbull.2013.05.040>.
- Zhang, Y., De Zhang, W., 2019. Ternary catalysts based on amino-functionalized carbon quantum dots, graphitic carbon nitride nanosheets and cobalt complex for efficient H₂ evolution under visible light irradiation. *Carbon N. Y.* 145, 488–500. <https://doi.org/10.1016/j.carbon.2019.01.052>.
- Zhang, J., Hu, S., Wang, Y., 2014. A convenient method to prepare a novel alkali metal sodium doped carbon nitride photocatalyst with a tunable band structure. *RSC Adv.* 4, 62912–62919. <https://doi.org/10.1039/C4RA11377B>.
- Zhang, J., Fu, J., Dai, K., 2022. Graphitic carbon nitride/antimonene van der Waals heterostructure with enhanced photocatalytic CO₂ reduction activity. *J. Mater. Sci. Technol.* 116, 192–198. <https://doi.org/10.1016/j.jmst.2021.10.045>.
- Zhang, S., Li, J., Zeng, M., Li, J., Xu, J., Wang, X., 2014. Bandgap engineering and mechanism study of nonmetal and metal ion codoped carbon nitride: C+Fe as an example. *Chem. – A Eur. J.* 20, 9805–9812. <https://doi.org/10.1002/chem.201400060>.
- Zhang, P., Li, X., Shao, C., Liu, Y., 2015. Hydrothermal synthesis of carbon-rich graphitic carbon nitride nanosheets for photoredox catalysis. *J. Mater. Chem. A* 3, 3281–3284. <https://doi.org/10.1039/C5TA00202H>.
- Zhang, Z., Lin, S., Li, X., Li, H., Cui, W., 2017. Metal free and efficient photoelectrocatalytic removal of organic contaminants over g-C₃N₄ nanosheet films decorated with carbon quantum dots. *RSC Adv.* 7, 56335–56343. <https://doi.org/10.1039/C7RA11205J>.
- Zhang, X., Ma, P., Wang, C., Gan, L., Chen, X., Zhang, P., Wang, Y., Li, H., Wang, L., Zhou, X., Zheng, K., 2022. Unraveling the dual defect sites in graphite carbon nitride for ultra-high photocatalytic H₂O₂ evolution. *Energy Environ. Sci.* 15, 830–842. <https://doi.org/10.1039/D1EE02369A>.
- Zhang, X., Liu, Y., Ren, M., Yang, G., Qin, L., Guo, Y., Meng, J., 2022. Precise carbon doping regulation of porous graphitic carbon nitride nanosheets enables elevated photocatalytic oxidation performance towards emerging organic pollutants. *Chem. Eng. J.* 433, <https://doi.org/10.1016/j.cej.2022.134551> 134551.
- Zhang, Y., Mori, T., Ye, J., Antonietti, M., 2010. Phosphorus-doped carbon nitride solid: enhanced electrical conductivity and photocurrent generation. *J. Am. Chem. Soc.* 132, 6294–6295. https://doi.org/10.1021/JA101749Y/SUPPL_FILE/JA101749Y_SI_002.PDF.
- Zhang, Y., Huang, Z., Dong, C.L., Shi, J., Cheng, C., Guan, X., Zong, S., Luo, B., Cheng, Z., Wei, D., Cheng Huang, Y., Shen, S., Guo, L., 2022. Synergistic effect of nitrogen vacancy on ultrathin graphitic carbon nitride porous nanosheets for highly efficient photocatalytic H₂ evolution. *Chem. Eng. J.* 431, <https://doi.org/10.1016/j.cej.2021.134101> 134101.
- Zhang, D., Ren, P., Liu, W., Li, Y., Salli, S., Han, F., Qiao, W., Liu, Y., Fan, Y., Cui, Y., Shen, Y., Richards, E., Wen, X., Rummeli, M. H., Li, Y., Besenbacher, F., Niemantsverdriet, H., Lim, T., Su, R., 2022. Photocatalytic abstraction of hydrogen atoms from water using hydroxylated graphitic carbon nitride for hydrogenative coupling reactions. *Angew. Chemie Int. Ed.* 61, e202204256. <https://doi.org/10.1002/anie.202204256>.
- Zhang, Y., Wang, T., Zheng, B., Shi, J., Cai, C., Mao, L., Cheng, C., Zong, S., Guo, X., Chen, Q., 2022. EDTA-dominated hollow tube-like porous graphitic carbon nitride towards enhanced photocatalytic hydrogen evolution. *J. Colloid Interface Sci.* 619, 289–297. <https://doi.org/10.1016/j.jcis.2022.03.127>.
- Zhang, G., Zhang, M., Ye, X., Qiu, X., Lin, S., Wang, X., Zhang, G., Zhang, M., Ye, X., Qiu, X., Lin, S., Wang, X., 2014. Iodine modified carbon nitride semiconductors as visible light photocatalysts for hydrogen evolution. *Adv. Mater.* 26, 805–809. <https://doi.org/10.1002/adma.201303611>.
- Zhang, H., Zhang, B., Liang, F., Fang, Y., Wang, H., Chen, A., 2022. Precise regulation of ultra-thin platinum decorated Gold/Graphite carbon nitride photocatalysts by atomic layer deposition for efficient degradation of Rhodamine B under simulated sunlight. *Arab. J. Chem.* 15, <https://doi.org/10.1016/j.arabj.2022.103951> 103951.
- Zhang, X., Zhang, J., Qiu, L., Lan, X., Zhu, C., Duan, J., Liu, Y., Li, H., Yu, Y., Yang, W., 2022. In-situ synthesis of dual Z-scheme heterojunctions of cuprous oxide/layered double hydroxides/nitrogen-rich graphitic carbon nitride for photocatalytic sterilization. *J. Colloid Interface Sci.* 620, 313–321. <https://doi.org/10.1016/j.jcis.2022.04.015>.
- Zhang, H., Zhao, L., Geng, F., Guo, L.H., Wan, B., Yang, Y., 2016. Carbon dots decorated graphitic carbon nitride as an efficient metal-free photocatalyst for phenol degradation. *Appl. Catal. B Environ.* 180, 656–662. <https://doi.org/10.1016/j.apcatb.2015.06.056>.
- Zhao, B., Gao, D., Liu, Y., Fan, J., Yu, H., 2022. Cyano group-enriched crystalline graphitic carbon nitride photocatalyst: Ethyl acetate-induced improved ordered structure and efficient hydrogen-evolution activity. *J. Colloid Interface Sci.* 608, 1268–1277. <https://doi.org/10.1016/j.jcis.2021.10.108>.
- Zhao, G., Li, W., Zhang, H., Wang, W., Ren, Y., 2022. Single atom Fe-dispersed graphitic carbon nitride (g-C₃N₄) as a highly efficient peroxymonosulfate photocatalytic activator for sulfamethoxazole degradation. *Chem. Eng. J.* 430, <https://doi.org/10.1016/j.cej.2021.132937> 132937.
- Zhao, Y., Qin, H., Wang, Z., Wang, H., He, Y., Tian, Q., Luo, Q., Xu, P., 2022. Facile synthesis of cadmium-doped graphite carbon nitride for photocatalytic degradation of tetracycline under visible light irradiation. *Environ. Sci. Pollut. Res.* 2022, 1–19. <https://doi.org/10.1007/S11356-022-21051-X>.
- Zhao, Z., Sun, Y., Dong, F., Zhang, Y., Zhao, H., 2015. Template synthesis of carbon self-doped g-C₃N₄ with enhanced visible to near-infrared absorption and photocatalytic performance. *RSC Adv.* 5, 39549–39556. <https://doi.org/10.1039/C5RA03433G>.
- Zhao, S., Tang, Z., Guo, S., Han, M., Zhu, C., Zhou, Y., Bai, L., Gao, J., Huang, H., Li, Y., Liu, Y., Kang, Z., 2018. Enhanced activity for CO₂ electroreduction on a highly active and stable ternary Au-CDots-C₃N₄ electrocatalyst. *ACS Catal.* 8, 188–197.

- https://doi.org/10.1021/ACSCATAL.7B01551/ASSET/IMAGES/LARGE/CS-2017-01551X_0007.JPEG.
- Zhong, Z., Chen, L., Zhang, L., Wu, F., Jiang, X., Liu, H., Lv, F., Xie, H., Meng, F., Zheng, L., Zou, J., 2022. Semi-chemical interaction between graphitic carbon nitride and Pt for boosting photocatalytic hydrogen evolution. *Chinese Chem. Lett.* 33, 3061–3064. <https://doi.org/10.1016/J.CCLET.2021.09.057>.
- Zhong, J., Ni, T., Huang, J., Li, D., Tan, C., Liu, Y., Chen, P., Wen, C., Liu, H., Wang, Z., Lv, W., Liu, G., 2022. Directional utilization disorder charge via In-plane driving force of functionalized graphite carbon nitride for the robust photocatalytic degradation of fluoroquinolone. *Chem. Eng. J.* 442,. <https://doi.org/10.1016/J.CEJ.2022.135943> 135943.
- Zhou, W., Yang, B., Liu, G., Xu, C., Ji, Q., Xiang, W., Sun, D., Zhong, Q., He, H., Yazici, L., Xu, Z., Qi, C., Li, S., Yang, S., 2022. Perylene diimide supermolecule (PDI) as a novel and highly efficient cocatalyst for photocatalytic degradation of tetracycline in water: A case study of PDI decorated graphitic carbon nitride/bismuth tungstate composite. *J. Colloid Interface Sci.* 615, 849–864. <https://doi.org/10.1016/J.JCIS.2022.02.003>.
- Zhou, Y., Zhang, L., Liu, J., Fan, X., Wang, B., Wang, M., Ren, W., Wang, J., Li, M., Shi, J., 2015. Brand new P-doped g-C3N4: enhanced photocatalytic activity for H₂ evolution and Rhodamine B degradation under visible light. *J. Mater. Chem. A.* 3, 3862–3867. <https://doi.org/10.1039/C4TA05292G>.
- Zhu, Y.P., Ren, T.Z., Yuan, Z.Y., 2015. Mesoporous phosphorus-doped g-C3N4 nanostructured flowers with superior photocatalytic hydrogen evolution performance. *ACS Appl. Mater. Interfaces* 7, 16850–16856. https://doi.org/10.1021/ACSAMI.5B04947/SUPPL_FILE/AM5B04947_SI_001.PDF.
- Zhu, Y., Sun, Y., Khan, J., Liu, H., He, G., Liu, X., Xiao, J., Xie, H., Han, L., 2022. NaClO-induced sodium-doped cyano-rich graphitic carbon nitride nanosheets with nitrogen vacancies to boost photocatalytic hydrogen peroxide production. *Chem. Eng. J.* 443,. <https://doi.org/10.1016/J.CEJ.2022.136501> 136501.